Copyright Warning & Restrictions

The copyright law of the United States (Title 17, United States Code) governs the making of photocopies or other reproductions of copyrighted material.

Under certain conditions specified in the law, libraries and archives are authorized to furnish a photocopy or other reproduction. One of these specified conditions is that the photocopy or reproduction is not to be "used for any purpose other than private study, scholarship, or research." If a, user makes a request for, or later uses, a photocopy or reproduction for purposes in excess of "fair use" that user may be liable for copyright infringement,

This institution reserves the right to refuse to accept a copying order if, in its judgment, fulfillment of the order would involve violation of copyright law.

Please Note: The author retains the copyright while the New Jersey Institute of Technology reserves the right to distribute this thesis or dissertation

Printing note: If you do not wish to print this page, then select "Pages from: first page # to: last page #" on the print dialog screen

ABSTRACT

DOPPLER ULTRASOUND TECHNIQUE USED TO DETERMINE THE BLOOD FLOW VELOCITY IN THE MIDDLE CEREBRAL ARTERY OF A CANINE ANIMAL MODEL

by

Raj P. Ganpath

The cerebral blood flow velocity in the middle cerebral artery of an canine animal model was measured using the Doppler Ultrasound technique. A transducer was designed with a 20 MHz piezoelectric crystal and used for the application. An *in vitro* calibration system was designed and machined for the purpose of testing and calibrating every transducer before using it *in vivo.* Preliminary tests included experiments on the *in vitro* system and measurement of blood flow velocity in the human wrist artery (metacarpal artery). The effect of using different transmission media (agarose and gelatin) was determined through the many *in vitro* and animal experiments. A design of surgical preparation and setup which included instrumentation and procedure was developed. The *in vivo* measures included blood flow velocity in the femoral, left gastric and mesenteric arteries of a mouse (14.5cm/s to 17.4cm/s; 12cm/s to 14cm/s; 25cm/s to 30cm/s respectively), middle cerebral artery (MCA) of a pig (7.5cm/s to 8.5cm/s), the MCA of a dog (5.5cm/s to 6cm/s) and drug response as an indication of instrument sensitivity (increase from 6cm/s to 10cm/s with introduction of Forskolin). The values obtained matched those in the published literature. Fast Fourier Transformations were used to write programs in MATLAB which served as the tool for data analysis.

DOPPLER ULTRASOUND TECHNIQUE USED TO DETERMINE THE BLOOD FLOW VELOCITY IN THE MIDDLE CEREBRAL ARTERY OF A CANINE ANIMAL MODEL

by

Raj P. Ganpath

A Thesis
Submitted to the Faculty of
New Jersey Institute of Technology
in Partial Fulfillment of the Requirements for the Degree of
Master of Science in Mechanical Engineering

Department of Mechanical Engineering

January 2006

APPROVAL PAGE

DOPPLER ULTRASOUND TECHNIQUE USED TO DETERMINE THE BLOOD FLOW VELOCITY IN THE MIDDLE CEREBRAL ARTERY OF A CANINE ANIMAL MODEL

Raj P. Ganpath

Dr. Nadine Aubry, Thesis Advisor — Date
Professor, Mechanical Engineering, NJIT

Dr. Pushpendra Singh, Committee member — Date
Professor, Mechanical Engineering, NJIT

Dr. Ernest S. Geskin, Committee member — Date
Professor, Mechanical Engineering, NJIT

BIBLIOGRAPHICAL SKETCH

Author: Raj P. Ganpath

Degree: Master of Science

Date: January 2006

Undergraduate and Graduate Education

- Master of Science in Mechanical Engineering
  New Jersey Institute of Technology (January 2006)

- Bachelor of Engineering (Honors) Mechanical Engineering
  Birla Institute of Technology and Science, Pilani, India (May 2004)

Major: Mechanical Engineering

Life is a lesson. You learn it when you're through.

To my dad, mom and sister for their support and encouragement and especially the faith they had in me.

To Nari, Lokesh, Anand, Karthik, Maapi and Yogesh for having shared both misery and fortune.

ACKNOWLEDGMENT

I would like to thank Dr. Nadine Aubry for providing me with this opportunity to work on such an interesting thesis and for her valuable contributions throughout the course of the thesis work. I thank Dr. Pushpendra Singh and Dr. Ernest Geskin for actively participating in the committee.

I am deeply indebted to Mr. Samuel C. Lieber for his input, involvement and guidance from the day I started working on this thesis and for his never failing efforts to make me a successful engineer.

Special thanks to Dr. Stephen Vatner and Dr. Nadine Aubry for having funded this project. I extend my gratitude to Mr. Brian Griffin and Mr. Milton Brown of UMDNJ for all their support.

I also thank surgeons Dr. Y T Shen of UMDNJ, Dr. Chull Hong of UMDNJ and Dr. Bruno Mantilla of NJIT without whom this project would never have been possible.

TABLE OF CONTENTS

TABLE OF CONTENTS
(Continued)

Chapter **Page**

TABLE OF CONTENTS
(Continued)

Chapter **Page**

TABLE OF CONTENTS
(Continued)

Chapter **Page**

LIST OF TABLES

Table **Page**

LIST OF FIGURES

Figure **Page**

LIST OF FIGURES
(Continued)

Figure **Page**

LIST OF FIGURES
(Continued)

Figure **Page**

LIST OF FIGURES
(Continued)

Figure **Page**

LIST OF FIGURES
(Continued)

Figure **Page**

CHAPTER 1

INTRODUCTION

1.1 Objectives

This project deals with blood flow velocity measurement using the Doppler Ultrasound Technique. The objective of this work is to design a complete system to measure the blood flow velocity in the brain of large animals. This includes the development of an *in vitro* calibration system to verify the operation and design of a transducer including the selection of size, geometry and crystal frequency, the development of the surgical methods applied, the testing in various *in vivo* models and the development of a data analysis method to determine blood flow velocity.

Initially transducers (also called probes), containing a 10MHz piezoelectric crystal, of different geometries and sizes will be iterated in a few preliminary experiments. Following this, an *in vitro* system, designed to calibrate the different frequency crystals, will be used as an exhaustive testing station. Each transducer will be tested *in vitro,* using particle suspended solutions mimicking blood flow, before being used on an animal. A clear comparison of the results obtained, when each of these transducers is used, will be formulated and then the transducer producing the best results will be selected. A design study on the shape of the transducer will be done to model one which can be comfortably used both *in vivo* and *in vitro*. Then the transducer producing the best results and with the most optimum shape will be used to deduce the blood flow velocities in various arteries of a mouse, in the MCA of a pig and the MCA of a dog.

1.2 Medical Background Explanation

The blood that flows through the brain distributes nutrients to the brain and removes wastes. This flow maintains the high rate of metabolism necessary for the brain to function. Restrictions in blood flow may occur from vessel narrowing (stenosis), clot formation (thrombosis), blockage (embolism), or blood vessel rupture (hemorrhage). Lack of sufficient blood flow (ischemia) threatens brain tissue and may cause a stroke.

The velocity of flow of blood through the arteries in the brain can be analyzed using Doppler ultrasonography. This is a form of ultrasound, in which high frequency sound waves bounce off or pass through body tissues. While most other types of ultrasonography create images of the tissue being studied, the results of Doppler Ultrasonography are audible sounds that the examiner listens to and records.

Doppler ultrasonography uses what is called the Doppler effect to measure the rate and direction of blood flow in the vessels. Just as a siren's pitch sounds higher when its source is moving toward you and lower as it moves away, so too will ultrasound waves change pitch, or frequency, as they bounce off the red blood cells moving in the blood. It is these pitch changes that produce the audible sounds during the exam.

Changes in frequency can be used to measure both the direction and the speed of blood flow. Faster blood flow causes a greater change in frequency. Combined with other tests, this information can be used to locate restrictions in the blood vessels in the brain, and to track changes in blood flow over time. In this way, Doppler Ultrasonography gives valuable information about the site of a stroke and the patient's progress after a stroke. It is also used to evaluate the contraction of blood vessels that can occur if a blood vessel ruptures.[1

CHAPTER 2

LITERATURE SURVEY

2.1 Brain Covering

The brain and spinal cord are delicate organs that have a jelly-like consistency. These highly vulnerable structures are protected by the skull and vertebral column, several membrane covers, and by the cerebrospinal fluid (CSF), which provides a cushion against compressive shock [68]. The three membranes covering the brain working from the skull inward, are the dura mater, the arachnoid mater, and the pia mater (see Fig. 2.1). The ***dura*** is a rather tough membrane that can only be torn by hand with some difficulty. It consists of two leaves: an outer periosteal layer that adheres to the inner surface of the skull, and an inner layer [67].

6 » EXTERNAL ANATOMY

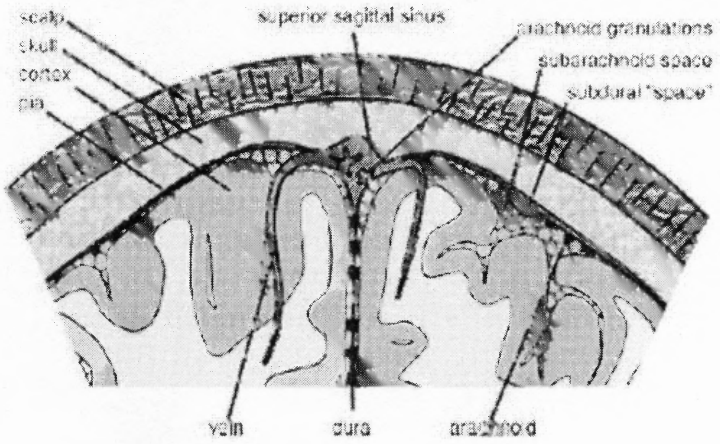

FIGURE 1.5. Coverings of the brain. Multiple layers of tissue enclose the brain. From outside-in, the main layers are the scalp, skull, dura, arachnoid membrane, and pia mater. Except for the pia, which is really part of the brain, fluids can collect in the "spaces" between these layers in pathologic states. (Note: In this figure the dura is drawn very thick to emphasize its structure. In life it is about the thickness of a piece of thin cardboard.)

Fig 2.1 Layers of the Brain
(Source: External Anatomy, WY003-01 WY003/Joseph November 19, 2003 19:1)

The two dural layers cannot be distinguished from one another except where they depart from the conformation of the skull, and dive into the brain forming the interhemispheric falx and the tentorium overlying the cerebellum, or where they split apart to form the ***venous sinuses*** [9].

Multiple layers of tissue enclose the brain. From outside-in, the main layers are the scalp, skull, dura, arachnoid membrane, and pia mater. Except for the pia, which is really part of the brain, fluids can collect in the "spaces" between these layers in pathologic states [67].

2.2 Cerebral Blood Flow

The basilar artery runs rostrally from the spinal cord and bifurcates into posterior cerebral arteries, which complete the arterial circle formed by trifurcation of bilateral internal carotid arteries (refer Fig. 2.2).

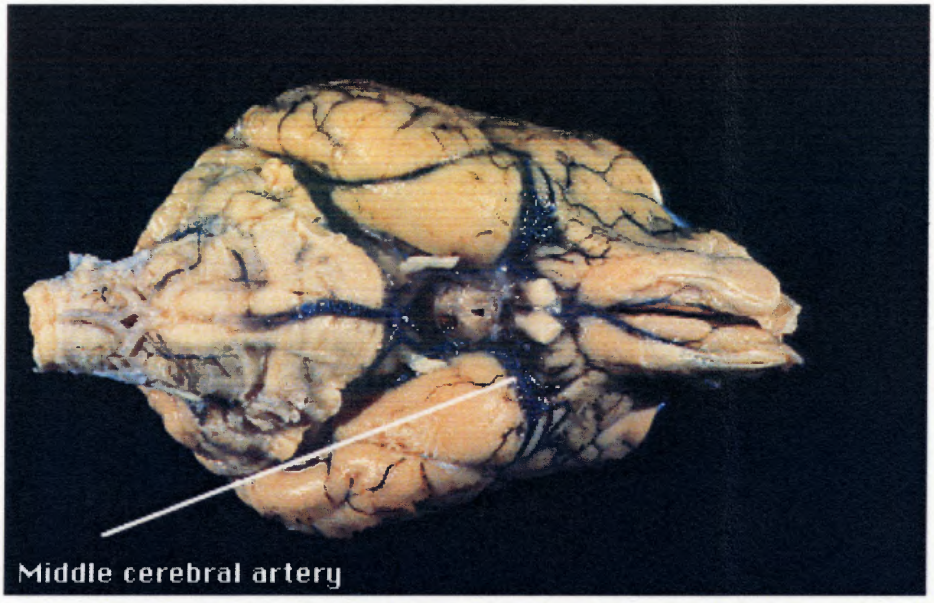

Fig 2.2 Brain of Dog showing Middle Cerebral Artery
(Source: Neurosciences; School of Veterinary Medicine, University of Pennsylvania)

Each internal carotid artery gives rise to: an anterior cerebral artery, a middle cerebral artery and a posterior communicating branch [10].

2.3 Red Blood Cells

The red blood cells are the most common type of cell found within the human body. They make up about 45% of the blood volume. There are roughly 250 million red blood cells in one tiny drop of blood [69]. A red blood cell will live anywhere from 3 - 4 months. Then it will die in the liver and spleen when it is attacked and destroyed by macrophages [12].

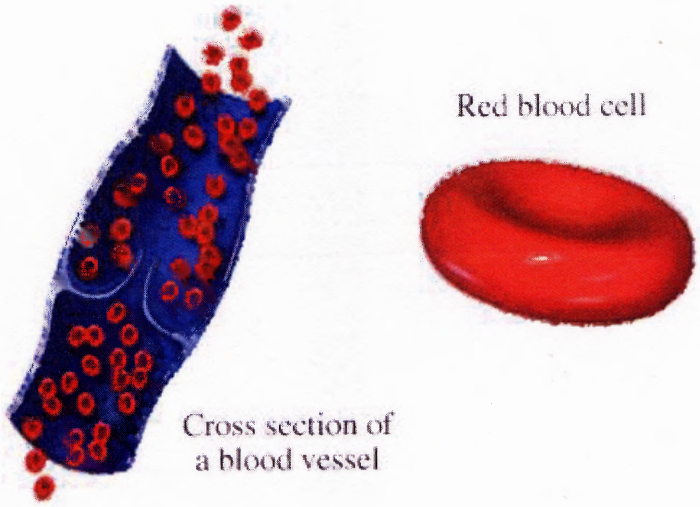

Fig 2.3 RBCs
(Source: WebMD Health)

Red blood cells have the main function or job to carry oxygen from the lungs to every cell in the body. A red blood cells make-up is composed mostly of a iron and protein compound called hemoglobin [69]. Red blood cells are packed with this compound; hence they do not have many common components of cells such as a nucleus. The outer layer of a red blood cell is like a little bubble that is extremely flexible (refer

Fig. 2.3). Its flexibility is necessary because the cell has to travel through the smallest blood vessels and capillaries to carry oxygen to wherever it's needed. Red blood cells are always disk shaped with a centered dent on each of its sides [12].

2.4 Cerebral Blood Flow Pharmacology

In the 1970s, researchers isolated a chemically active ingredient in the herb and called it forskolin. Now available in supplement form, this extract is commonly recommended for treating hypothyroidism, a condition in which the thyroid gland produces too little thyroid hormone. Forskolin is believed to stimulate the release of thyroid hormone, thus relieving such hypothyroidism symptoms as fatigue, depression, weight gain, and dry skin. Specifically, forskolin is thought to increase thyroid function by activating an enzyme that raises levels of a key cell-regulating substance called cAMP (cyclic adenosine monophosphate). Forskolin is typically taken over the long-term for hypothyroidism; it should not be used in addition to thyroid hormone replacement therapy, however. Forskolin causes the arteries to relax. Because this can lower blood pressure, forskolin should not be used in tandem with blood pressure-lowering medications [70].

Isoproterenol is a bronchodilator. It works by relaxing muscles in the airways to improve breathing. Isoproterenol inhalation is used to treat conditions such as asthma, bronchitis, and emphysema. [58].As a result of relaxing muscles, arteries are also relaxed which in turn reduces pressure. A reduction in pressure proves an increase in velocity of blood flow through the respective artery.

2.5 Blood Flow in the Brain

The brain has a high metabolic rate, receivi ng 16% of cardiac output and accounting for 20% of oxygen consumption. There are five pairs of major arteries that supply the brain with oxygenated blood. Four of these pairs are linked to form Cerebral Arterial Circle (or Circle of Willis) on the ventral surface of the brain (refer Fig. 2.4). The last pair forms a tributary of the circle.

Rostral Cerebral Arteries - supply the medial aspect of the cerebral hemispheres.

Middle Cerebral Arteries - supply the lateral and ventrolateral aspects of the cerebral hemispheres.

Caudal Cerebral Arteries - supply the occipital lobes.

Rostral Cerebellar Arteries - supply the rostral aspects of the cerebellum.

Caudal Cerebellar Arteries - supply the caudal and lateral aspects of the cerebellum. They usually arise from the basilar artery.

The circle is completed by a Rostral Communicating Artery between the two rostral cerebral arteries, and two Caudal Communicating Arteries between the internal carotid and caudal cerebral artery (refer Fig. 2.5). There are several smaller arteries which leave the basilar artery to supply the lateral parts of the brain stem which contain the Vital Centers. Note that there is little anastomosis between these areas, so occlusion will lead to permanent damage.

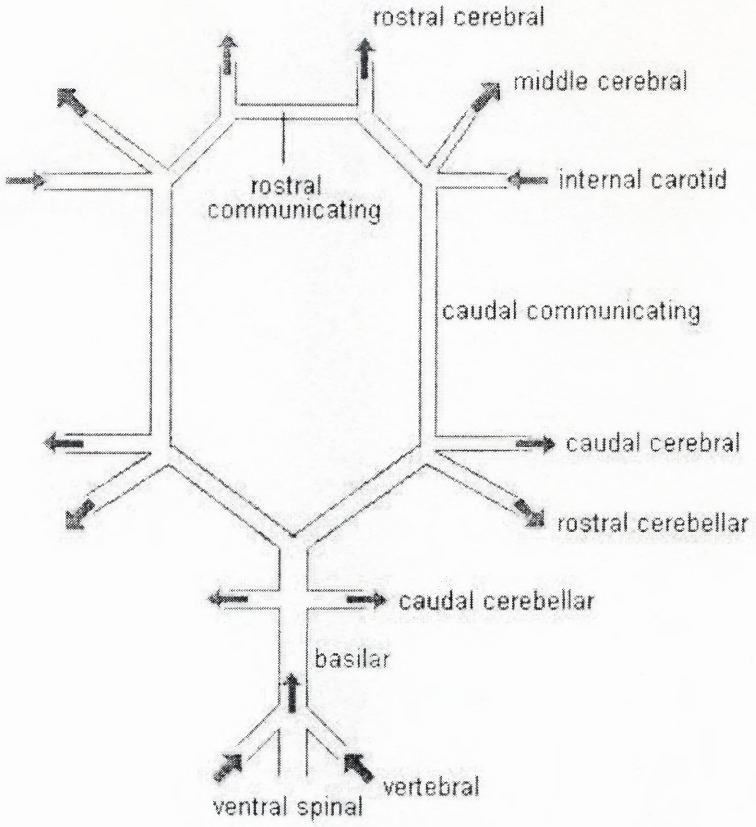

Fig 2.4 Blood flow in the Brain - Schematic Diagram

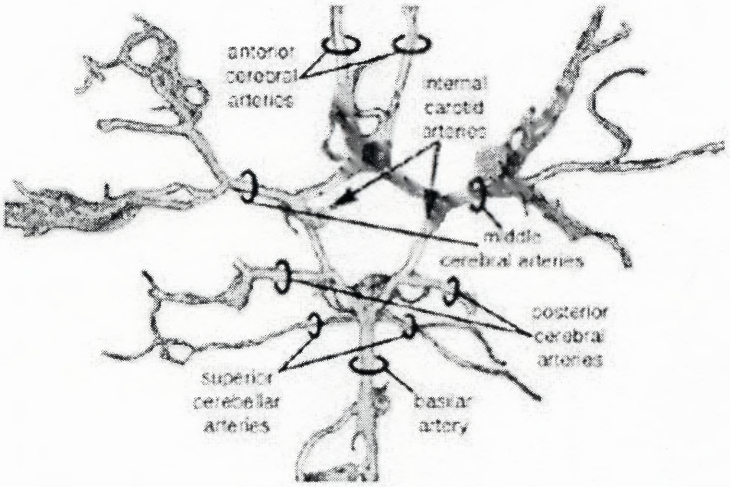

Fig 2.5 Blood flow in the Brain through various arteries

2.6 Doppler and Ultrasound Principles

Doppler ultrasonography makes use of two different principles.

a). The ultrasound principle is that when a high-frequency sound is produced and aimed at a target, it will be reflected by its target and the reflected sound can be detected back at its origin [2]. In addition, it is known that certain crystals (called piezoelectric crystals) produce an electrical pulse when vibrated by a returning sound [2].

b). The Doppler principle is simply that sound pitch increases as the source moves toward the listener and decreases as it moves away [60]. A classic example of this is the difference in sound of an arriving train and that of a one which is departing [59].

2.7 Doppler Ultrasonography

This principle, mentioned above, is applied in practice by mounting a piezoelectric crystal that emits and receives high frequency sound waves [3]. The transducer sends out ultrasound signals, at a particular frequency (10MHz Pulsed-wave probe in our case) which bounce off the Red Blood Cells present in the blood (refer Fig. 2.6). Therefore there is a shift between the frequency of sound waves that are emitted and those that are received (echo). This phase shift is processed and displayed.

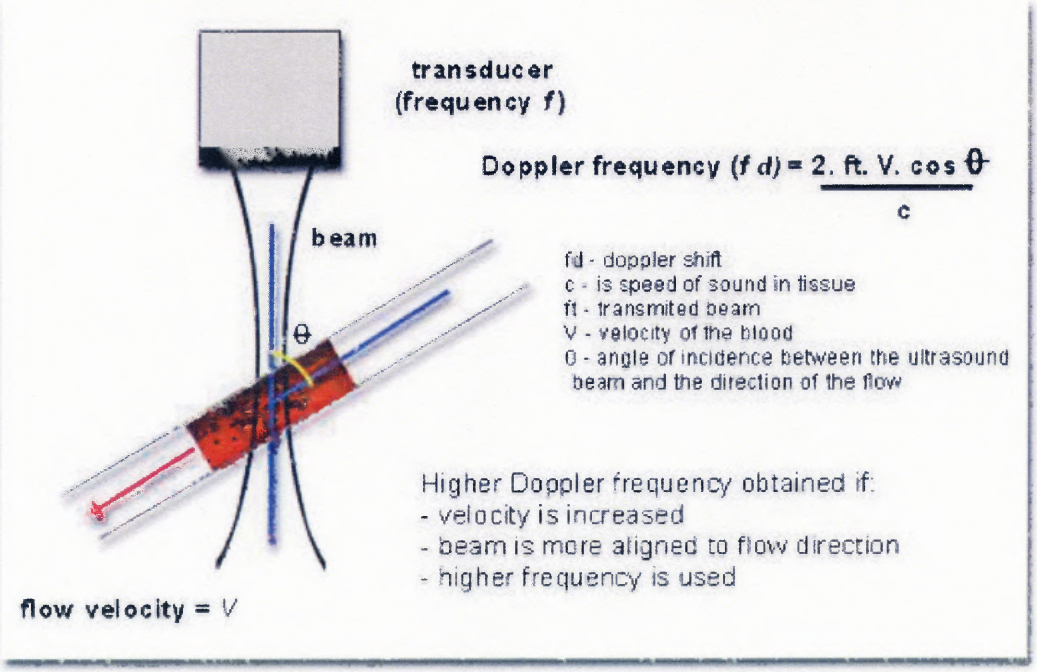

Fig 2.6 Doppler Technique
(Source: Doppler Ultrasound: "Principles and practice" by Colin Deane)

These echoes from scattering elements take some time to return to the receiver. The probe being a pulsed-wave probe, emits waves at regular time intervals and during the no-emission time interval receives the reflected waves [34], [35]. So from the time difference (which we can calculate from the change in the frequency of the reflected wave) the velocity of blood can be deduced

$$F_d = \frac{2 \times F_1 \times V \times \cos\theta}{c}$$

Therefore,

$$V = \frac{(F_1 - F_0) \times C}{2 \times F_0 \times \cos\theta}$$

V = velocity of blood flow

F_0 = returning frequency

F_1 = transmitting (transducer) frequency

F_d = doppler shift

C = constant: speed of sound in blood [61]

θ = angle of incidence.

There are two kinds of Doppler Ultrasonography, namely Pulsed-Wave Doppler and Continuous –Wave Doppler. The main different between the two types being that the continuous wave transducer has two elements, one for sending waves and another for receiving, while the pulsed wave transducer has just one element, which sends and receives signals [60].

2.8 Pulsed Wave Doppler Ultrasound Technique

This is a kind of Doppler ultrasound technique for measurement of blood-flow velocity using the pulse echo method. Short pulses of ultrasound are transmitted with a certain frequency, the pulse repetition frequency (PRF). Between pulse transmissions, echoes are continuously returning to the transducer (refer Fig. 2.7), but most of them are not analyzed. A receiver gate opens only once between each pulse transmission to allow estimation of the Doppler frequency shift from only one predetermined range along the ultrasound beam, the sample volume [62].

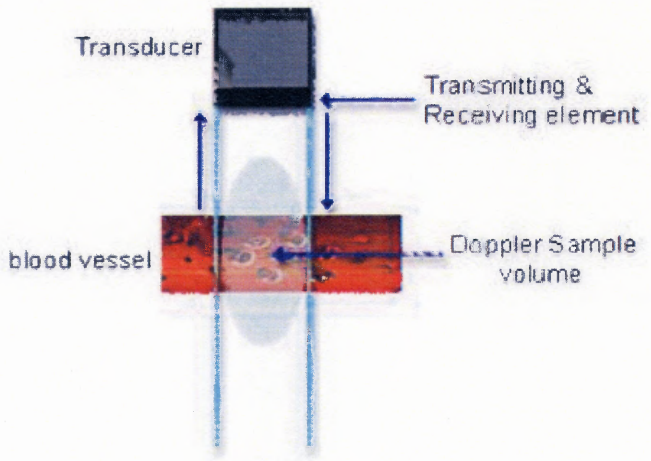

Fig 2.7 Pulsed Wave Transducer
(Source: Doppler Ultrasound: "Principles and practice" by Colin Deane)

The Doppler technique is based upon measurement of small changes in ultrasound frequency from transmission of the pulse to reception of the echo. It is therefore important that the transmitted pulse contains a uniform, narrow bandwidth frequency (i.e. small frequency range) [63].

2.9 Transducer

A **transducer** is a device that converts one type of energy to another, or responds to a physical parameter [4]. A transducer is in its fundamental form a passive component. It is actuated by energy from one system and supplies energy usually in another form to a second system [5]. In the Doppler technique, piezoelectric transducers are used [64]. The principle of the piezoelectric crystal is one of the most important ones in this thesis.

2.9.1 Piezoelectricity

In a piezoelectric crystal, the positive and negative electrical charges are separated, but symmetrically distributed, so that the crystal overall is electrically neutral. When a stress is applied, this symmetry is disturbed, and the charge asymmetry generates a voltage. A 1 cm cube of quartz with 500 lb (2 kN) of correctly applied pressure upon it, can produce 12,500 V of electricity.

Piezoelectric materials also show the opposite effect, called **converse piezoelectricity**, where application of an electrical field creates mechanical stress (distortion) in the crystal [66]. Because the charges inside the crystal are separated, the applied voltage affects different points within the crystal differently, resulting in the distortion [66].

The bending forces generated by converse piezoelectricity are extremely high, of the order of tens of millions of pounds (tens of meganewtons), and usually cannot be constrained. The only reason the force is usually not noticed is because it causes a displacement of the order of one billionth of an inch (a few nanometres) [6].

In other words, the use of ultrasound as a medical imaging modality became practical with the development of small piezoelectric crystal transducers. "Piezo" means pressure, so piezoelectric means that pressure is generated when electrical energy is applied to the crystal [65]. The quartz crystal in your watch is an example of this type of material. When electrical energy is applied to the face of the crystal, the shape of the crystal changes as a function of the polarity of the applied electrical energy (refer Fig. 2.8). As the crystal expands and contracts it produces compressions and rarefactions, and corresponding sound waves [8].

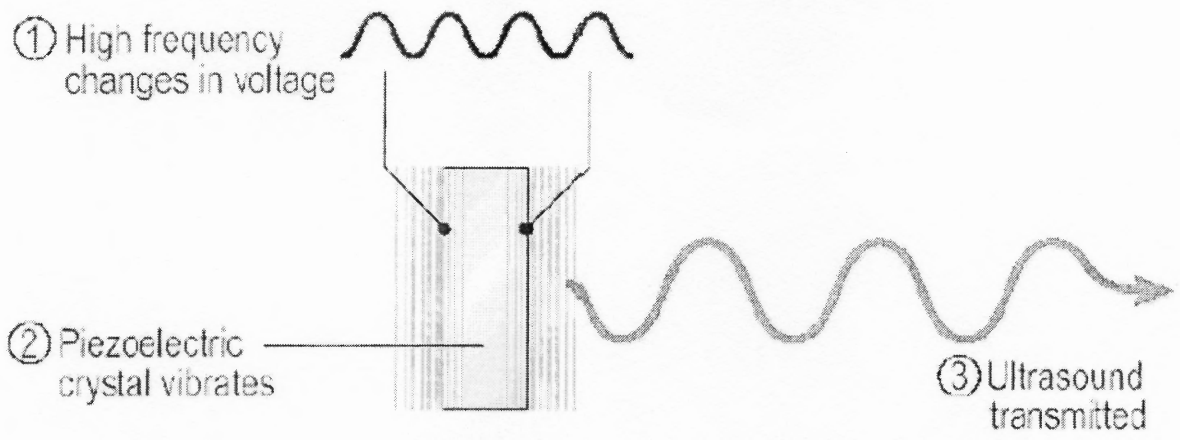

Fig 2.8 Working of Piezoelectric Crystal
(Source: Department of Biomedical Engineering, University of Texas at Austin)

2.9.2 Angle of Insonation

In Doppler ultrasound blood flow velocity measurement, the angle between the Doppler ultrasound beam and the direction of blood flow is a very important measurement. The Doppler instrument "sees" only the blood flow velocity component being directed straight towards the transducer, i.e. along the Doppler ultrasound beam [8]. This component is equal to (v cos θ), where "v" is the true blood flow velocity in the vessel, and "θ" is the Doppler angle. Owing to the cosine relationship between the relative and true blood flow velocity, the consequence of an error in measurement of the Doppler angle on the estimation of true blood flow velocity, increases with increasing Doppler angle [33]. At Doppler angles less than 45^{o}, a 5^{o} overestimation of the Doppler angle will give overestimations of the true blood flow velocity less than 10%. At Doppler angles larger than 70^{o}, the consequences of a small overestimation of the Doppler angle may become dramatic [38].

2.10 Fourier Transform and Signal Filtering

The Fourier Transform

The Fourier Transform is a mathematical method that converts an input signal from the Time Domain to the Frequency Domain. The time domain is displayed as a Waveform of voltage versus time, whereas the frequency domain is shown as a Spectrum of magnitude or power versus frequency. The Fourier Transform and its kin operate by analyzing an input waveform into a series of sinusoidal waves of various frequencies and amplitudes [46].

Somewhat closer to intuitive understanding but mathematically less general than the Laplace transformation is the Fourier transformation

$$f(t) = \frac{1}{2\pi}\int_{-\infty}^{\infty} \tilde{F}(\omega)\, e^{j\omega t}\, d\omega, \qquad \tilde{F}(\omega) = \int_{-\infty}^{\infty} f(t)\, e^{-j\omega t}\, dt$$

The signal is here assumed to have a finite energy so that the integrals converge. The condition that no signal is present at negative times can be dropped in this case. The Fourier transformation decomposes the signal into purely harmonic waves $e^{j\omega t}$ (the tilde over F is meant to remind you of this). The direct and inverse Fourier transformations are also known as a harmonic analysis and synthesis [47].

Fast Fourier Transformation

A **fast Fourier transform** (**FFT**) is an efficient algorithm to compute the discrete Fourier transform (DFT) and its inverse. FFTs are of great importance to a wide variety of applications, from digital signal processing to solving partial differential equations to algorithms for quickly multiplying large integers. This article describes the algorithms, of which there are many; see discrete Fourier transform for properties and applications of the transform [46].

Let x_0, ..., x_{n-1} be complex numbers. The DFT is defined by the formula

$$f_j = \sum_{k=0}^{n-1} x_k e^{-\frac{2\pi i}{n} jk} \qquad j = 0, \ldots, n-1.$$

Evaluating these sums directly would take $O(n^2)$ arithmetical operations (see Big O notation). An FFT is an algorithm to compute the same result in only $O(n \log n)$ operations. In general, such algorithms depend upon the factorization of n, but (contrary to popular misconception) there are $O(n \log n)$ FFTs for all n, even prime n. Since the inverse DFT is the same as the DFT, but with the opposite sign in the exponent and a $1/n$ factor, any FFT algorithm can easily be adapted for it as well [48].

Signal Filtering

In signal processing, the function of a filter is to remove unwanted parts of the signal, such as random noise, or to extract useful parts of the signal (refer Fig. 2.9), such as the components lying within a certain frequency range [50].

Filters are signal conditioners. Each functions by accepting an input signal, blocking pre-specified frequency components, and passing the original signal minus those components to the output [49].

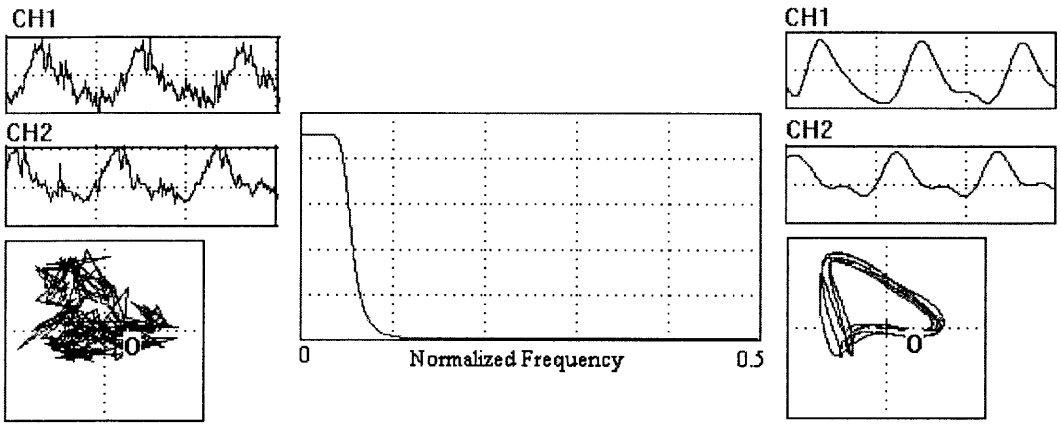

Fig 2.9 Filtering

There are two main kinds of filter, *analog* and *digital*. They are quite different in their physical makeup and in how they work [71].

An *analog filter* operates directly on the analog inputs and is built entirely with analog components, such as resistors, capacitors, and inductors [49]. Such filter circuits are widely used in such applications as noise reduction, video signal enhancement, graphic equalizers in hi-fi systems, and many other areas.

There are well-established standard techniques for designing an analog filter circuit for a given requirement. At all stages, the signal being filtered is an electrical voltage or current which is the direct analogue of the physical quantity (e.g. a sound or video signal or transducer output) involved [74].

A *digital filter* takes a digital input, gives a digital output, and consists of digital components. In a typical digital filtering application, software running on a digital signal processor (DSP) reads input samples from an A/D converter, performs the mathematical manipulations dictated by theory for the required filter type, and outputs the result via a D/A converter [49]. A digital filter uses a digital processor to perform numerical calculations on sampled values of the signal. The processor may be a general-purpose computer such as a PC, or a specialized DSP (Digital Signal Processor) chip.

Note that in a digital filter, the signal is represented by a sequence of numbers, rather than a voltage or current [50].

Lowpass filters

A third filter type is the low-pass. A low-pass filter passes low frequency signals, and rejects signals at frequencies above the filter's cutoff frequency. Low-pass filters are used whenever high frequency components must be removed from a signal [72]. If a low-pass filter is placed at the output of the amplifier, and if its cutoff frequency is high enough to allow the desired signal frequencies to pass, the overall noise level can be reduced [71].

Bandpass Filter

Bandpass filters are often used in front of detectors to eliminate or reduce noise due to light at wavelengths different from the wanted signal wavelength. Bandpass filters can be ordered with different bandwidths depending on the need [71]

CHAPTER 3

MATERIALS AND EXPERIMENTAL METHODS

3.1 Design and Materials

3.1.1 Transducer Design

The piezoelectric crystal is placed inside a casing flushed onto the surface on one side. The crystal is placed in way that the sound waves are not hindered by the casing to any extent. As the crystal goes into the head of the dog along with the casing, it is important that the casing material has to be biocompatible so that it does not affect any part of the body. Also, Optical clarity is an important quality in medical devices or diagnostic equipment that rely on visual inspection and therefore require a high level of transparency [13].Polycarbonate and delrin were chosen as the materials for the casing (for different transducers).

3.1.1.1 Materials for casing

Polycarbonate

Polycarbonate occupies a unique niche in the medical device market. Engineers have tapped its key characteristics of toughness, rigidity, and strength for critical device applications in which safety and performance are vital [76]. The ease of sterilizability of polycarbonate gives designers wide latitude in developing products that are not dependent on a single sterilization method [75].

These features are further complemented by polycarbonate's high clarity, a key benefit when visual assessment of patients and their prescribed therapies is indispensable [76].

Delrin

Delrin acetal resin, is formed from the polymerization of formaldehyde. The tightly interlocked helical molecules and high crystallinity result in excellent mechanical properties [77]. One of the important characteristics separating Delrin from other engineering plastics such as polyamides (nylons) is its very low water absorption and the small effect of aqueous solutions on its properties [78]. A couple of transducers were made with casing using delrin. These were for the preliminary tests and the *in vitro* calibration purposes. Delrin used here though is biocompatible [15], lacks the property of transparency, which is a very required aspect during surgery and implantation.

3.1.1.2 Experimental Designs for 10 MHz Transducer

Initially the experiment was done using a 10MHz probe. Two design proposals were made for the probe and bought from *Iowa Doppler Products, Iowa City, Iowa 52244 USA.*

(i) Polycarbonate Casing 10MHz Transducer Design – 1

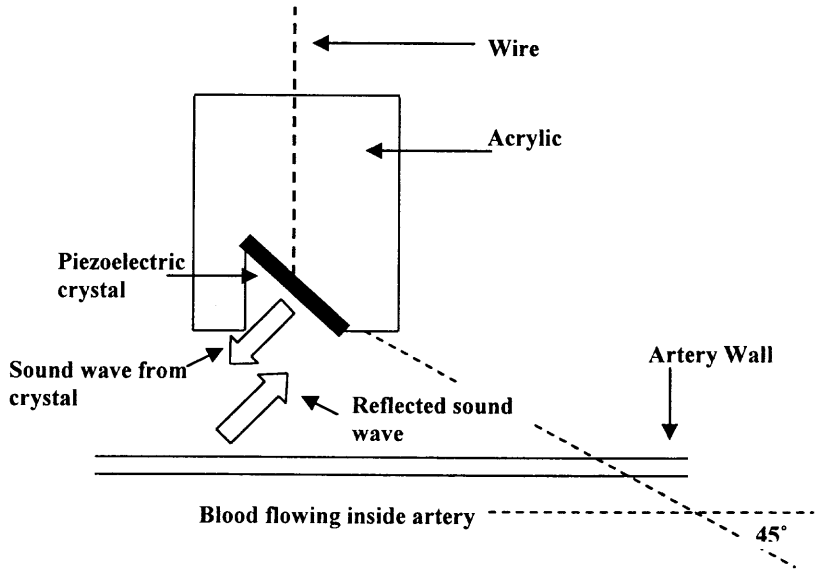

Fig 3.1 Polycarbonate Casing 10MHz Transducer Design – 1

A rectangular piece of piezoelectric crystal is embedded in a solid cylinder of polycarbonate at an angle of 45° (refer Fig. 3.1). The probe was made in such a way so that the crystal is maintained at 45° throughout the course of the surgery/experiment, as authentic results are obtained at that angle and as advised by very experienced researchers and producers [16]. The transducer was 3mm tall and 3mm in diameter and the crystal is buried such that one of the ends of the crystal is flushed to the bottom surface of the cylinder of polycarbonate.

During a chronic implantation, the transducer will need to be positioned so that it continuously gives information that will help in calculating the velocity. The geometry of the polycarbonate casing enables the probe to be buried in properly in the bone and the open end of the casing rests on the artery comfortably, because the casing is a cylindrical block it has a large surface area at the bottom. This provides stability even during spasmic movements of the artery.

(ii) Polycarbonate Casing 10MHz Transducer Design – 2

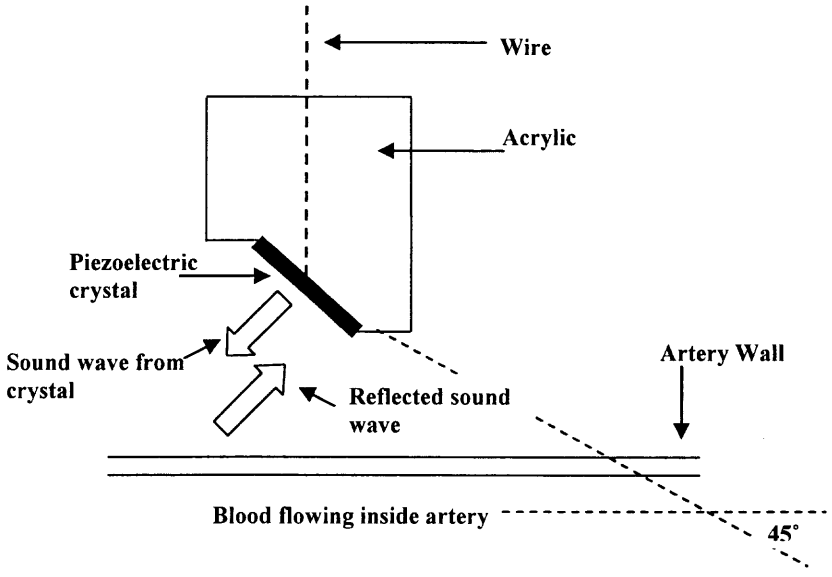

Fig 3.2 Polycarbonate Casing 10MHz Transducer Design – 2

Another transducer was made as shown above. The difference between the previous design and this one is that one side of the polycarbonate casing is grounded off (refer Fig. 3.2). This exposes the crystal more than in the previous one. Such a design change was carried out to deduce if the polycarbonate casing hinders the flow of sound waves, which will in turn affect the quality and reception of signals.

3.1.1.3 Experimental Design for 20 MHz Transducer

Two 20MHz transducers were designed and made to order from *Iowa Doppler Products, Iowa City, Iowa 52244 USA* one without any casing and another with a different shape of casing.

(i) Delrin Casing 20MHz Transducer Design – 1

A casing for the naked transducer was made using Delrin. This casing was a cylindrical block 6mm tall and of diameter 6mm. The naked probe of diameter 0.8mm was slid into a narrow hole drilled through the delrin block and sealed at the top surface of the block using silicon gel, with just the wire coming out. The design was similar to the first design of the 10MHz transducer, the only differences being the use of Delrin instead of polycarbonate and the size. This transducer was made larger in purpose to increase stability and ease of use during surgery.

(ii) Polycarbonate Casing 20MHz Transducer Design – 2

A final design of the 20MHz transducer (refer Fig. 3.3) was worked on and made to order from Iowa Doppler Products.

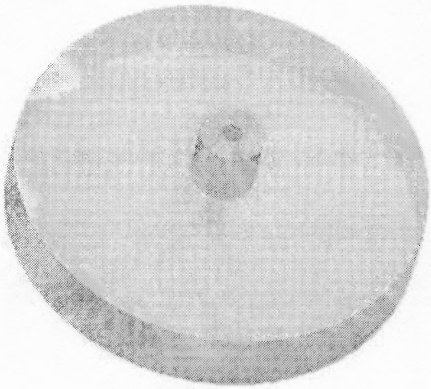

Fig 3.3 Polycarbonate Casing 20MHz Transducer Design – 2

The casing was made of Polycarbonate for the reason that it is transparent. The dimensions are as below.

Table 3.1 Dimensions - Polycarbonate Casing 10MHz Transducer Design – 2

S. No	Part	Diameter	Height
1	Lower cylinder	19.05mm	3.125mm
2	Upper cylinder	3mm	3mm

The upper cylinder was designed for convenience in holding the transducer while positioning it and moving it around.

3.1.2 System for *In vitro* Testing and Calibration

A system for testing the transducer and other equipments and for calibration was designed and machined.

3.1.2.1 Acrylic Chamber

A block of Acrylic was cut out and a channel was drilled through the length of the block. A 15 gauge stub needle will be used to induce flow through this channel, which will induced by a peristaltic pump (refer Fig.3.4).

The diameter of this though hole was a little larger than the outer diameter of the needle. The stud needles, otherwise called nipples, were glued into the two sides of this through hole by using epoxy. Another hole was drilled on the top surface of the acrylic block, the depth of which was a little lower than the distance between the top surface and the channel. This will be the niche in which the transducer will sit.

As an extension of this hole, a counter bore was drilled up to a depth that it opens up to the channel. This hole will make sure that the transducer does not fall into the channel and block the stream of flow and at the same time, give enough space through which it can send in sound waves and receive the reflected sound waves.

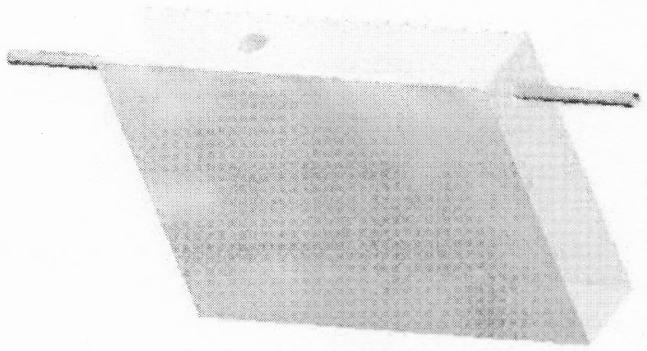

Fig 3.4 Acrylic Chamber which can accommodate Polycarbonate Casing 10MHz Transducer Design 1 and 2

Table 3.2 Dimensions Acrylic Chamber

S. No.	Dimension	Measure (inches)
1	Length of Acrylic Block	2
2	Height of Acrylic Block	1.5
3	Thickness of Acrylic Block	0.4
5	Diameter of channel	0.079
6	Diameter of Hole-1 on top surface	0.14
7	Diameter of counter bore hole	0.125
8	Position of Hole-1 on top surface	0.7

Another similar block was designed to test the new design of the transducer (refer Fig. 3.5). This one had the same concept involved with a few improvements as given below.

- Introduction of a silicon sheet to avoid leakage of fluid and to nail down the transducer in place (refer Fig. 3.6 and 3.7).
- Addition of an extra layer of Acrylic, to make sure that enough pressure is applied on the transducer that it does not pop out due to fluid pressure (refer Fig. 3.6 and 3.7).

Fig 3.5 Acrylic Chamber which can accommodate Polycarbonate Casing 20MHz Transducer Design – 2

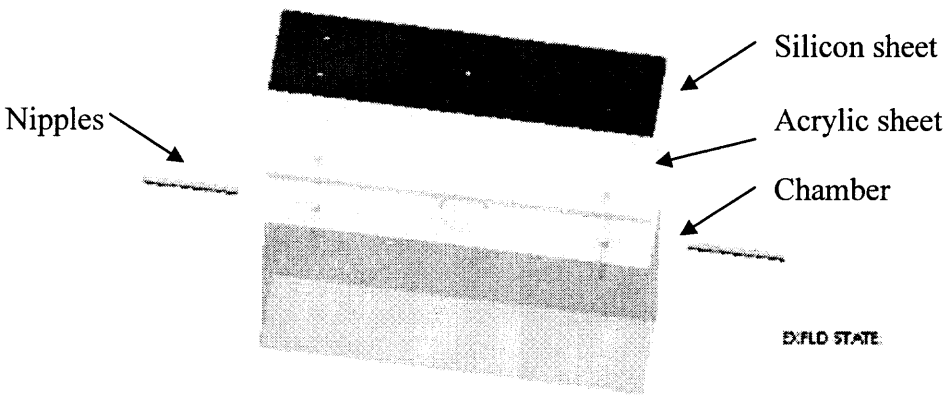

Fig 3.6 Exploded View of Setup for *In vitro* testing of Polycarbonate Casing 20MHz Transducer Design – 2

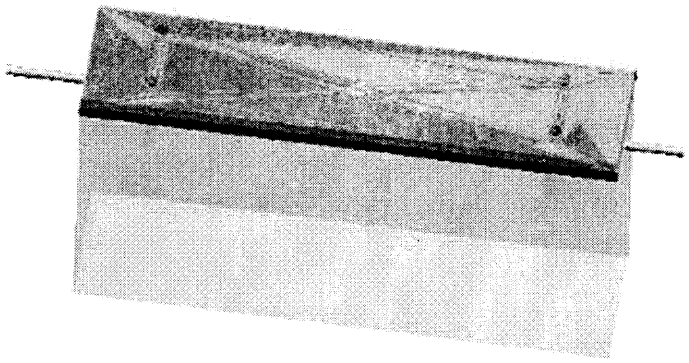

Fig 3.7 Setup for *In vitro* testing of Polycarbonate Casing 20MHz Transducer Design – 2

Table 3.3 Dimensions Acrylic Chamber - 2

S. No.	Dimension	Measure (inches)
1	Length of Acrylic Block	4
2	Height of Acrylic Block	2
3	Thickness of Acrylic Block	1
5	Diameter of channel	0.079
6	Diameter of Hole-1 on top surface	0.5
7	Depth of screw holes	0.5
8	Diameter of screw holes	0.1
9	Position of Hole-1 on top surface	2

3.1.2.2 Hollow Glass Particles

A solution, similar to blood with respect to density and concentration of particles was made using water and hollow glass spheres. The comparison of properties of blood and this solution is tabulated below.

Table 3.4 Comparison – Blood vs. Suspension with Hollow Glass Spheres

S.No	Property/Component	Blood	Solution
1	Composition	Plasma, RBCs, WBCs, Platelets	Water and hollow glass spheres
2	Maximum composition	Red Blood Cells	
3	Component that reflects sound waves	Red Blood Cells	Hollow Glass Spheres
4	Density	1.06 gm/ml	1.05-1.15 gm/ml
5	Concentration of reflection components	2.5 to 5million per micro liter	2.65million per micro liter

6	Diameter of reflection components	5-10 micro meters	8-12 micro meters
7	Hematocrit	42% – 54%	45%

These particles were purchased from *TSI Corporation.* The schematic representation of the *in vitro* setup is shown below.

3.1.3 Gels

As the speed of sound in air is very less compared to that in water, gel or other body tissues and fluids, acoustic gels are used to transmit the sound waves from the transducer to the body part or fluid.

Aquagel

Fig 3.8 Aquasonic Transmission Gel
(Copyright: Parker Laboratories)

Aquasonic 100 Ultrasound Transmission Gel (Parker Laboratories, Inc.) was used for this purpose. The gels are warmed using Thermosonic Gel Warmer (Parker Laboratories, Inc.) before they are used [44].

Agarose Gel

For the same purpose, agarose gels can also be used. The advantage of using agarose gel is that it can withstand body conditions for a longer time span hence proving more use with regard to chronic implantation.

The effect of the gel varies with concentration. Seakem LE Agarose gel from *Cambrex,* was one of the many agarose gels available. Its properties are listen below.

Table 3.5 Seakem LE Agarose Properties
(Copyright: Cambrex)

S. No	Property	Measure
1	Strength	Very high
2	Gelling temperature	36°C ±1.5°C
3	Melting temperature	>90°C
4	Gel strength (1%)	>1,200 g/cm^2

Seakem LE Agarose with a high gelling temperature was preferred as enough time is available to work on before it gels and more importantly will not have drastic temperature drop or rise effects on the brain surface, when in contact.

3.1.4 Adhesives

Bone Cements

These chemicals will be used to glue to transducer (the polycarbonate casing) to the skull once the chronic implantation is done and are generally used during prosthetics [41]. *Generation 4™ Bone Cement and VacPac™ Mixing and Delivery System* from *Biomet* was used for this purpose (refer Fig. 3.9).

Fig 3.9 Generation 4™ Bone Cement and VacPac™ Mixing and Delivery System
(Copyright: Biomet)

Dental Acrylic

Dental acrylic would also serve the purpose of gluing plastics with the skull [43]. For this purpose, *Nexus® 2™ and Nexus® 2™ Dual Syringe* from *Kerr Dentistry* was used (refer Fig. 3.10).

Fig 3.10 Nexus® 2™ and Nexus® 2™ Dual Syringe
(Copyright: Kerr Dentistry)

3.1.5 Gigli Wire Saw

A wire saw to remove a piece of skull bone of regular geometry was purchased from *Surgical Tools,* manufactured by *Miltex.* This is a type of wire saw used generally by neurosurgeons to perform cranial (referring to the cranium or skull) surgeries [30] (refer Fig. 3.10).

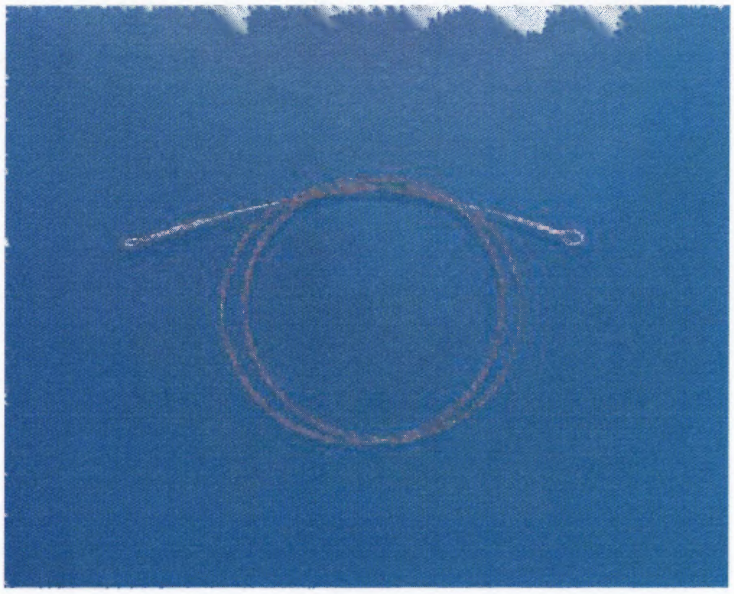

Fig 3.11 Gigli Wire Saw
(Copyright: Surgical Tools)

More details are tabulated below.

Table 3.6 Gigli Wire Saw Details
(Copyright: Surgical Tools)

S. No.	Dimension	Measure
1	Length	508mm
2	Diameter of sawing part of wire	1mm
3	Diameter of end loop	6mm
4	Material	Stainless Steel
5	Type	Standard Twisted

3.1.6 Carbide Burrs and Dremel

Carbide burrs (refer Fig. 3.11) of the following dimensions were used during the surgery to open the skull.

Head dia 1/4"; shaft dia 1/8"
Head dia 1/2"; shaft dia 1/4"
Head dia 3/4"; shaft dia 1/4"

The burrs were used with a dremel (refer Fig. 3.12) which can accommodate shaft diameters of up to 1/8".

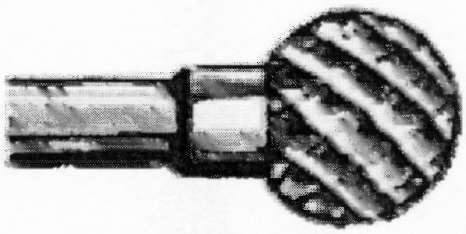

Fig 3.12 Carbide Burr
(Copyright: McMaster-Carr)

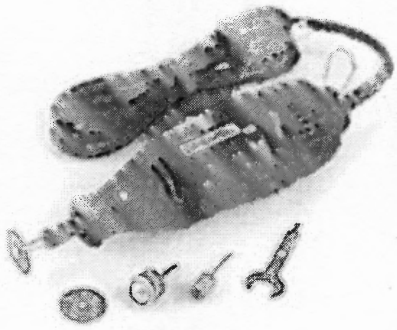

Fig 3.13 Dremel – Rotary Tool
(Copyright: Dremel Ltd.)

3.2 *In Vitro* Experimental Methods

3.2.1 *In vitro* Calibration and Testing with 10MHz Transducer using Aquagel

A system to test and calibrate the transducer *in vitro* was designed and machined (refer 'System for *in vitro* testing and calibration' in Materials). The transducer was tight fitted into the hole drilled for the purpose, by using a rubber grommet which is available in syringes. A peristaltic pump (*Dynamax RP-1* by *Rainin*) was used to induce a continuous flow through the channel. The solution was prepared using water and hollow glass spheres. The transducer was connected to the *BCM Multichannel Doppler Ultrasound Measuring System,* which was connected to a filter and the filter in turn to an oscilloscope (refer Fig. 3.14).

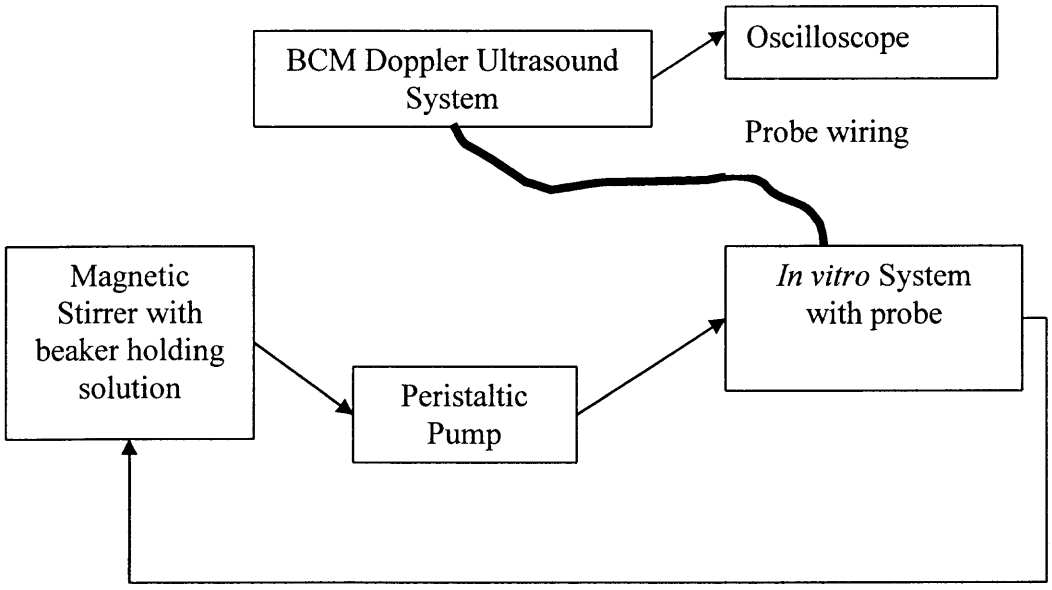

Fig 3.14 Experimental Setup for *In vitro* Calibration and Testing

Settings

Probe	:	10MHz piezoelectric crystal embedded at 45° in Polycarbonate
Peristaltic Pump	:	Dynamax RP-1 by Rainin
Tubing	:	PVC 1.52mm ID (Max. Flow = 9.5ml/min)
Filtering	:	300Hz – Low Pass
Gel	:	Aquagel
Particles Used	:	Hollow Glass Spheres
Particle Size	:	8-12 microns
Density	:	1.05 – 1.15 g/ml
Mixture	:	Water – 1.0ml; Particle – 0.5g

As a comparison criterion, the velocity of the fluid flow was calculated using the traditional beaker method. A calibrated beaker is filled with water at different RPMs of the peristaltic pump and the corresponding time is noted. With the volume flow rate and the cross-sectional area, the velocity of fluid flow is calculated.

3.2.2 *In vitro* Calibration and Testing with 20MHz Transducer using Aquagel

A similar experiment was performed using the 20 MHz transducer. The transducer was connected to the *Doppler Ultrasound system from Triton.* The unit from Triton comes with an inbuilt filter, which is a 25Hz low pass filter.

Settings

Probe	:	20MHz piezoelectric crystal embedded 45° in Delrin
Peristaltic Pump	:	Dynamax RP-1 by Rainin
Tubing	:	PVC 1.52mm ID (Max. Flow = 9.5ml/min)
Filtering	:	25Hz – Low Pass
Gel	:	Aquagel
Particles Used	:	Hollow Glass Spheres
Particle Size	:	8-12 microns
Density	:	1.05 – 1.15 g/ml
Mixture	:	Water – 1ml; Particle – 0.5g

3.2.3 *In vitro* Calibration and Testing with 20MHz Transducer using different concentration of Agarose Gel -1

Seakem Gold Agarose gels of different concentrations were prepared to be tested on the *in vitro* system.

Agarose preparation

Initially a stock solution of 2% Seakem Agarose was prepared, from which the other concentrations were diluted. 2.041gms of Seakem agarose powder was mixed with 100gms of water and simultaneously heated to over 90°C in an autoclaved 300ml beaker. The mixing and heating was done using a heated magnetic stirrer setup. The mixing was done carefully making sure no chunks were formed and the resulting agarose gel solution is a purely homogenous one (refer Fig. 3.15).

Density of Water (kg/m^3)	1000

1 cubic meter = 1,000,000 milliliter

Density of Water (g/ml)	1

SeaKem Stock Solution 2%

Percentage	0.02

Total Vol(ml)	H2O Mass(g)	Agarose Mass (g)
100	100	2.041

Further % From Stock

Total Volume (ml)	Amount of Stock (ml)	Amount of Distilled H2O (ml)	%	Factor
10	10	0	0.02	1
10	7.5	2.5	0.015	0.75
10	5	5	0.01	0.5
10	2.5	7.5	0.005	0.25

TOTAL STOCK FOR EXP (ml)	25

Fig 3.15 Recipe for Agarose preparation

The *in vitro* experiment was carried out as before thrice to compare results when agarose concentrations of 0.5%, 1% and 1.5% were used.

3.2.4 *In vitro* Calibration and Testing with 20MHz Transducer using different concentration of Agarose Gel - 2

Seakem agarose gels of concentrations 0.6%, 0.7%, 0.8%, 0.9% and 1.0% were prepared as before and the experiment was carried out 5 times to make a comprehensive comparison.

3.2.5 *In vitro* Calibration and Testing with 20MHz Transducer for different Particle Concentrations

The final step was to simulate the flow of blood at various conditions. In a healthy body, each micro liter of blood would contain between 2.5 million to 5 million red blood cells. If the body is anemic, the worst case would be that one milli liter of blood will contain 2 million red blood cells. This is a huge difference and so is important to make sure that the device and hence the technique works well, even when it is used on blood which is short of red blood cells (anemic) [45].

For this purpose, the experiment was carried out using different particle concentrations. The range was from 1.6 million particles per ml to 2.65 billion particles per ml. When the particle number went below 1.6 million per ml, the signal strength decreased.

The concentrations were as tabulated.

Table 3.7 Concentrations and Particle numbers

S. No	Mass of particles per ml of water (mg)	No. of particles per ml of water
1	0.2	1.6 million
2	1	5.3 million
3	3	16 million
4	10	53 million
5	30	160 million
6	100	530 million
7	500	2.65 billion

3.2.6 Bone – Plastic glue test

These were the experiments conducted to analyze the bonding strength of dental luting cements and cone cements when they are used to glue bone and plastics, as that will be the case during a chronic implantation.

Dental Luting Cement

A piece of pig skull bone was taken as the type of bone in the top surface of the skull is the similar to that of a dog. The plastic used was polycarbonate. *Nexus® 2™ and Nexus® 2™ Dual Syringe* from *Kerr Dentistry* was used to prepare the glue. Different components of the Nexus package were mixed at required amounts and concentrations.

A small depression like hole was drilled on the bone and the plastic was placed inside it, jutting out at the top. The glue was smeared onto the layer of the bone in a fashion that the plastic was buried with some amount of its height sticking out. The glue was light cured for a time span of 5minutes and then tested for rigidity.

Bone Cements

The same piece of bone as used above was used. Polycarbonate was the plastic used in this case too. *Generation 4™ Bone Cement and VacPac™ Mixing and Delivery System* from *Biomet* was the bone cement to be tested.

The contents of the pack were mixed as per instructions and kneaded meticulously to make a homogenous mixture. A similar arrangement as in the previous experiment was made to seat the plastic in the bone and the bone cement was smeared over the bone and plastic. Light curing was not necessary. The glue was air dried for 15minutes.

3.3 *In Vivo* Experimental Methods

3.3.1 Wrist Method with 10MHz Transducer

As a traditional testing method, the transducer was tested on the human wrist. The transducer was connected to the *BCM Multichannel Doppler Ultrasound Measuring System* which was in turn connected to an oscilloscope to view the peaks. The transducer was placed vertically on the human wrist, such that the bottom surface of the polycarbonate casing was sitting flat on the layer of the skin. This maintains the angle of insonation at 45°, as the crystal is embedded at 45° to the horizontal. The experiment was performed using both the designs of transducers mentioned earlier (refer Transducer Design).

As an inference from both the experiments, it was clear that there was very little difference in the signal quality in both cases and the values obtained different negligibly. The reason for the fluctuation in values is because of the inaccuracy in positioning, as this is a very preliminary test. One major difference between the two designs, was the ease of positioning as expected. Design – 1 with a larger surface area at the bottom surface was much easier handle, while working with design – 2 a little too complicated. One had to make sure that the bottom surface (with extremely small surface area) was placed flat on the skin. Considering the fact that this experiment was done outside the body, using such a design *in vivo* during a chronic implant will in no way be user friendly for the surgeon. Hence, it can be said that design – 2 is not the best design to be used.

3.3.2 Experiment on MCA of Dog with 10MHz Transducer

The transducer selection was done based on the size and transparency. Design -1 Polycarbonate Casing 10MHz Transducer was chosen for the reason that it offers higher surface area which aids in ease of positioning and stability.

Mongrel dogs of approximately 15Kgs were anesthetized. The part of the skull above the middle cerebral artery area was removed by experiences surgeons at the University of Medicine and Dentistry of New Jersey, Newark. A small glob of aquagel was placed on the transducer. The transducer was connected to the *BCM Multichannel Doppler Ultrasound Measuring System* which was in turn connected to an oscilloscope to view the peaks. The transducer was placed on the layer of the brain and slid gently to reach the point where best signal was received.

3.3.3 Experiment on Femoral Artery, Left Gastric Artery and Mesenteric Artery of Mouse using 20MHz Transducer

5 month old FVB male mice were weighed and anesthetized using a mixture of Ketamine 65mg/Kg, Acepromazine 2mg/Kg and Xylamine 13mg/Kg using a dilution ratio of 1 : 10. The dosage of anesthesia was 0.085ml/10g of Body weight.

3.3.3.1 Femoral Artery

As decided earlier, a 20MHz transducer was to be used and the design – 1 was used owing to its smaller size in comparison to the other one, because the experiment was on a small animal (refer Fig. 3.16).

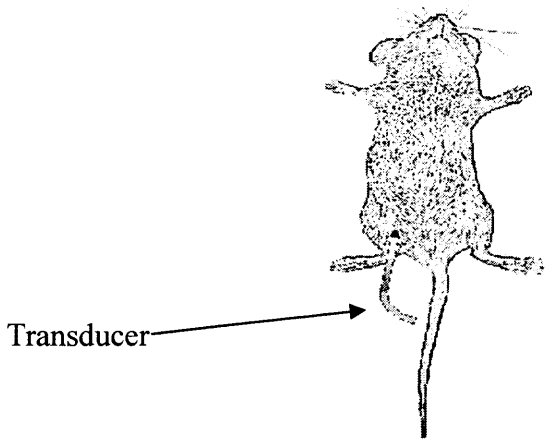

Fig 3.16 Position of Transducer – Femoral Artery Experiment
(Copyright: Indus Instruments)

The transducer was placed on the femoral artery (diameter ~ 400 micro meters) of the right leg and in turn connected to the Triton system. Aquagel was used due to easy warming and storage facilities. The transducer was ranged at 3mm to sample the flow with the trigger in a full turn CW position. The output of the system was connected to a computer and the results were recorded using Notocord and analyzed in excel.

3.3.3.2 Left Gastric Artery

The transducer was now placed on the left gastric artery and the similar procedure was followed.

3.3.3.3 Mesenteric Artery

Next, the transducer was placed on the mesenteric artery (the aim here being to go on to smaller arteries on each step). The diameter of the vessel is approximately 300 micro meters. A similar procedure was followed as before.

A second experiment was performed on the same artery with the use of Agarose gel in place of aquagel.

3.3.4 Experiment on MCA of Dog using 20MHz transducer

The transducer selection was done based on the size and transparency. Design -2 Polycarbonate Casing 20MHz Transducer was chosen for the reason that it offers higher surface area which enables the transducer to sit on the area of interest without any external force, the larger size of the transducer and in turn the weight plays an important role in tolerating the random flow blood during the surgery i.e. the weight keeps the transducer from sliding/floating off along with the blood and the transparency helps immensely in identifying the spot of velocity measurement.

Mongrel dogs of approximately 15Kgs were anesthetized. The part of the skull above the middle cerebral artery area was removed using a *Cranial Hand Drill* purchased from *Medtronic* (drill bit – ¼") by experienced surgeons at the University of Medicine and Dentistry of New Jersey, Newark. A small glob of aquagel was placed on the transducer. The transducer was placed on the layer of the brain and slid gently to reach the point where best signal was received.

The results were in the form of sound. The sound was recorded in a tape, and the data was imported into Notocord by replaying it. Time ranges where best quality signal was received were grabbed and exported to Excel for further analysis.

3.3.5 Experiment on MCA of Pig using 20MHz Transducer

A similar surgery was performed on the middle cerebral artery of a sacrifice pig. The part of the skull above the middle cerebral artery area was removed using a *Cranial Hand Drill* initially and then Carbide Burrs (fit with a Dremel) were used to open enough of the skull to perform the experiment. A small glob of aquagel was placed on the transducer. The transducer was placed on the layer of the brain and slid gently to reach the point

where best signal was received as before. Once the best signal was obtained the transducer was left undisturbed for a few minutes to monitor its stability. It was found that good quality signals were obtained consistently. Then a required amount of Biomet Bone Cement mixture was smeared on the transducer, gluing it to the side surface of the drilled skull bone. A few minutes were provided for the cement to solidify and then the skin was sutured to put the muscle back in place supporting the transducer below.

The sound signals were recorded in a tape and replayed hence transferring the same into Notocord. Then data analysis was performed.

3.3.6 Experiment on MCA of Dog using 20MHz Transducer – Drug Response

As a final step, the experiment was performed on another Mongrel dog to monitor the effect of drugs (Isoproterenol and Forskolin). After the initial anesthetization, the normal experiment was done to determine the baseline values. Then the pCO2 concentration was varied gradually to see the effect of increase in pCO2. Once the values were recorded, the pCO2 was brought back to the concentration at baseline and Isoproterenol was introduced. The concentration of the drug was gradually increased from 0.05 micro gram per kilogram per minute to 0.1 micro gram per kilogram per minute and then finally to 0.4 micro gram per kilogram per minute. Signals were recorded and a good amount of time was given for the respiration to get back to baseline value. Then Forskolin was injected into the dog. Initially a concentration of 25 nanogram per kilogram per minute was injected which was gradually increased to 50 nanogram per kilogram per minute. The results which were obtained are plotted in the results section.

CHAPTER 4

RESULTS AND DISCUSSION

4.1 Design Conclusions - Geometry

Design 1 and 2 of 10MHz Transducer

Table 4.1 Comparative study – 10MHz Transducer Design 1 and 2

S.No	Polycarbonate Casing 10MHz Transducer Design – 1	Polycarbonate Casing 10MHz Transducer Design – 2
1	Polycarbonate casing might hinder flow out and reception of sound waves i.e. few signals can be lost	Polycarbonate casing grounded off appropriately to make sure waves are not bothered
2	Large surface area at bottom	Very little surface area (not even enough to sit the probe on its own)
3	More comfortable with regard to positioning during surgery as this design offers a large surface area at the bottom	Delicate positioning is necessary. If not carefully positioned, might result in losing signals indefinitely
4	Properly insulated from outside noise	Chances of picking up waves from else where due to open geometry at one side.

From various experiments, it was clear that Design 1 did not lose any signals due to its geometry. So gauging the positives and negatives of both transducers, Design 2 was chosen.

Design 1 and 2 of 10MHz transducer

The second design with the 20MHz transducer was chosen for the following reasons.

- Larger surface area helps immensely in stability while positioning
- Larger surface area aids in restricting motion during chronic implantation
- As the transducer occupies a lot of space, the remaining void can be filled in easily when the hole made on the skull has to be blocked eventually (for chronic implantation)

4.2 *In vitro* Calibration and Testing with 10MHz Transducer using Aquagel

The results using the Doppler technique are obtained in terms of Voltage. This is converted to KHz of Doppler shift using the calibration criterion specified which when substituted in the formula

$$F_d = \frac{2 \times F_1 \times V \times \cos\theta}{c}$$

The results obtained are tabulated below.

Table 4.2 Results - Flow Velocity Measurements – 10MHz Transducer

S. No	RPM at pump	Voltage at Oscilloscope (mV)	Frequency Shift (KHz)	Velocity using Doppler Technique (mm/sec)	Velocity using Beaker Method (mm/sec)
1	24	105	0.42	45.7	46.7
2	30	135	0.54	58.8	60.9
3	36	160	0.64	69.7	72.7
4	42	190	0.76	82.7	84.5
5	48	220	0.88	95.8	100.7

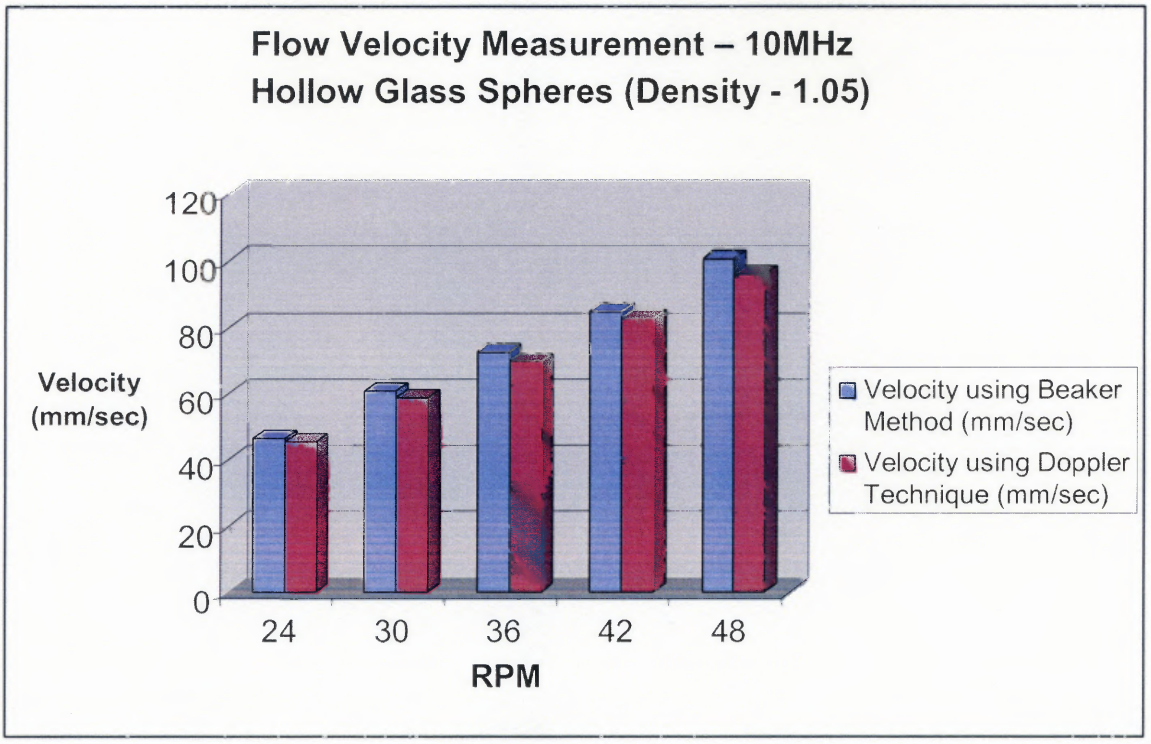

Fig 4.1 Results - Flow Velocity Measurements – 10MHz Transducer

As can be observed, there is a slight variation and the error is ±4.8% (refer Table 4.2 and Fig. 4.1). The deviation would be a result of non uniform cross-section through which the fluid is flowing. The non-uniform cross-section is due to the many different tubes used to complete the circuit.

4.3 *In vitro* Calibration and Testing with 20MHz Transducer using Aquagel

The results obtained are tabulated below.

Table 4.3 Flow Velocity Measurements – 20MHz Transducer

S. No	RPM at pump	Voltage at Oscilloscope (mV)	Frequency Shift (KHz)	Velocity using Doppler Technique (mm/sec)	Velocity using Beaker Method (mm/sec)
1	24	180	0.76	41.4	46.7
2	30	260	1.04	56.6	60.9
3	36	320	1.28	69.7	72.7
4	42	380	1.52	82.7	84.5
5	48	440	1.76	95.8	100.7

As in the previous case, slight variations can be observed, giving rise to an error of ±6.1% (refer Table 4.3 and Fig 4.2). The reason for the deviation is the same as above.

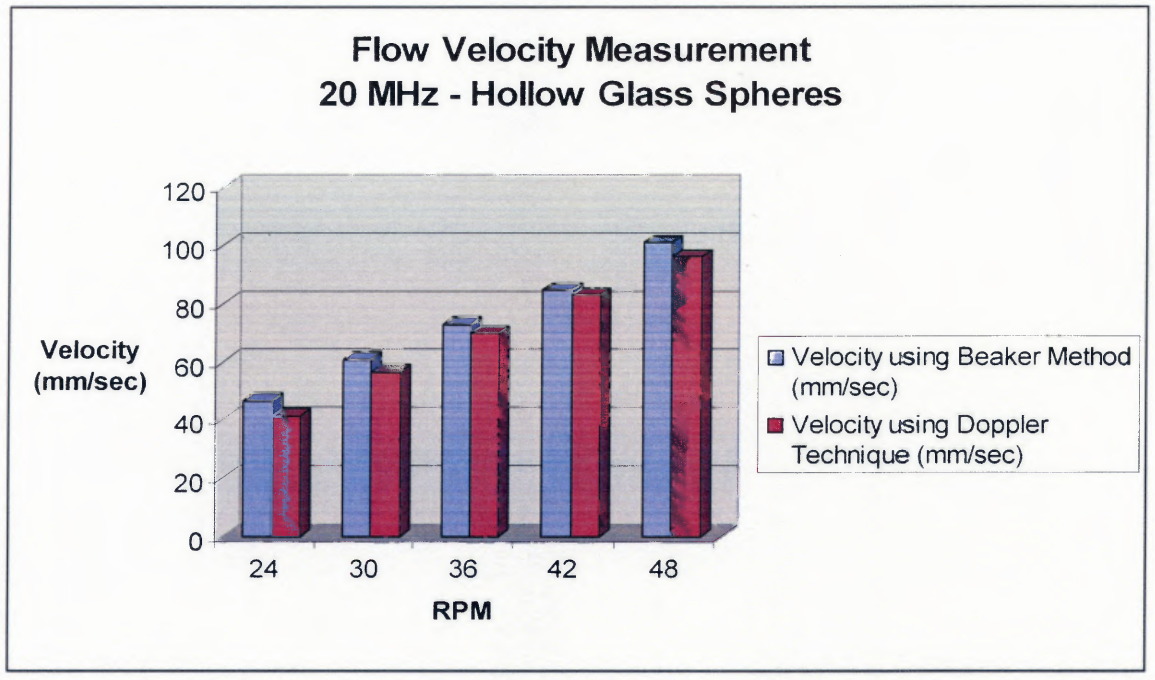

Fig 4.2 Results - Flow Velocity Measurements – 10MHz Transducer

Though the results obtained using both the 10MHz and the 20MHz transducers are the same in this case, it cannot be concluded that they will produce the same results on the animal. It should be noted that this is an *in vitro* system where in the flow and the particles used are spotted by both the transducers.

4.4 *In vitro* Calibration and Testing with 20MHz Transducer using different concentration of Agarose Gel – 1

The *in vitro* experiment was carried out as before thrice to compare results when agarose concentrations of 0.5%, 1% and 1.5% were used. Results are tabulated below.

Table 4.4 Results - Flow Velocity Measurements – Agarose Gel Concentrations 1

RPM	Velocity using Doppler Technique				Velocity using Beaker Method (mm/sec)
	Aquagel	0.5% Agarose	1.0% Agarose	1.5% Agarose	
24	45.7	41.4	43.5	52.3	46.7
30	58.8	52.3	56.6	74	60.9
36	69.7	69.7	74	98	72.7
42	82.7	88.4	82.7	108.9	84.5
48	95.8	87.1	95.8	130.7	100.7

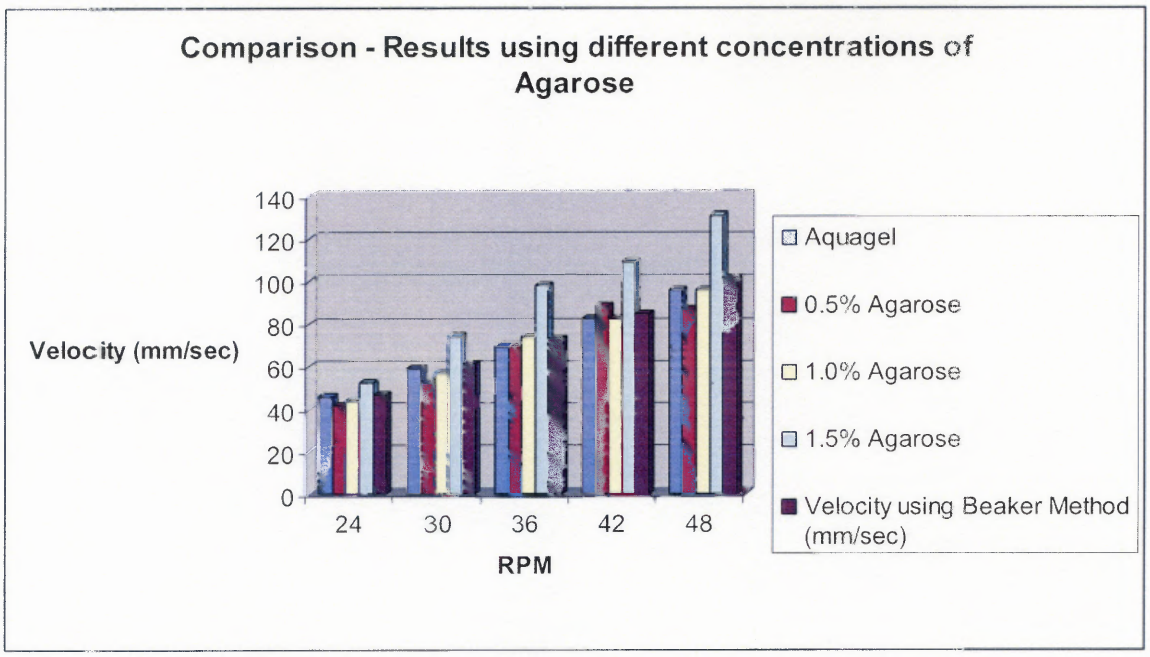

Fig 4.3 Results - Flow Velocity Measurements – Agarose Gel Concentrations 1

It is clearly seen that the results diverge when the concentration of agarose reaches 1.5% (refer Table 4.3 and Fig. 4.3). The reason for this could be because as the agarose gel starts getting hard to an extent, the sound waves seem to bounce off the agarose gel particles themselves, resulting in such high values. So a 2% concentration of agarose was not tried.

One more inference is that very good results were obtained for 0.5% and 1% agarose concentrations. Hence another experiment performing a comparison between closer ranges of different concentrations was carried out to calculate the best possible concentration of agarose.

4.5 *In vitro* Calibration and Testing with 20MHz Transducer using different concentration of Agarose Gel – 2

The results obtained are tabulated below.

Table 4.5 Results - Flow Velocity Measurements – Agarose Gel Concentrations 2

RPM	Velocity using Doppler Technique (mm/sec) with						Velocity using Beaker Method (mm/sec)
	Aquagel	0.6% Agarose	0.7% Agarose	0.8% Agarose	0.9% Agarose	1% Agarose	
24	39.2	41.4	42.5	42.5	43.5	44.6	46.7
30	54.3	52.3	54.3	50.1	55.5	56.6	60.9
36	69.7	69.7	70.7	74.0	75.1	74.0	72.7
42	76.2	74.0	78.4	79.5	79.5	82.7	84.5
48	91.5	93.6	93.6	96.9	94.7	95.8	100.7

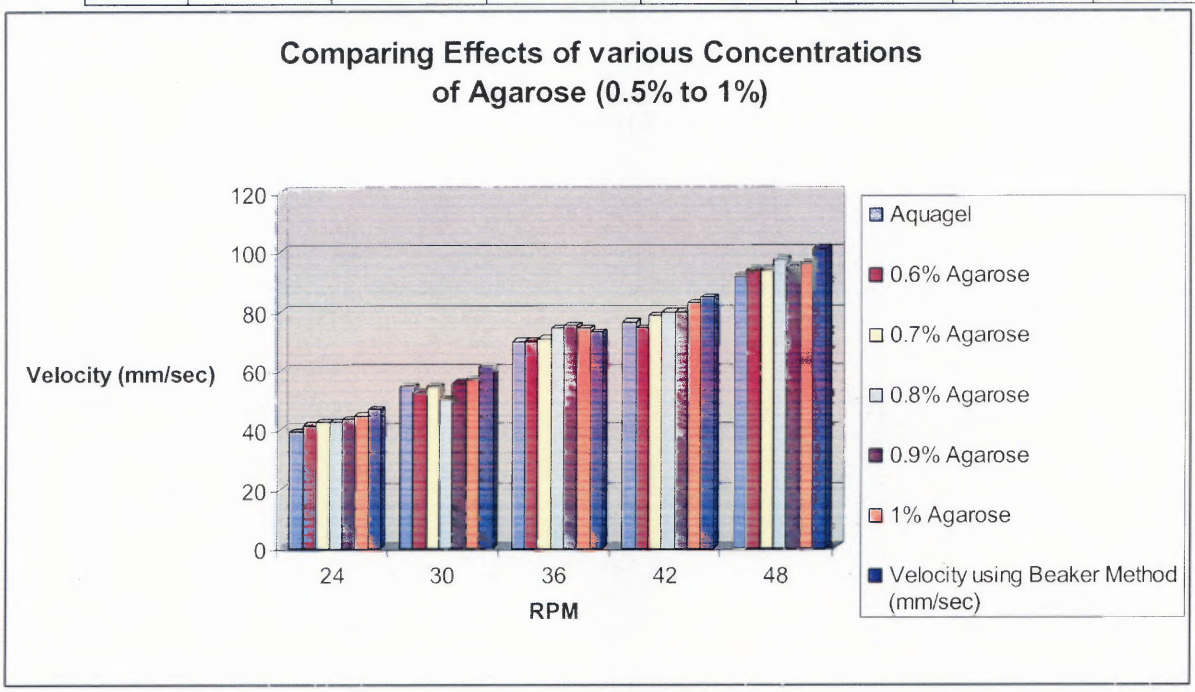

Fig 4.4 Results - Flow Velocity Measurements – Agarose Gel Concentrations 2

From the results (especially the graph) it is clear that the concentration of agarose between 0.5% and 1.0% does not hinder the signals in anyway (refer Table 4.5 and Fig. 4.4). Experimentally it was observed that the 0.5% concentration agarose gels were very soft and so had the following disadvantages.

- Took time to harden

- Kept flowing i.e. care should be taken to not move the transducer when this concentration of agarose gel is being applied and to hold that position till it hardens

Finally after all these experiments it can be said that the 1% agarose gel concentration will be the most optimum for this experiment considering all the criteria, because it gives accurate results and is hard enough not to flow away at the same time soft enough not to hinder the penetration of sound waves.

4.6 *In vitro* Calibration and Testing with 20MHz Transducer - Particle Concentrations

The results of this experiment are as follows.

Table 4.6 Results – Flow Velocity Measurements – Particle Concentrations

RPM	Velocity using Doppler Technique (mm/sec) using Aquagel							Velocity using Beaker Method (mm/sec)
	0.2mg in 1ml water	1mg in 1ml water	3mg in 1ml water	10mg in 1ml water	30mg in 1ml water	100mg in 1ml water	500mg in 1ml water	
24	43.5	41.4	41.4	40.3	43.5	39.2	45.7	46.7
30	57.7	56.6	52.3	54.4	56.6	56.6	58.8	60.9
36	69.7	69.7	69.7	69.7	74	74	69.7	72.7
42	82.7	82.7	82.7	80.6	84.9	81.6	82.7	84.5
48	98	95.8	100.2	93.6	95.8	95.8	95.8	100.7

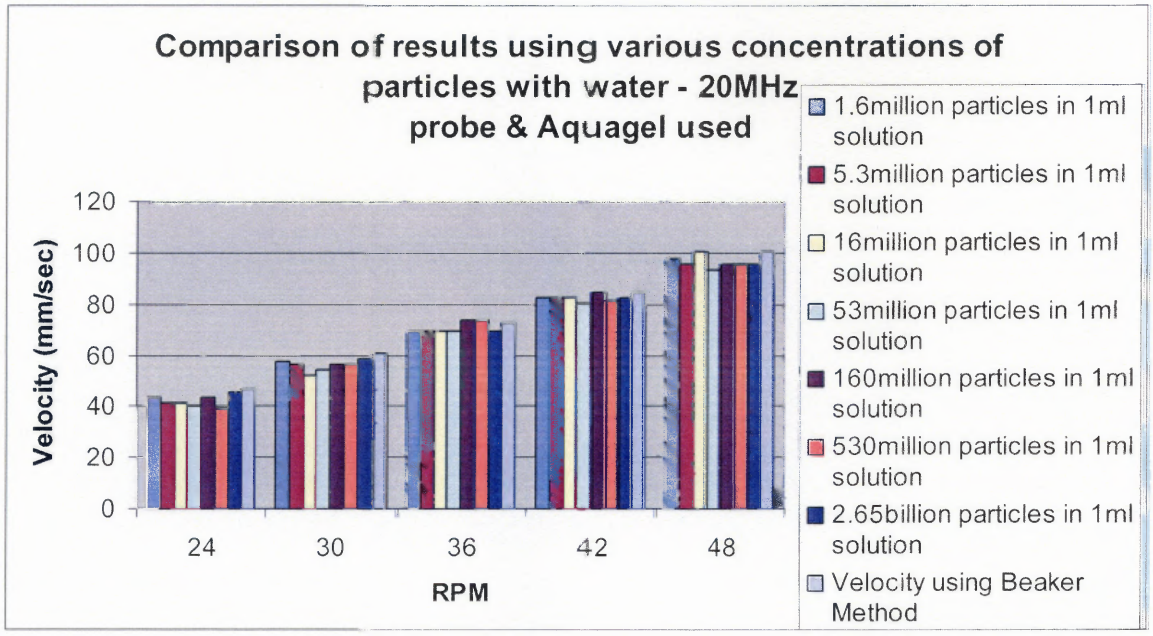

Fig 4.5 Results – Flow Velocity Measurements – Number of Particles

Results (refer Table 4.6 and Fig. 4.5) prove that the device will work even during the worst situations when the blood has very little red blood cells available.

4.7 Bone – Plastic glue test

Dental Luting Cement

It was observed that the glue was strong enough to bond the bone and the plastic. Extreme manual force was applied to test the quality of the bond. It should be noted that not too much force is expected to be applied on the transducer when inside the head of the dog.

Bone Cements

The resulting bond was a strong one. When maximum manual mechanical force was applied, no part of the glue withered off, promising to be a very good bet when used in the head (refer Fig. 4.6 and 4.7).

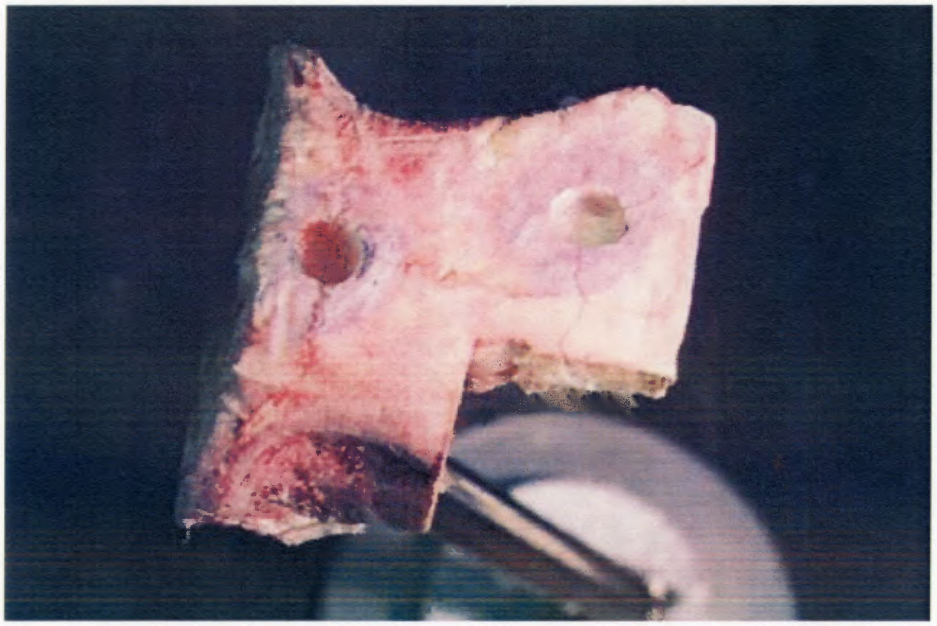

Fig 4.6 Pig Skull Bone – Arrangement for gluing

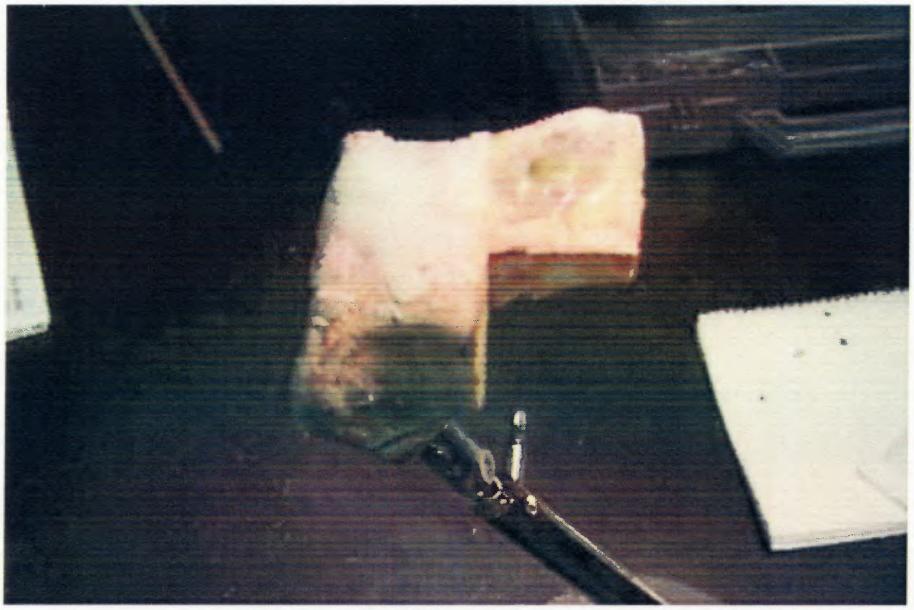

Fig 4.7 Pig Skull Bone and Polycarbonate - Glued

It is a known fact that all such hardening reactions are exothermic. One important observation was the amount of heat produced when the cement hardens. Temperatures up to a maximum of 60°C were observed. Though these are cements used on bone for prosthetics, the conditions in the arm or the knee is very different from that in the brain.

The Cerebrovascular (cerebro – brain ; vascular – vessels), pertaining to blood vessels of the brain, area is much more delicate and cannot sustain such high temperatures.

So a thermal analysis was performed to find out if the brain will be exposed to high temperatures. The thermal conductivity of resins are between 0.2 and 0.4, which is very low in any standards. Also, the thermal conductivity of the Cerebrospinal Fluid (refer *Brain Covering* in Literature Survey) is roughly around 0.55 and that of the Dura (refer *Brain Covering* in Literature Survey) is roughly 0.25. This gives a total thermal coefficient of 0.34. So considering the fact that the bone cement will be smeared on top of the plastic, the heat will have to pass through 2 layers, one is the plastic and the other is a combination of Dura and Cerebrospinal Fluid, to reach the brain. The total thermal conductivity value of 0.34 is a very low value and in no way will permit a large amount of heat to flow.

Also, another observation was that the heat developed from the bone cement was dependent on the volume of the glue used i.e. a cube of bone cement with volume $8cm^3$ will develop way too much more heat than a layer of bone cement with thickness 1mm and length 5cm. The more compact the molecules of the cement are, more the amount of heat developed. In the case of a chronic implant in a dogs head, it is expected to use very small volumes of the bone cement, saving the brain material from excessive heat.

4.8 Wrist Method with 10MHz Transducer

The results obtained from the human wrist using design – 1 are as follows.

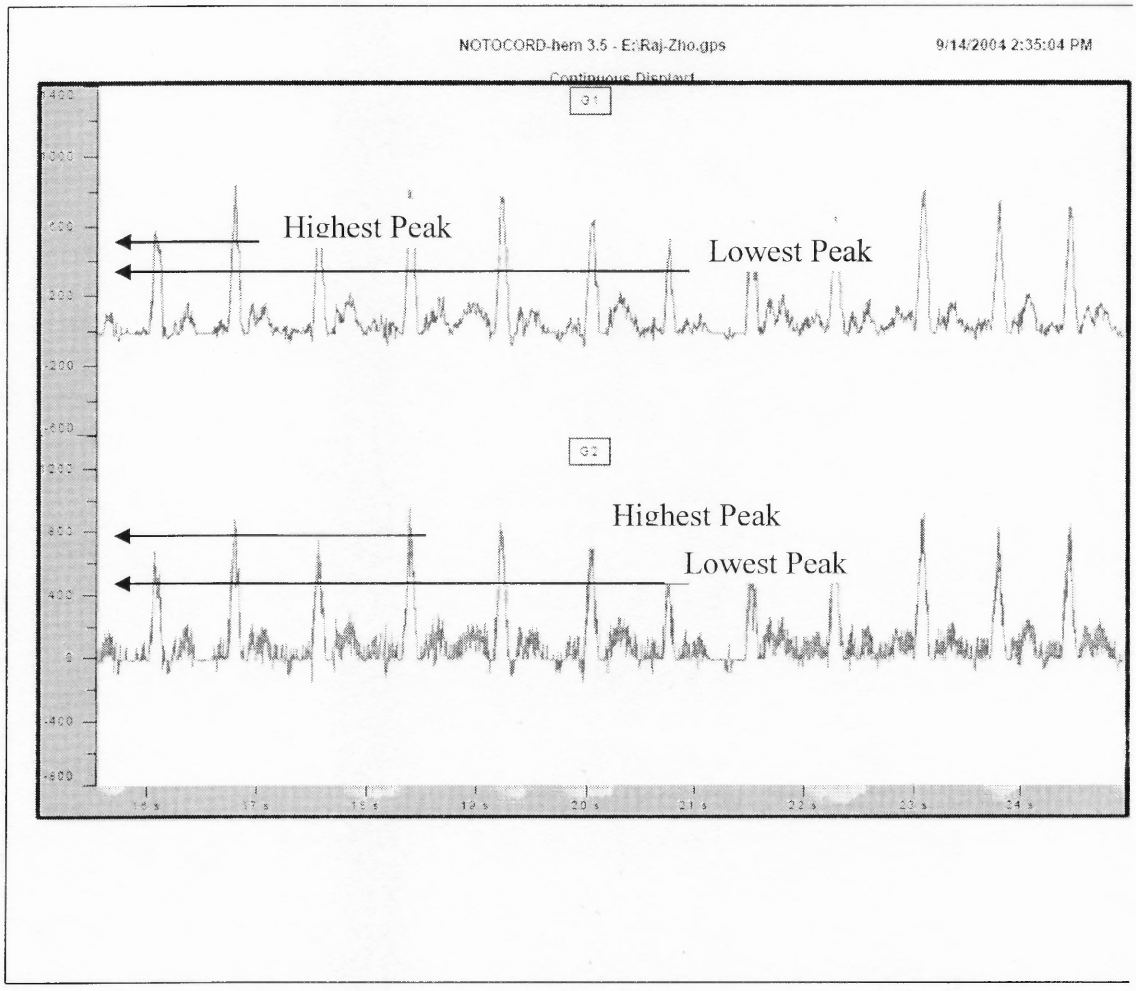

Fig 4.8 Results – Wrist Method

Calculation

Calibration criterion - **250mV ~ 1 KHz of Doppler Shift (F_d)**

The Y-axis gives the voltage in milli volts and the X-axis gives time in seconds.

Considering the highest peak,

Voltage = 970mV (Approx)

This corresponds to a Doppler shift (F_d) = 970/250 = 3.8KHz (approx)

The formula for calculating the velocity of blood is

$$F_d = \frac{2 \times F_1 \times V \times \cos\theta}{c}$$

$$= [(1540000\text{mm/sec}) * (3.8 * 10^3\text{Hz})] / [2 * (10 * 10^6\text{Hz}) * (\cos 45)]$$

Velocity (V) = 41.5cm/sec

Considering the lowest peak,

Voltage = 570mV (Approx)

This corresponds to a Doppler shift (F_d) = 570/250 = 2.25KHz(approx)

Using this value we get,

Velocity (V) = 24.0 cm/sec

The velocity of blood flow in the carpal artery (wrist artery) varied between 24.0 to 41.5cm/sec.

The most important inference is the frequency of occurrence of peaks. It can be observed from the graph that there is a peak every 0.8 seconds. This translates to about 75 peaks every minute. Considering the fact that every peak refers to a gush of blood, the frequency of peaks can be considered as a monitor for the heart rate. The human heart rate varies between 65 and 85 beats per minute [24].

One negative inference from the results is the amount of noise reported. This noise could be because the transducer is placed on the skin and the flow is inside the artery. Between the crystal and the blood flow, there is about 3-4mm of skin, tissue and fluid. The sound waves might bounce off some components of these and the reflected waves are portrayed as noise.

4.9 Experiment on MCA of Dog with 10MHz Transducer

Results obtained were in no way close to the expected results and excessive noise was observed. The reasons for this might be

- Lack of accuracy in positioning
- Frequency value of 10MHz is too low to track the flow inside the artery

As the positioning was done with utmost care and several times (taking advantage of the fact that it was not a chronic implant) the issue with positioning was given lower priority and a decision to try the experiment using a 20MHz probe was taken.

4.10 Experiment on Femoral Artery, Left Gastric Artery and Mesenteric Artery of Mouse using 20MHz Transducer

After the results were obtained, the data for each experiment was analyzed using Matlab. A Fast Fourier Transform was done on each set of data to find out the most powerful frequency and the overall power spectrum.

4.10.1 Femoral Artery

The following plot was obtained as result.

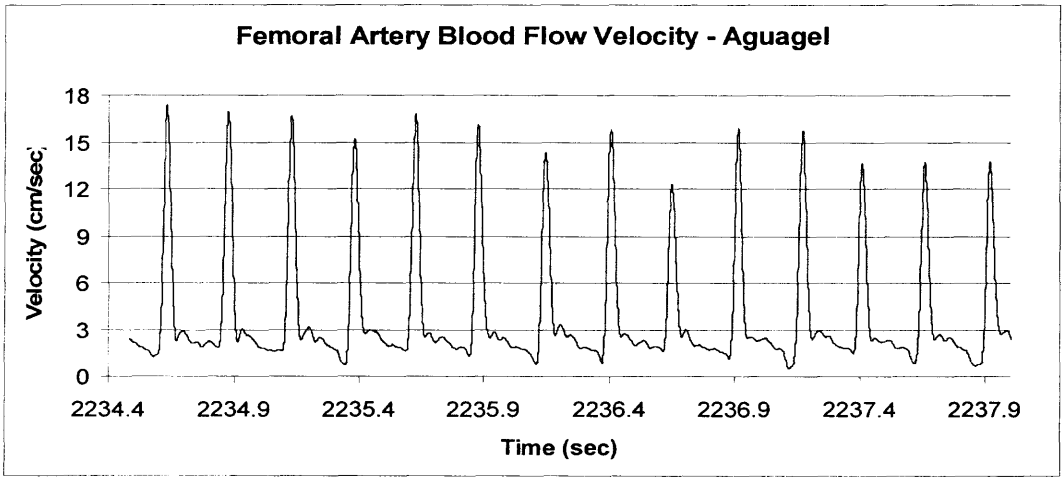

Fig 4.9 Results – Femoral Artery Blood Flow Velocity

Rhythmic and uniform peaks were obtained and the velocity of blood flow in the femoral artery of the mouse can be observed to vary between 14.5cm/s and 17.4cm/s (from data in excel file). The values obtained from the literature point at 17.5cm/s. [17], [18].

A program was written in Matlab to plot the power spectrum of the data obtained. The power spectrum is displayed below.

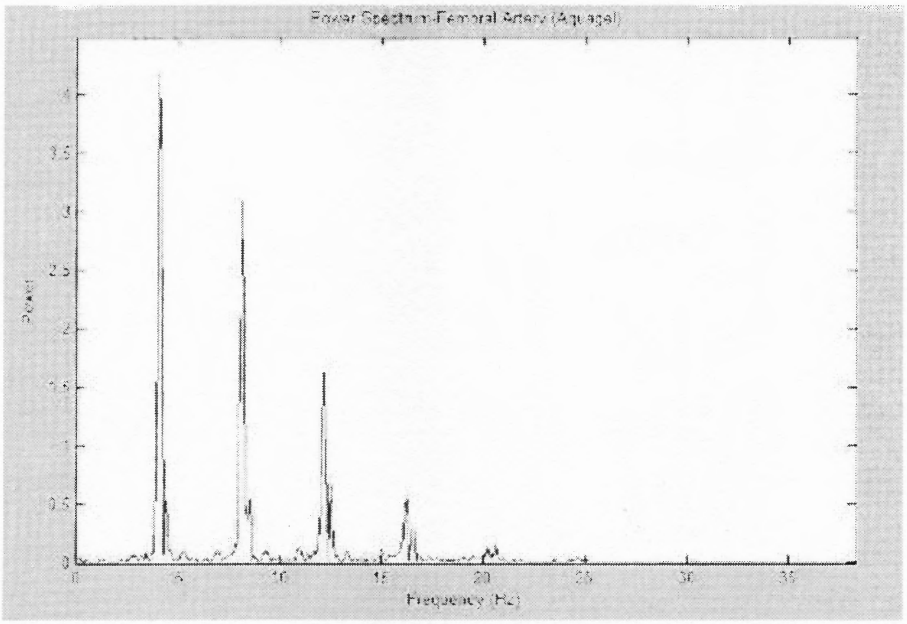

Fig 4.10 Results – Power Spectrum of Femoral Artery Blood Flow Velocity

It is clear from the power spectrum that the most powerful frequency is 4 and that is the number of peaks that occur each second.

Another program to count the number of peaks within each meaningful velocity range was written. The results of that program are tabulated below.

Table 4.6 Distribution of peaks – Femoral Blood Flow Velocity

S. No	Velocity Range (cm/s)	No. of Peaks
1	0 - 3	74
2	3 - 6	189
3	12 - 18	19

Within the velocity range of 0cm/s to 6cm/s there are about 263 peaks. It is obvious that this is mere noise. All the meaningful peaks occur within the velocity range 12cm/s to 18cm/s. This shows the uniform occurrence and distribution (most powerful frequency is 4) of the meaningful peaks.

To get a better understanding of the Power Spectrum, each noticeable powerful peak was isolated and an inverse FFT was performed to get the shape of the curve.

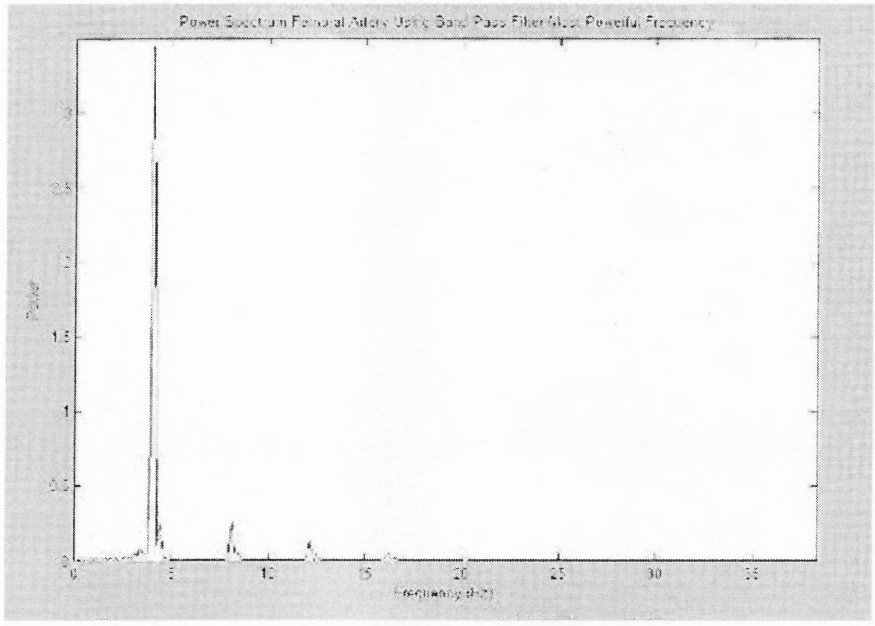

Fig 4.11 Isolation of most powerful frequency – Femoral Artery

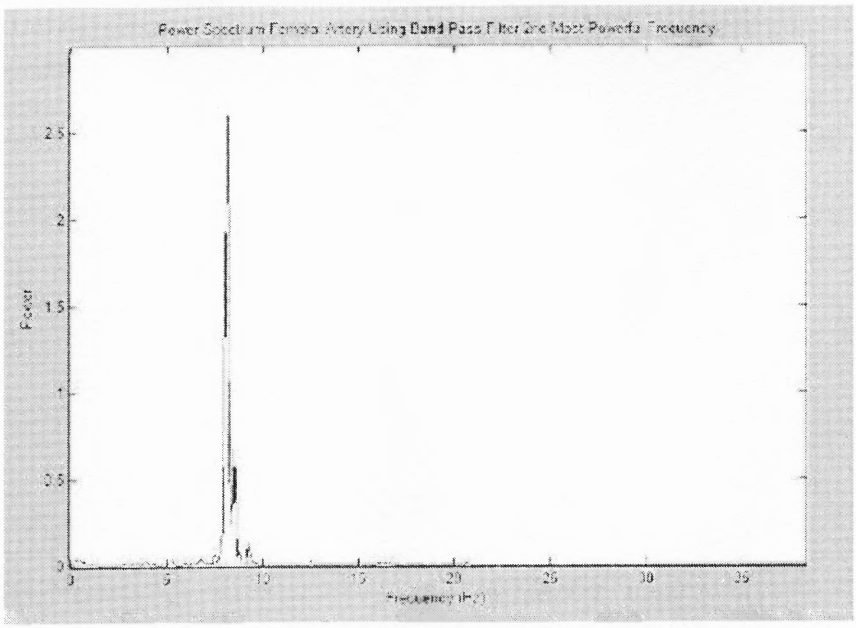

Fig 4.12 Isolation of 2nd most powerful frequency – Femoral Artery
The shape of each curve is shown below.

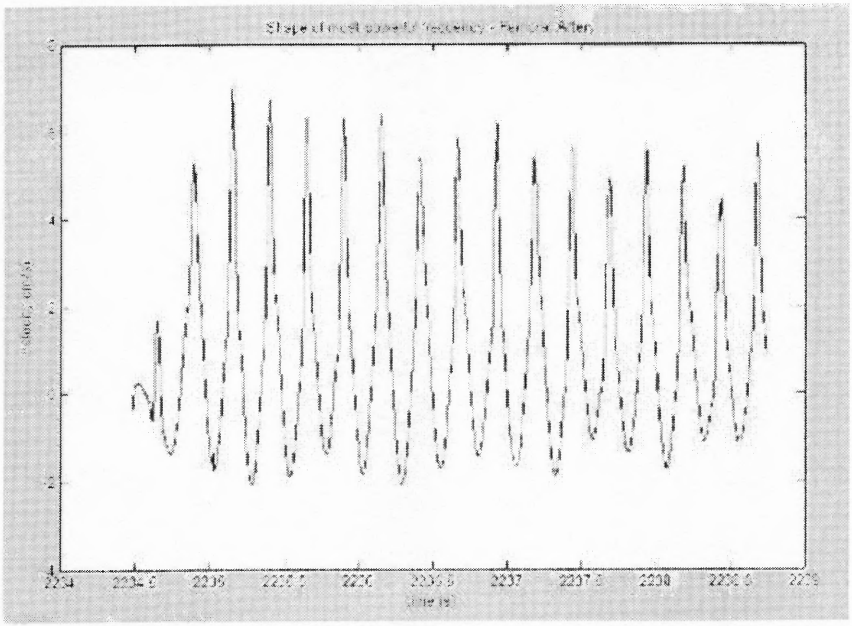

Fig 4.13 Shape of waveform of most powerful frequency – Femoral Artery

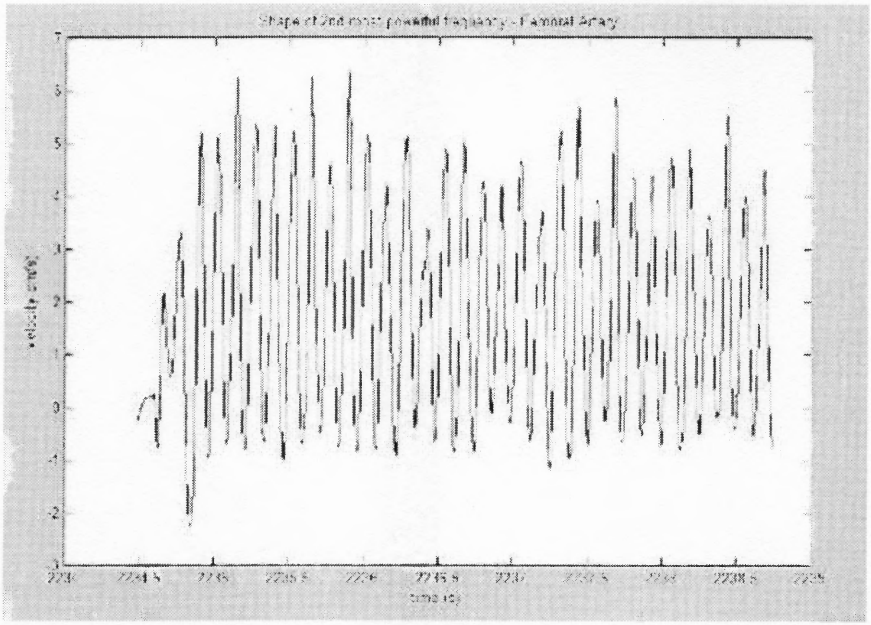

Fig 4.14 Shape of waveform of 2nd most powerful frequency – Femoral Artery

When all the peaks, however small they may be, in the power spectrum are converted to their respective waveforms and put together, the original curve (Fig.4.7) can be obtained.

It was observed that using a Bandpass filter to isolate the curves filtered some of the required signals too. It can be seen in the plots that the magnitude of the isolated waves are much lower than the original magnitude of velocity. In order to avoid to reduction in magnitude, a technique of threshold was performed. The resulting plot is shown below.

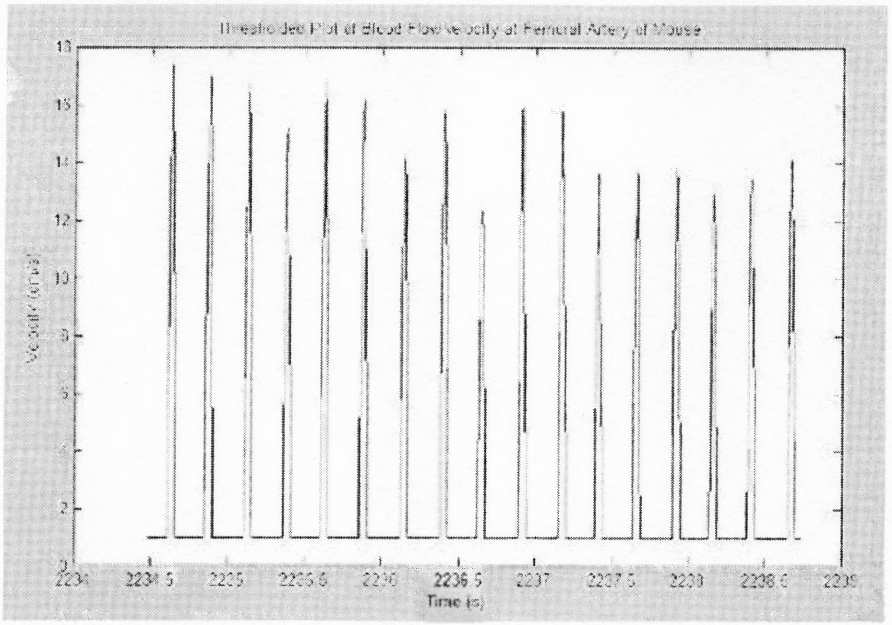

Fig 4.15 Time – Velocity plot after Thresholding – Femoral Artery

4.10.2 Left Gastric Artery

The follow result was obtained.

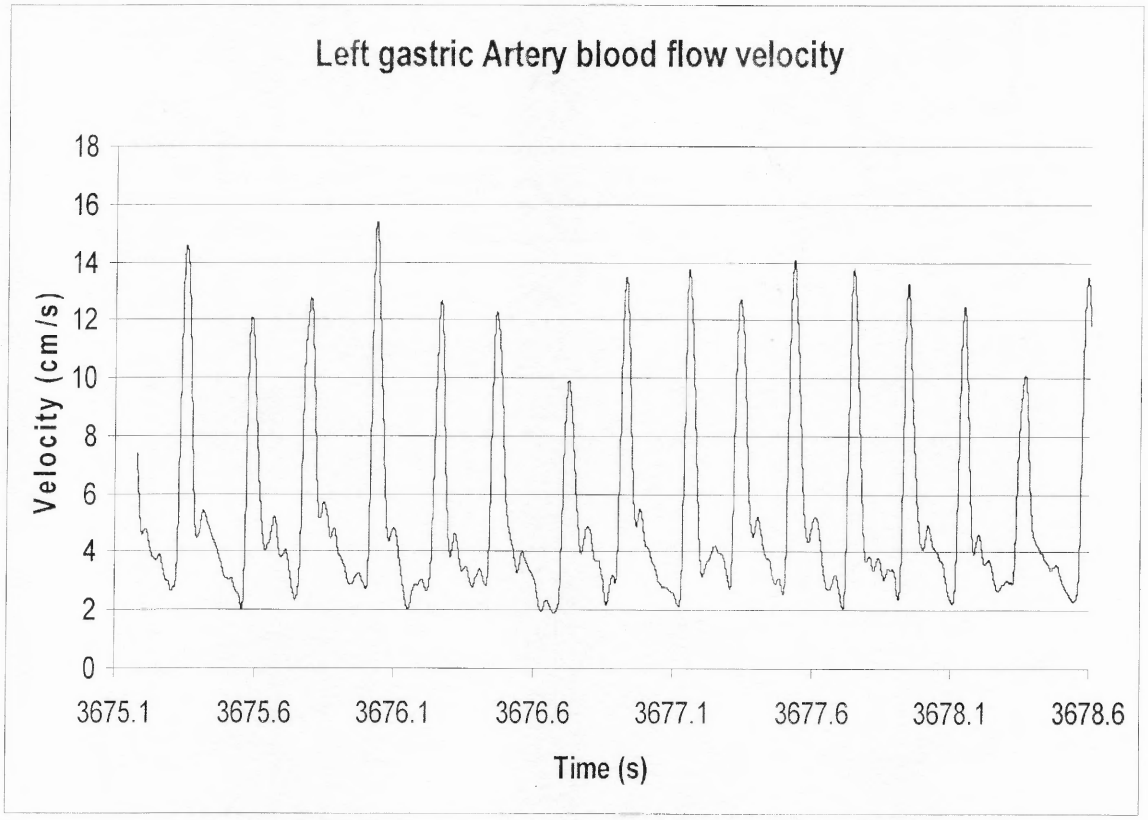

Fig 4.16 Results – Left Gastric Artery Blood Flow Velocity

Here too almost uniform peaks can be observed. As, not much research has been done on the blood flow velocity in the gastric arteries, the values were not quite compared.

The data analysis using Matlab gives the following results.

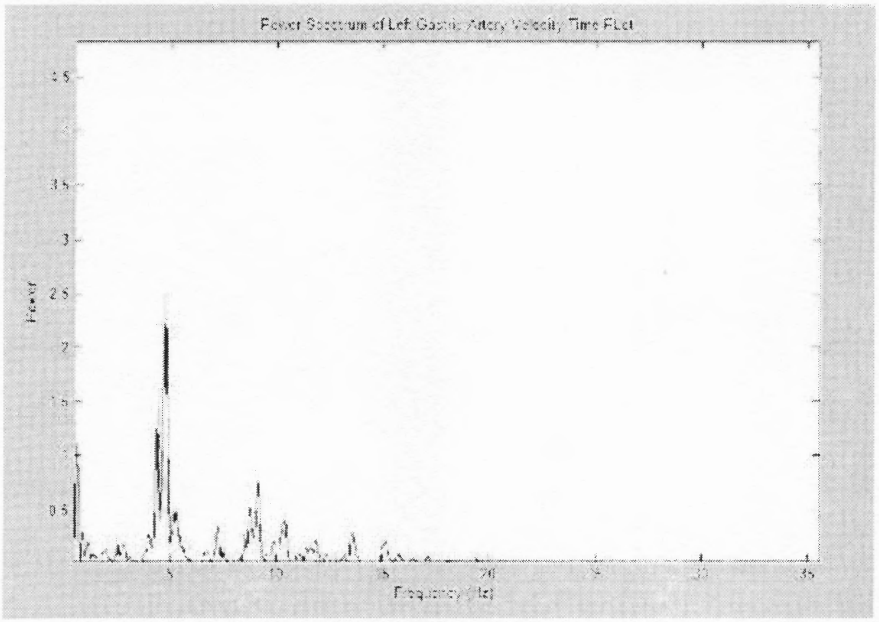

Fig 4.17 Results – Power Spectrum Left Gastric Artery Blood Flow Velocity

The most powerful frequency is 5 and that translates to the number of meaningful peaks every second. The distribution of peaks is given by

Table 4.7 Distribution of peaks – Left Gastric Artery Blood Flow Velocity

S. No	Velocity Range (cm/s)	No. of Peaks
1	0 - 6	263
2	10 -12	1
3	12 - 14	16
4	14 - 16	3

Again, the 263 peaks with then 0cm/s to 6cm/s can be ignored as noise and the majority of peaks (16 out of 21) occur within the range 12cm/s to 14cm/s. Uniformity of occurrence and distribution proved.

4.10.3 Mesenteric Artery

Results obtained are plotted below.

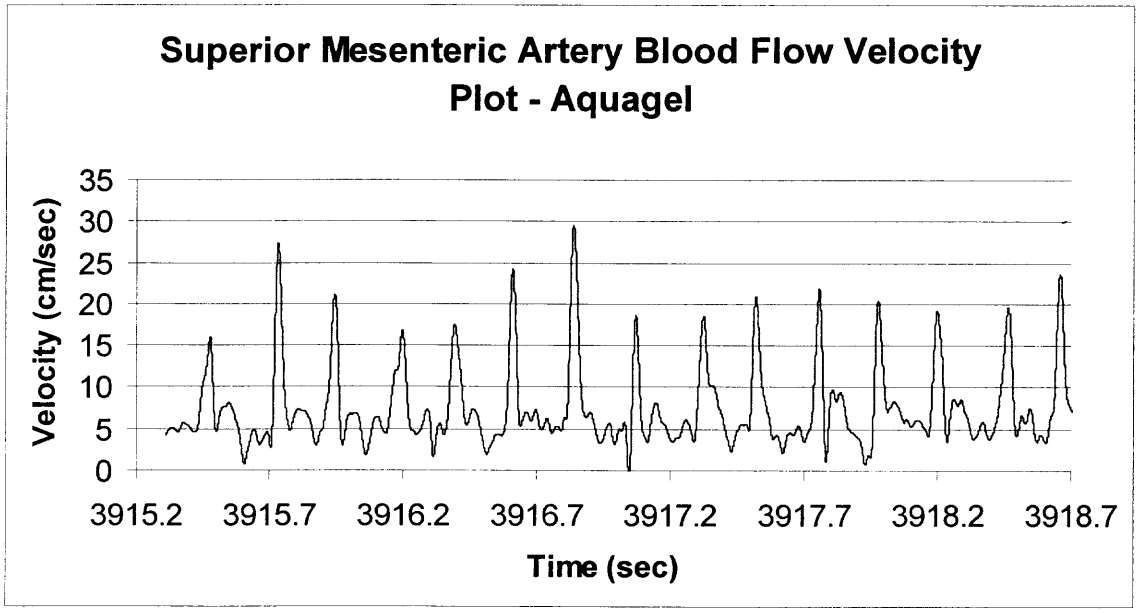

Fig 4.18 Results – Mesenteric Artery Blood Flow Velocity using Aquagel

Though the result is not uniform the peaks indicate the expected value. Literature points at value between 25cm/s and 31cm/s.

Data analysis using Matlab gives the following power spectrum and table which shows the distribution of peaks. Following the FFT performed to plot the power spectrum, isolation of curves was done to study the shape of each individual prominent frequency, as done with the femoral artery. In this case too the magnitude of velocity seemed to be affected, so the technique of thresholding was performed. The results

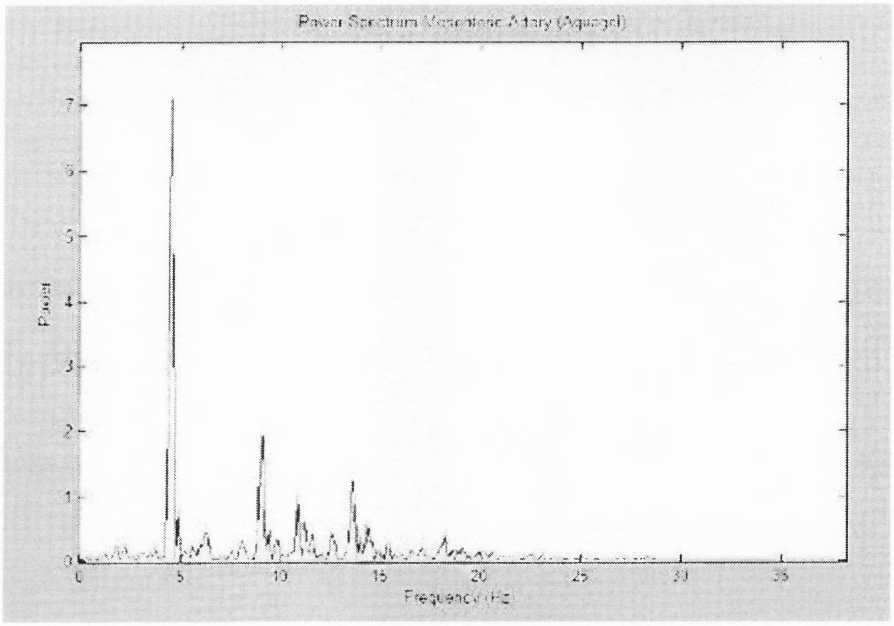

Fig 4.19 Results – Power Spectrum of Mesenteric Artery Blood Flow Velocity using Aquagel

Table 4.8 Distribution of peaks – Mesenteric Blood Flow Velocity (Aquagel)

S. No	Velocity Range (cm/s)	No. of Peaks
1	0 - 5	36
2	5 - 10	77
3	10 - 16	6
4	16 - 22	15
5	22 - 25	2
6	25 - 30	2

Again isolation and shape of curves were determined.

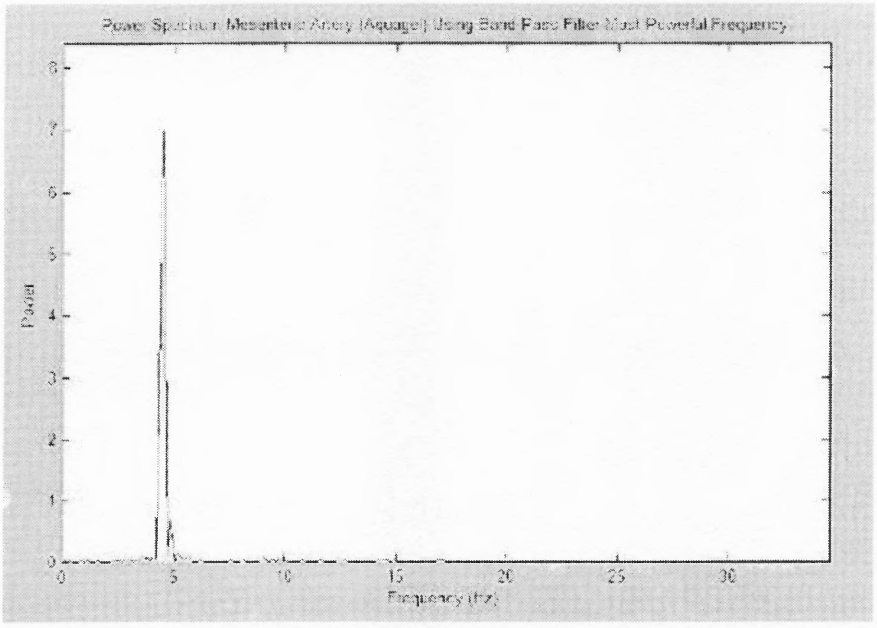

Fig 4.20 Isolation of most powerful frequency – Mesenteric Artery (Aquagel)

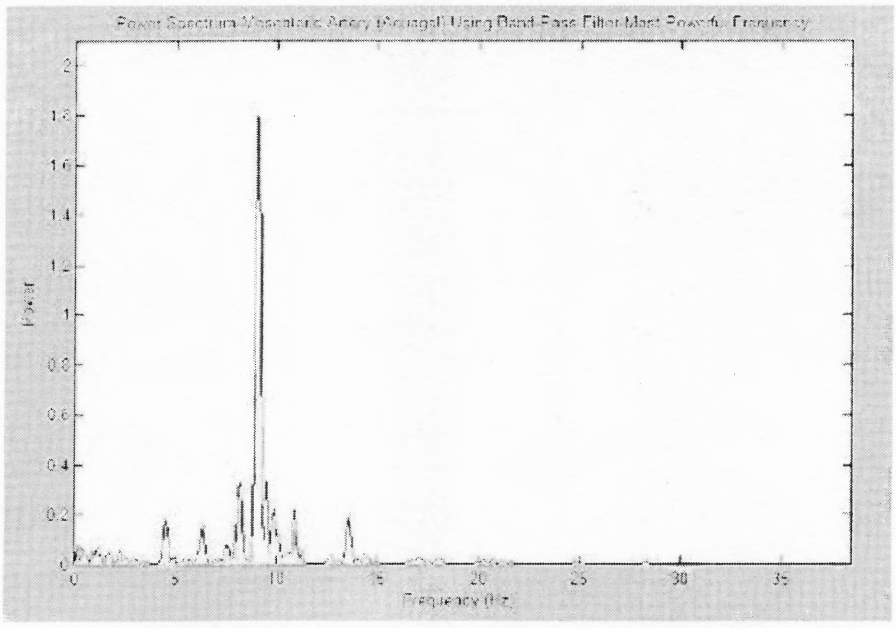

Fig 4.21 Isolation of 2nd most powerful frequency – Mesenteric Artery (Aquagel)

Similarly the shape of the curves were determined.

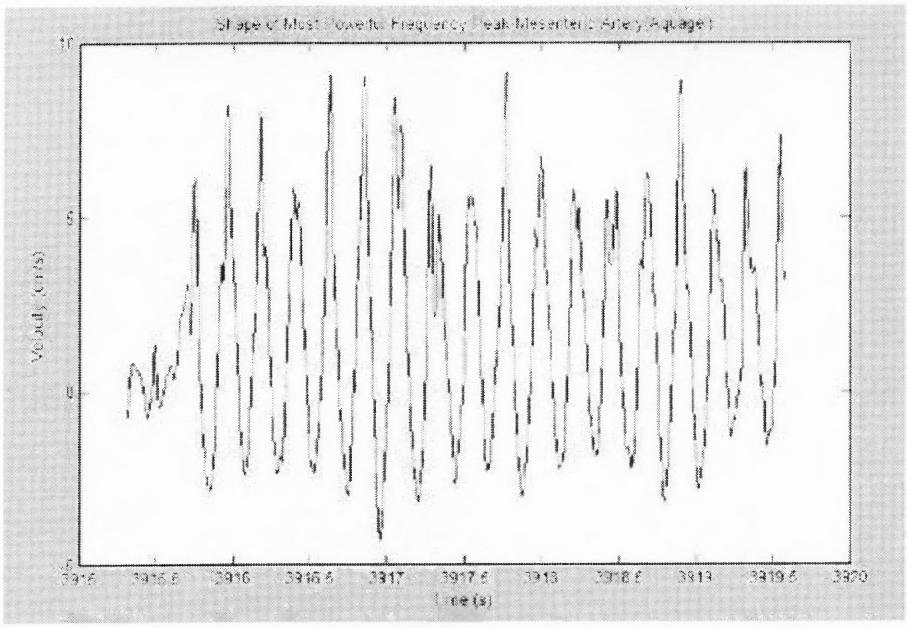

Fig 4.22 Shape of most powerful frequency – Mesenteric Artery (Aquagel)

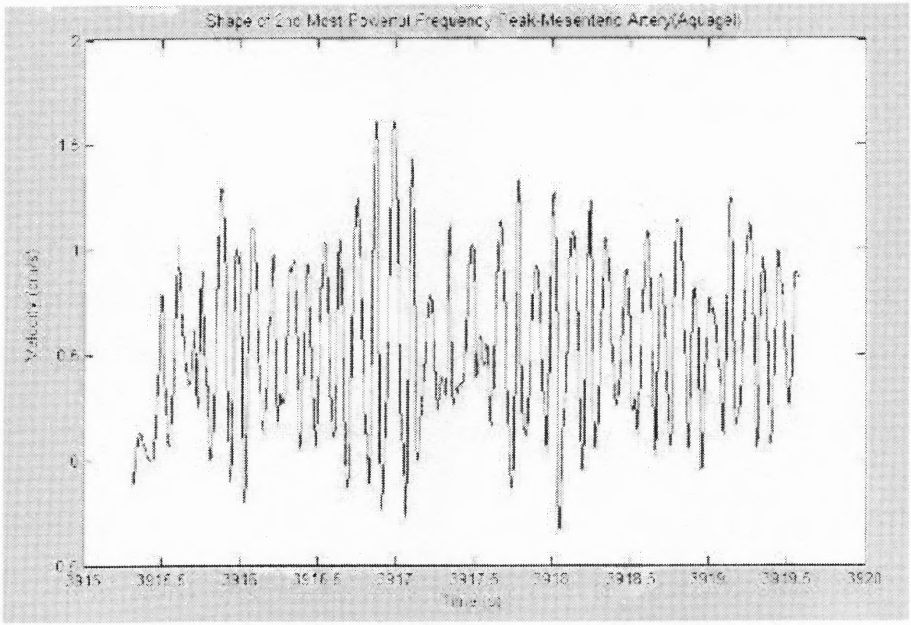

Fig 4.23 Shape of 2nd most powerful frequency – Mesenteric Artery (Aquagel)

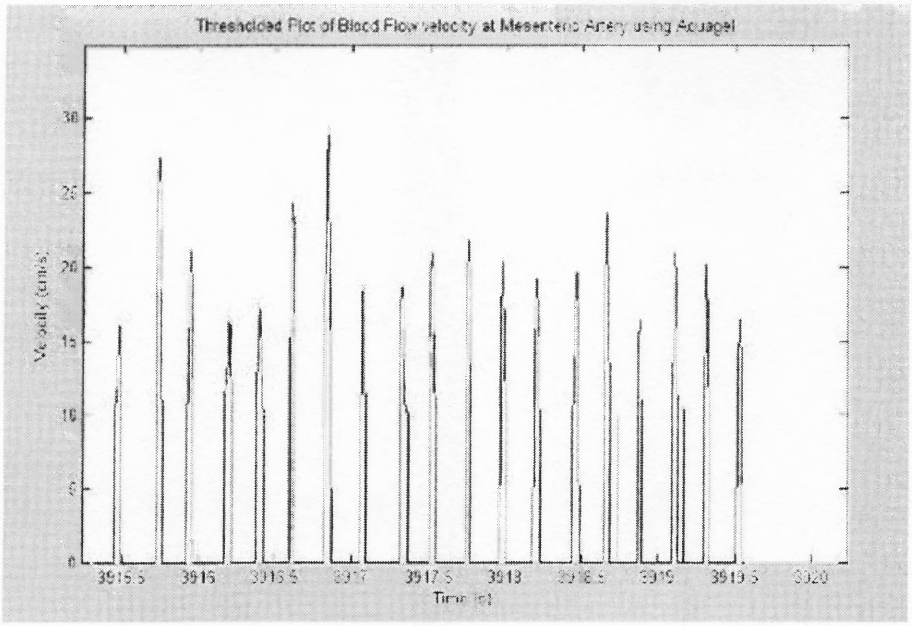

Fig 4.24 Time-velocity plot after thresholding – Mesenteric Artery (Aquagel)

But when the experiment was repeated using agarose gel of 1% concentration, a much better plot was obtained.

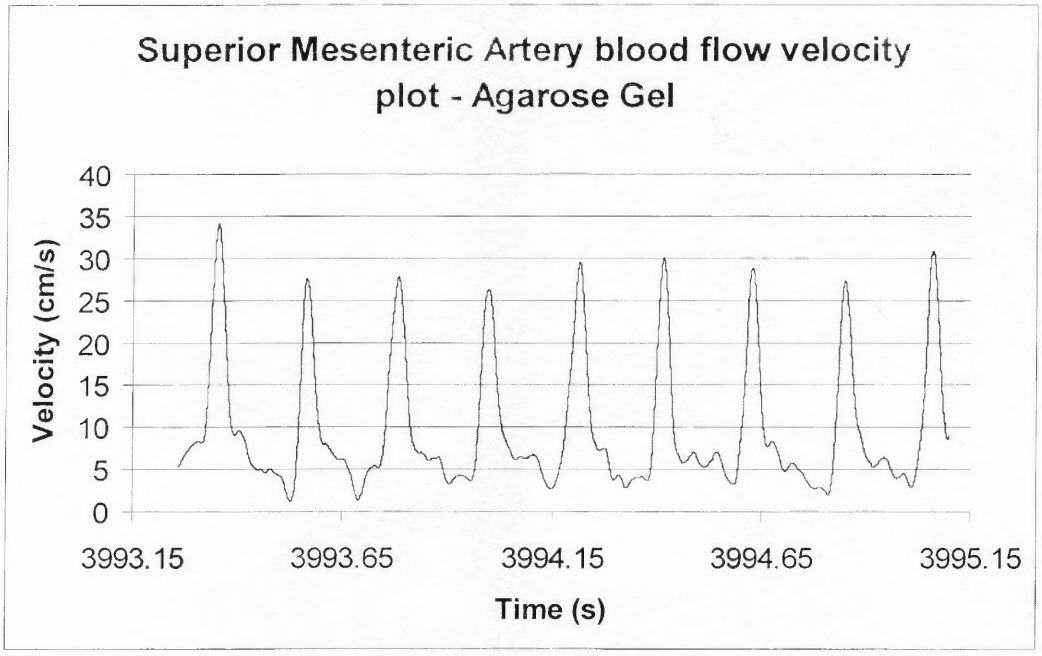

Fig 4.25 Results – Mesenteric Artery Blood Flow Velocity using Agarose Gel

To be noted here, the results are well in the range and also the peaks occur uniformly. Data analysis using Matlab gave the following power spectrum.

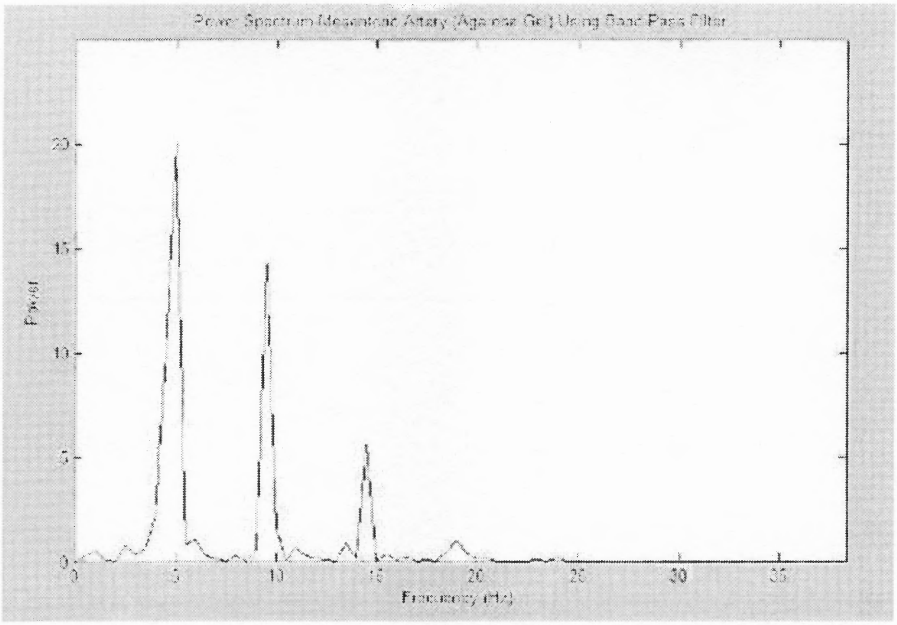

Fig 4.26 Results – Power Spectrum of Mesenteric Artery Blood Flow Velocity using Agarose Gel

To be noted is the power. On a comparative scale (with respect to the other power spectrums when Aquagel was used), the most powerful signal is obtained in this experiment. Also the frequency at which the most powerful signal occurs is the frequency of meaningful peaks in the experiment.

Table 4.9 Distribution of peaks – Mesenteric Blood Flow Velocity (Agarose)

S. No	Velocity Range (cm/s)	No. of Peaks
1	5 – 10	50
2	25 – 30	12
3	30 – 35	3

Clearly the peaks occurring between 5cm/s and 10cm/s are noise. The maximum number of peaks occurs between 25cm/s and 30cm/s which is in the correct range.

A similar isolation procedure followed by the thresholding technique was performed for analysis.

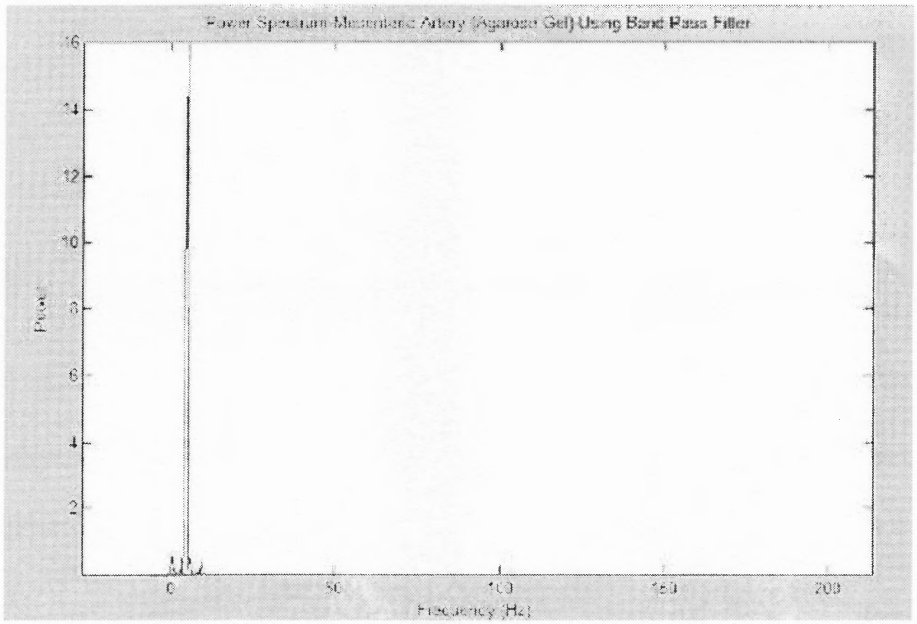

Fig 4.27 Isolation of most powerful frequency – Mesenteric Artery (Agarose)

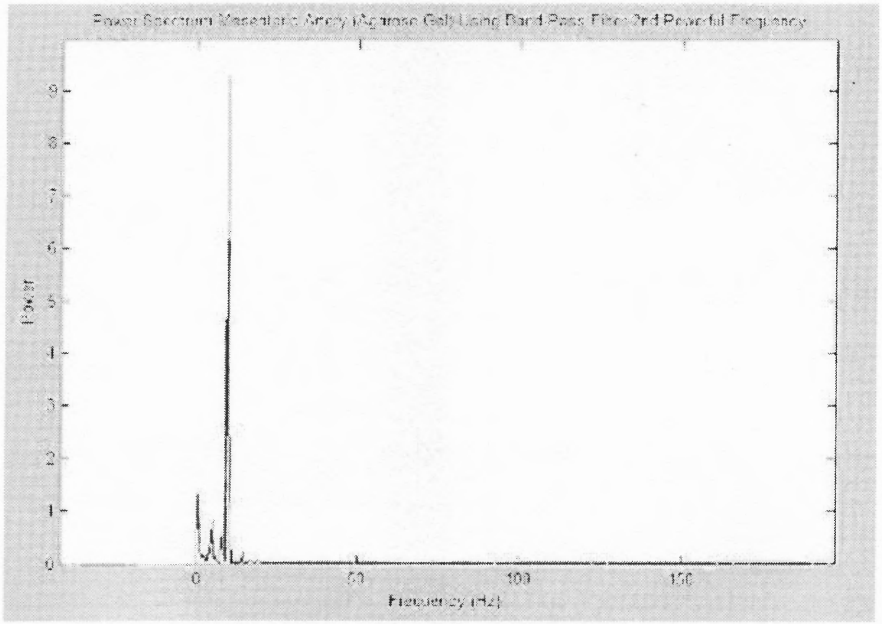

Fig 4.28 Isolation of 2nd most powerful frequency – Mesenteric Artery (Agarose)

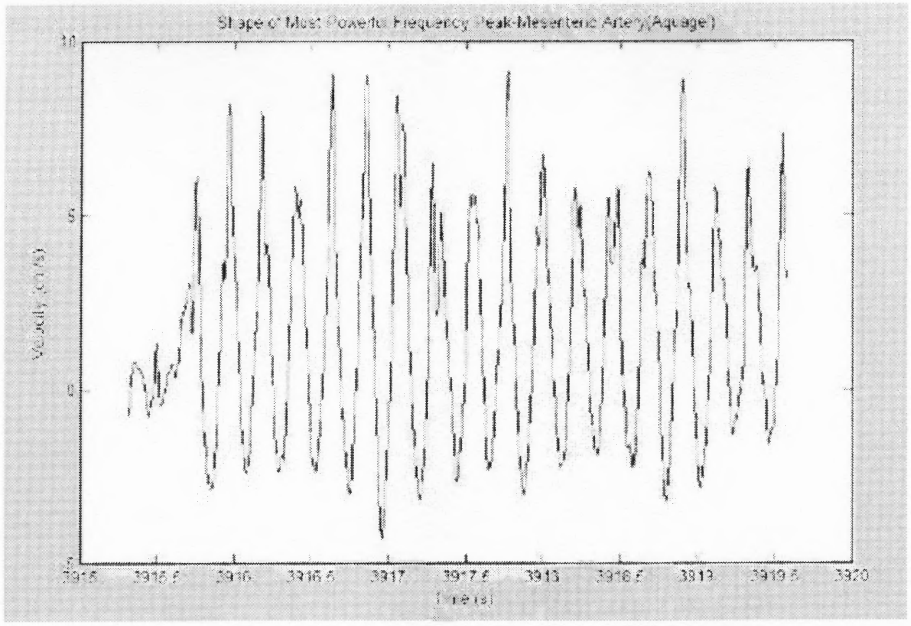

Fig 4.29 Shape of most powerful frequency – Mesenteric Artery (Agarose)

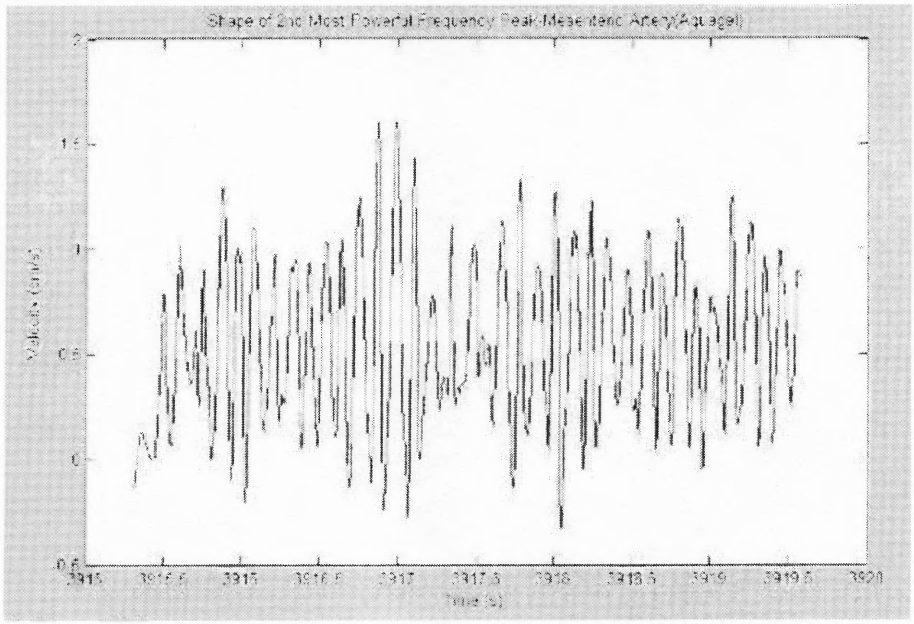

Fig 4.30 Shape of 2nd most powerful frequency – Mesenteric Artery (Agarose)

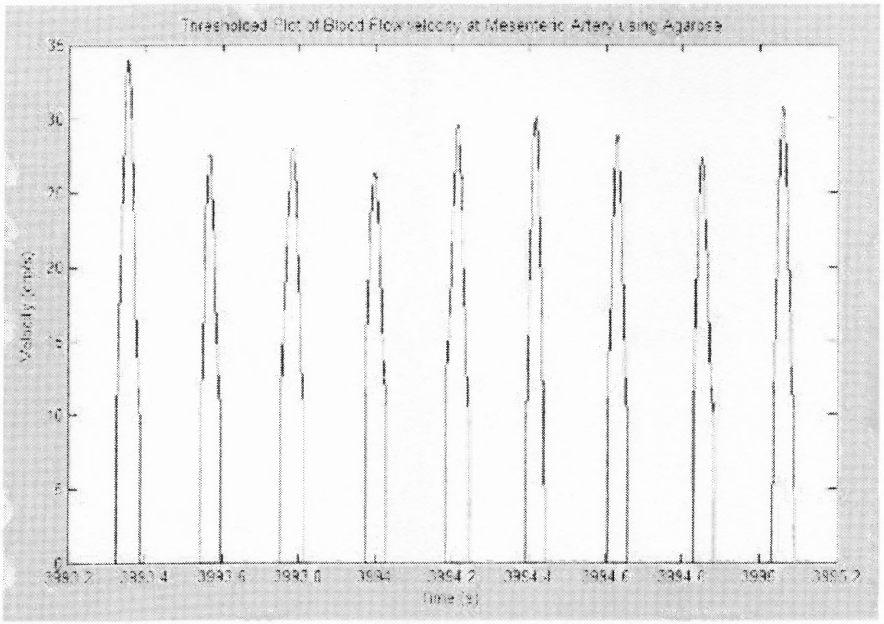

Fig 4.31 Time-velocity plot after thresholding – Mesenteric Artery (Agarose)

4.11 Experiment on MCA of Dog using 20MHz Transducer

The result obtained is plotted below.

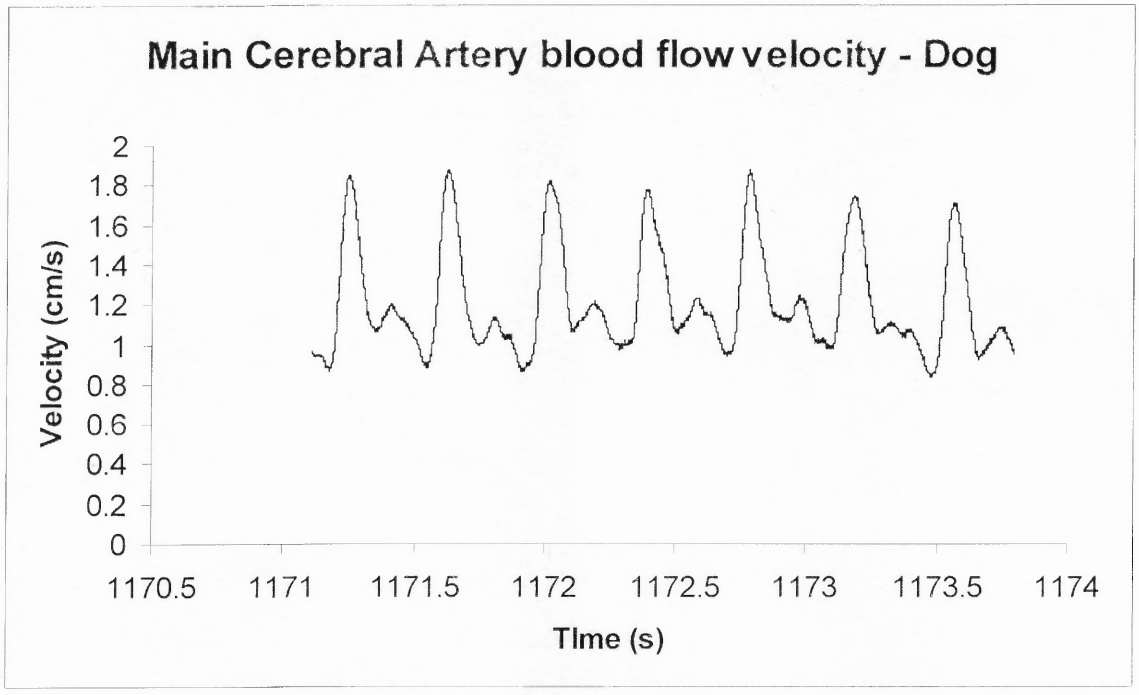

Fig 4.32 Results – MCA of Dog Blood Flow Velocity

The results exhibit a uniform occurrence of peaks and the frequency of this occurrence is about 2.2 peaks per second. This translated to the heart rate of the dog approximately. Though the data confers with the heart rate, the value of peak velocities do not fall within the expected range [37].

A data analysis using Matlab was done to confirm that the frequency of peaks was the heart rate of the dog. A power spectrum was obtained as a result of the analysis.

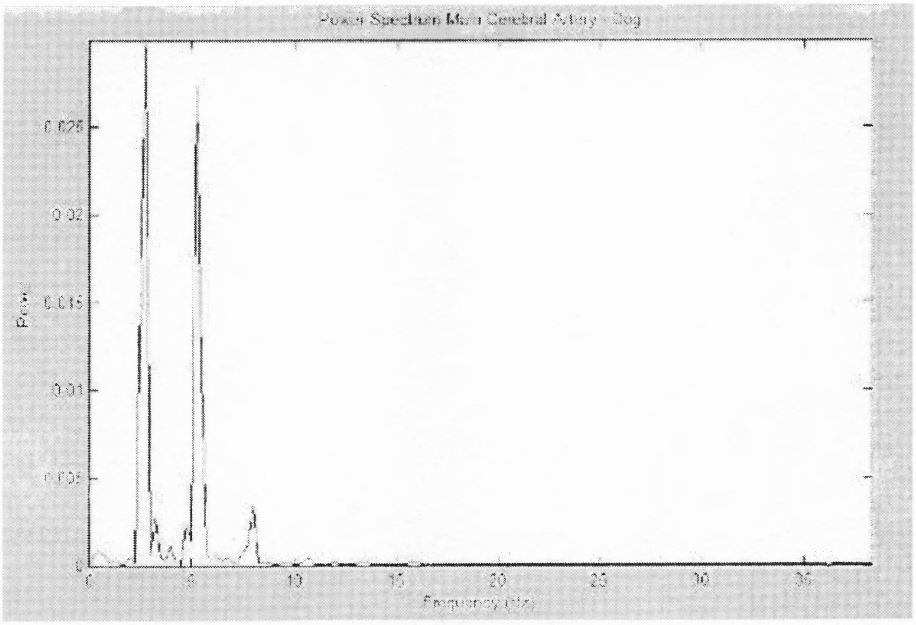

Fig 4.33 Results – Cerebral Blood Flow Velocity of Dog Power Spectrum

It can be seen that the most powerful frequency occurs at a frequency of approximately 2.5Hz. So proof again that the measured flow is the flow of blood pumped from the heart in the middle cerebral artery.

One more point to be noted is that the power of the 2.5Hz frequency is only 0.04, which is much lower than the power of frequencies obtained when tried on mice.

Waveform analysis was done. Results are shown below.

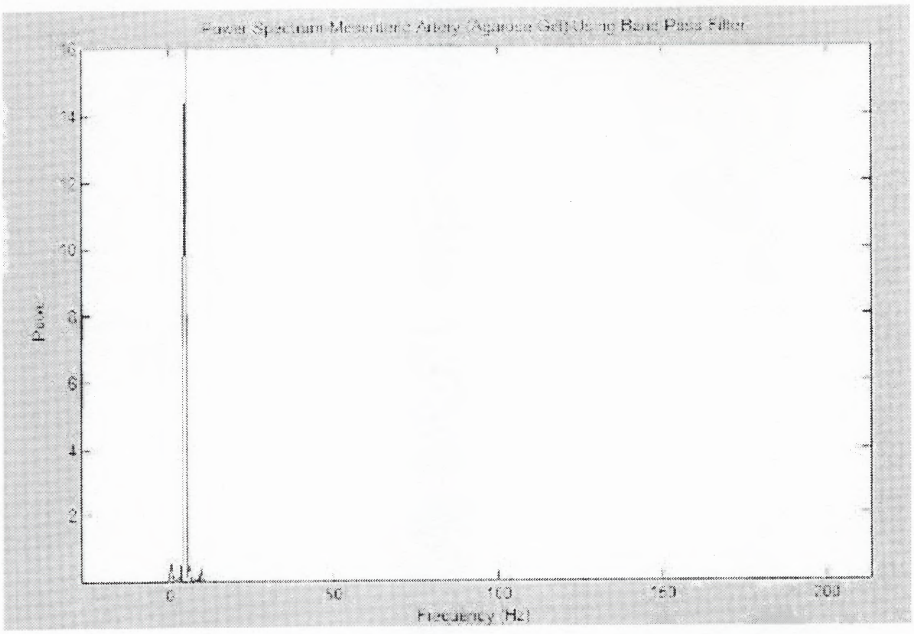

Fig 4.34 Results - Isolation of the most powerful frequency – Middle Cerebral Artery of Dog

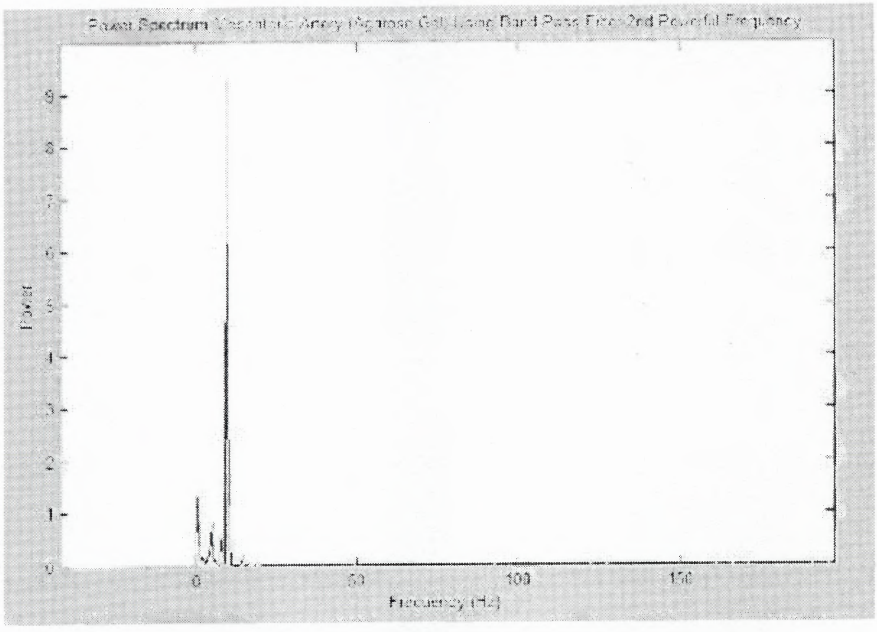

Fig 4.35 Results - Isolation of the 2nd most powerful frequency – Middle Cerebral Artery of Dog

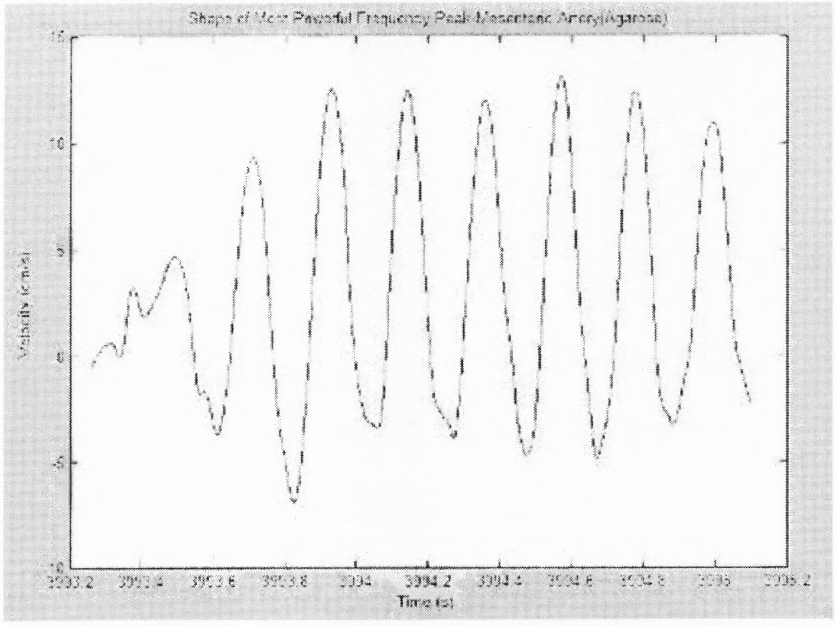

Fig 4.36 Results - Shape of the most powerful frequency – Middle Cerebral Artery of Dog

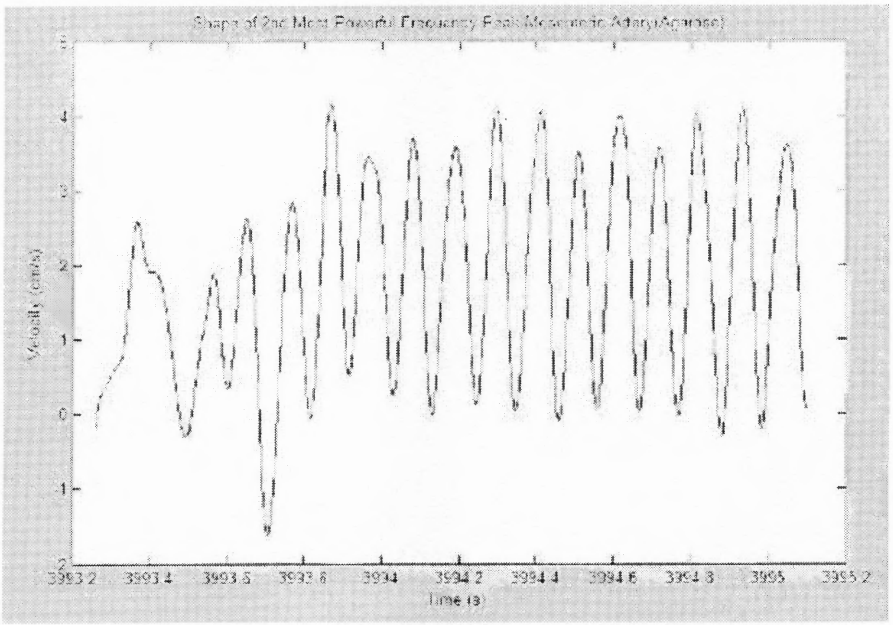

Fig 4.37 Results - Shape of the 2nd most powerful frequency – Middle Cerebral Artery of Dog

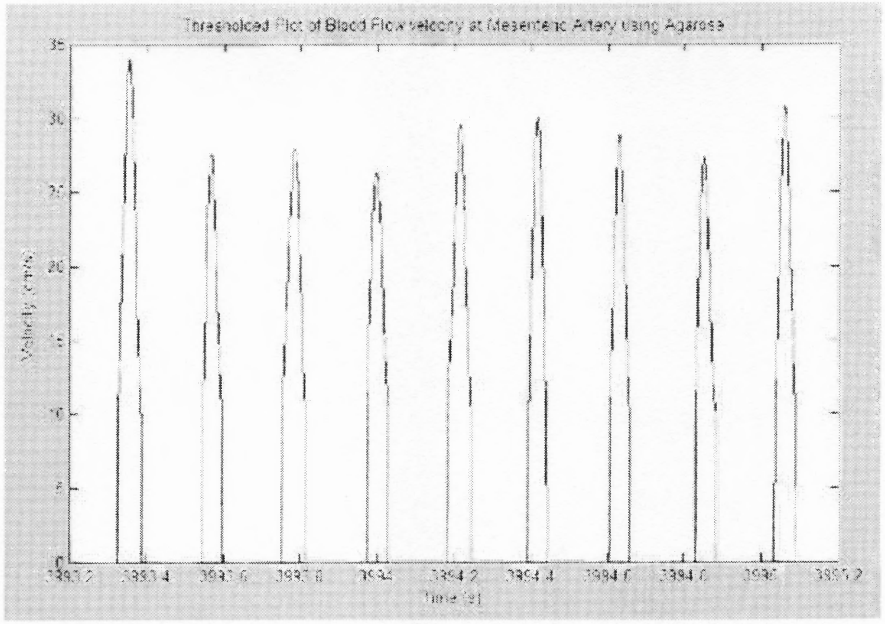

Fig 4.38 Time-velocity plot after thresholding – Middle Cerebral Artery of Dog

4.12 Experiment on MCA of Pig using 20MHz Transducer

The results obtained are plotted below.

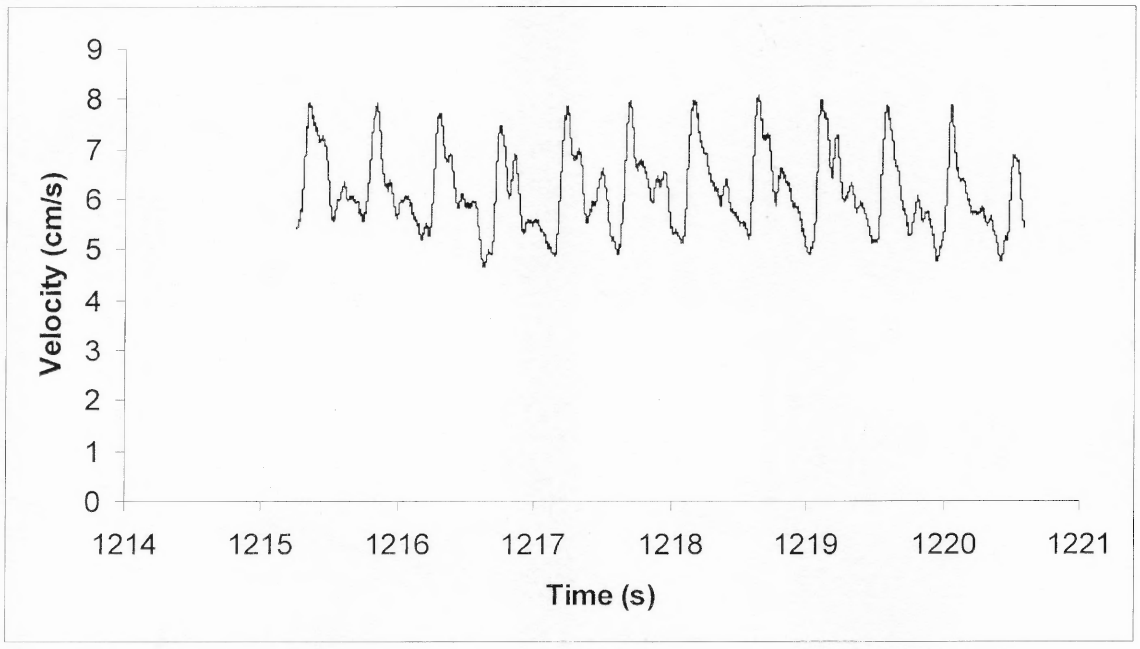

Fig 4.39 Cerebral Blood Flow Velocity pattern of Pig – High Peaks
(Results obtained before Implantation)

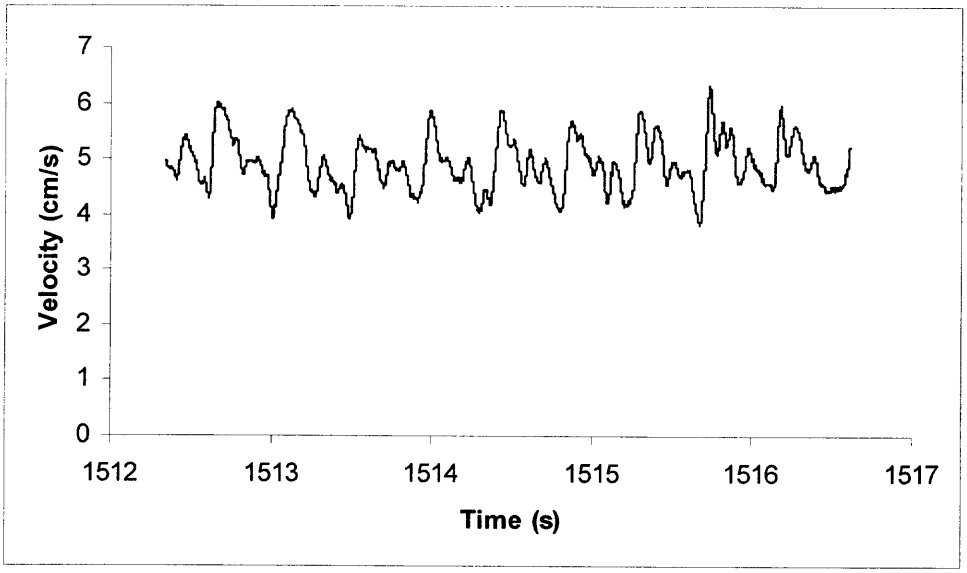

Fig 4.40 Cerebral Blood Flow Velocity pattern of Pig – Lower Peaks
(Results obtained before Implantation)

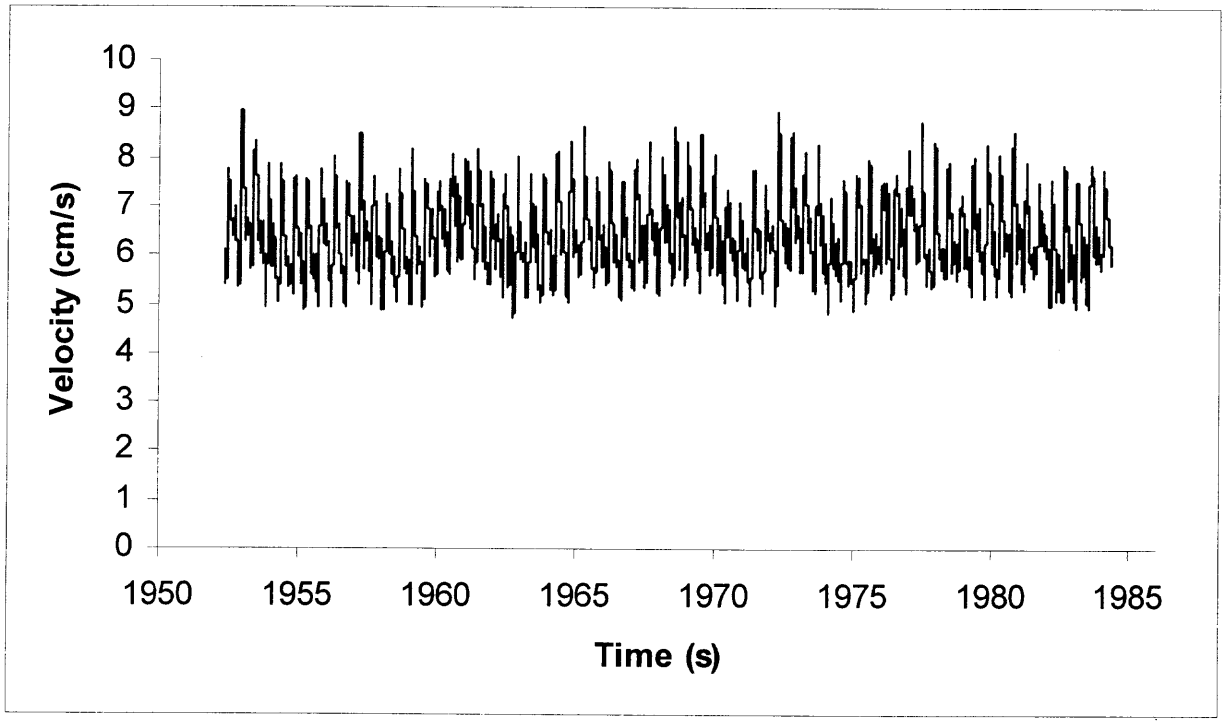

Fig 4.41 Cerebral Blood Flow pattern of Pig
(Longer time scale showing uniformity)

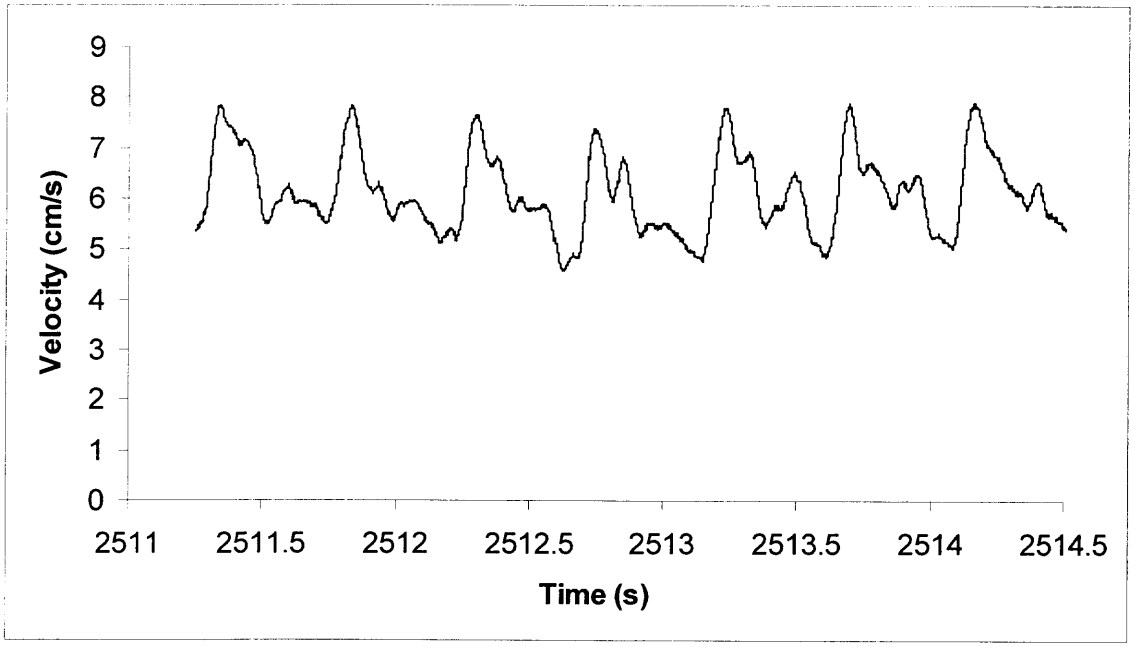

Fig 4.42 Cerebral Blood Flow Velocity pattern of Pig
(Results obtained after Implantation)

Data analysis was done using Matlab and the following plots for Power Spectrum were obtained.

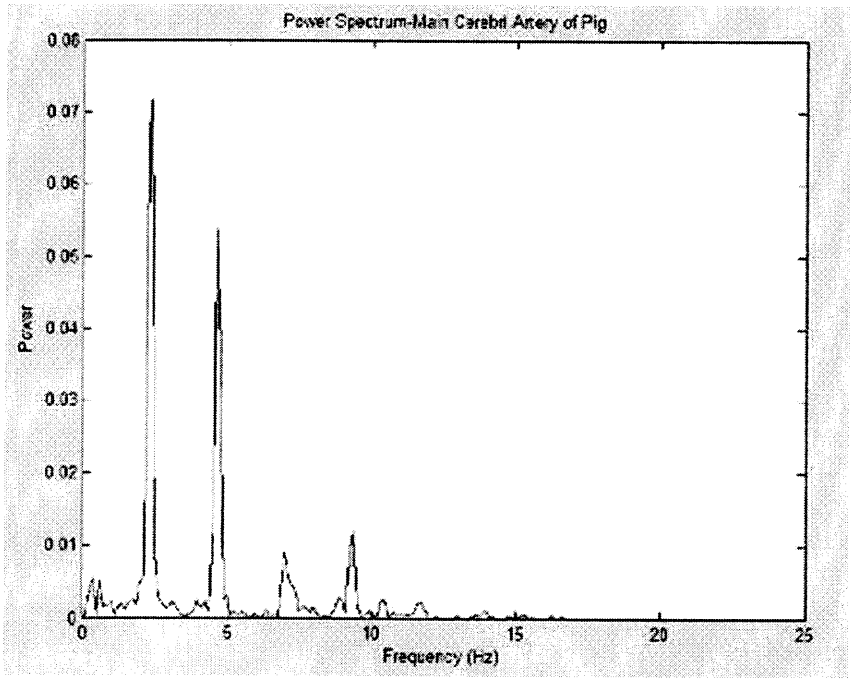

Fig 4.43 Cerebral Blood Flow Velocity of Pig – Power Spectrum
(Results obtained before Implantation)

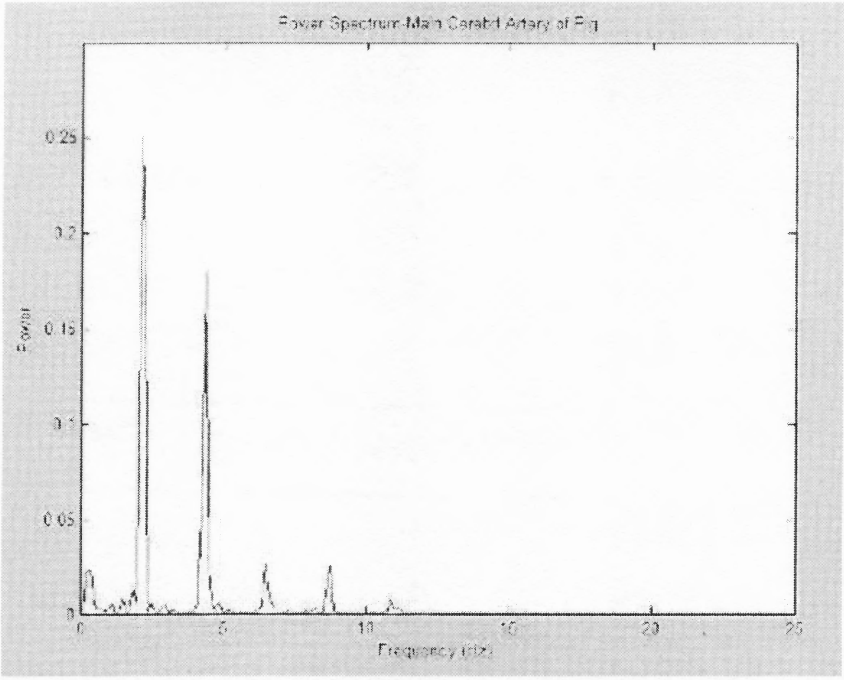

Fig 4.44 Cerebral Blood Flow Velocity of Pig – Power Spectrum
(Results obtained after Implantation)

It can be clearly seen that a better signal has been recorded when the probe was implanted (compare Y-axis values of Power). The reason for this would be because once the probe is implanted, there is a lot of muscle, in addition to the hardened bone cement, surrounding the probe holding it well in place. This is a positive point as the signal was found to be not only uniform and non-wavering after implantation, but also stronger.

4.13 Experiment on MCA of Dog using 20MHz Transducer

- Drug Response

The results obtained are as below.

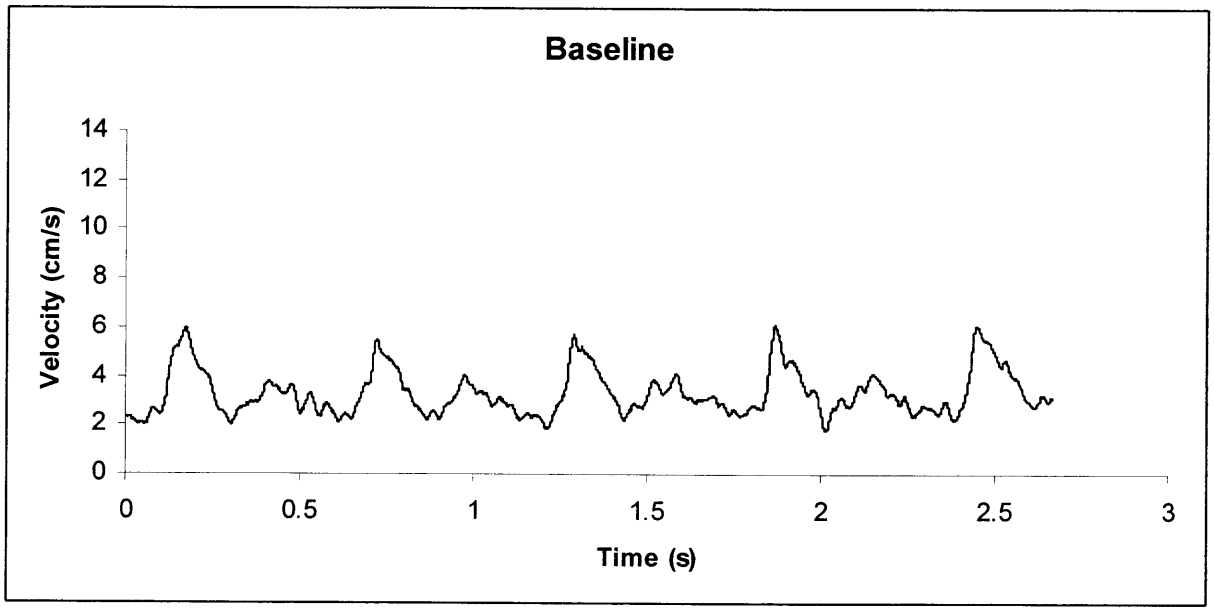

Fig 4.45 Cerebral Blood Flow Velocity pattern in Dog – Baseline Values

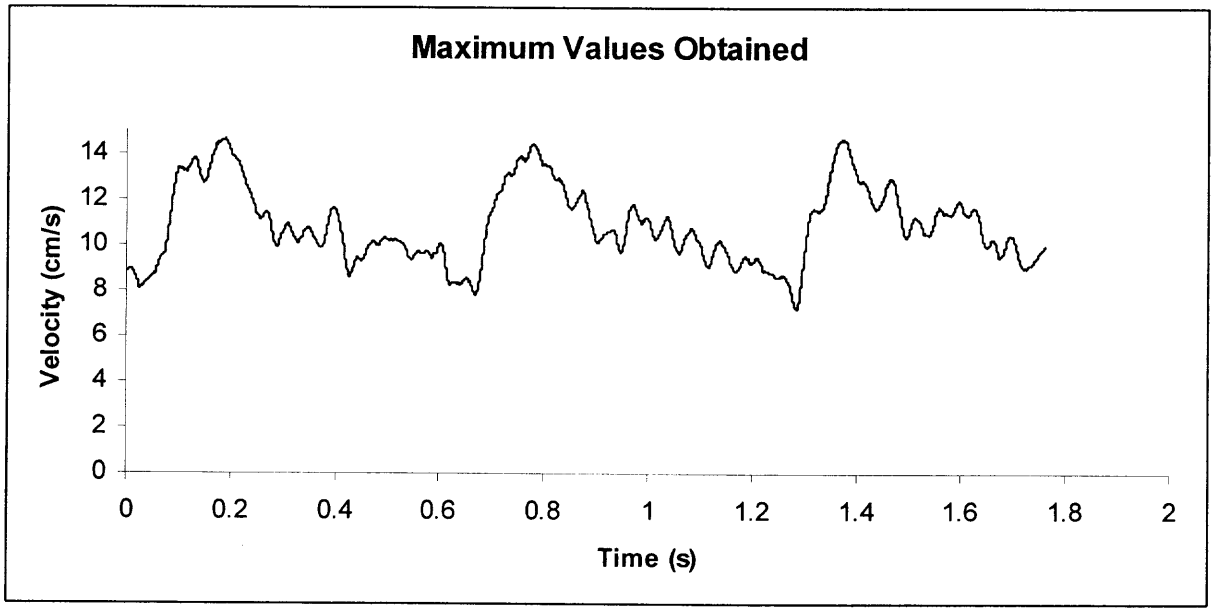

Fig 4.46 Cerebral Blood Flow Velocity pattern in Dog – Maximum Values

An increase in velocity values was observed with the gradual increase in pCO2 concentration as expected. Using a mathematical lowpass at 12Hz using Matlab, gave the above shown . It can be inferred that the required signals (magnitude) of the values are not affected.

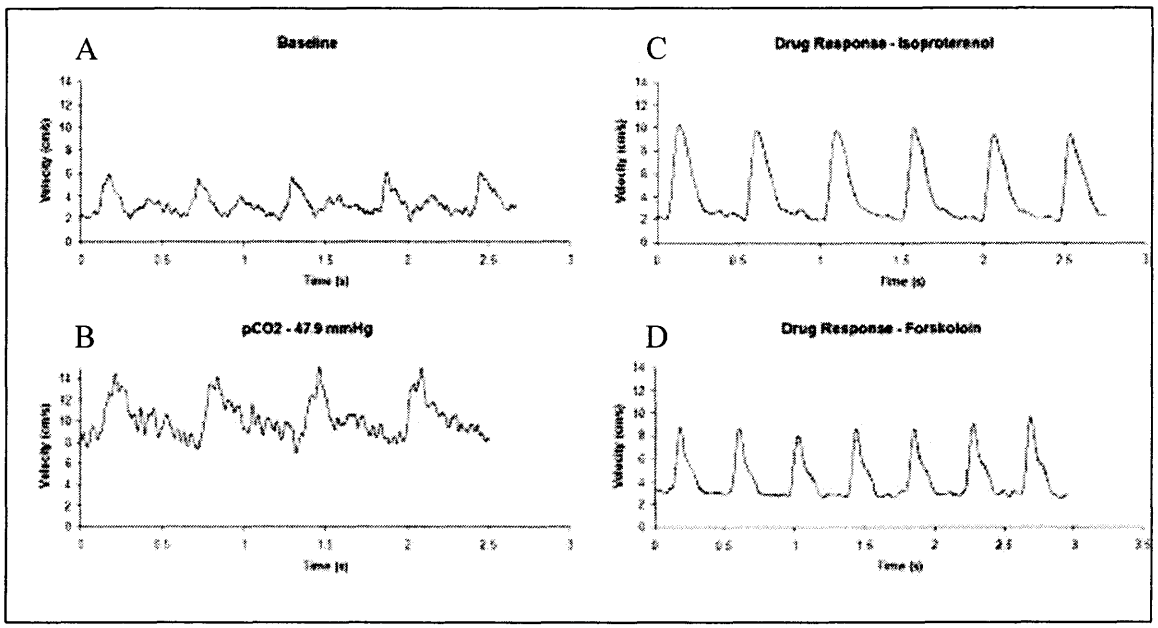

Fig 4.47 Cerebral Blood Flow Velocity pattern in Dog – (A). Baseline values (B). Increase in velocity with increase of pCO2 concentration (C, D). Increase in velocity values with introduction of Isoproterenol and Forskolin Response

It can be clearly seen from the above picture that the velocity values (Y-axis in cm/sec) increase in all the three cases. As the pCO2 values reach a maximum of 47.9mmHg (a 63% increase in comparison with its concentration during baseline measurement), the cerebral blood flow velocity varies 6cm/s to 14cm/s. This is the expected result. Next, with the introduction of Isoproterenol, there was a significant increase in the velocity of blood flow. Finally, with the introduction of Forskolin (after the effect of Isoproterenol subsided) the velocity values were found to increase from 6cm/s to 10cm/s. [56], [57].

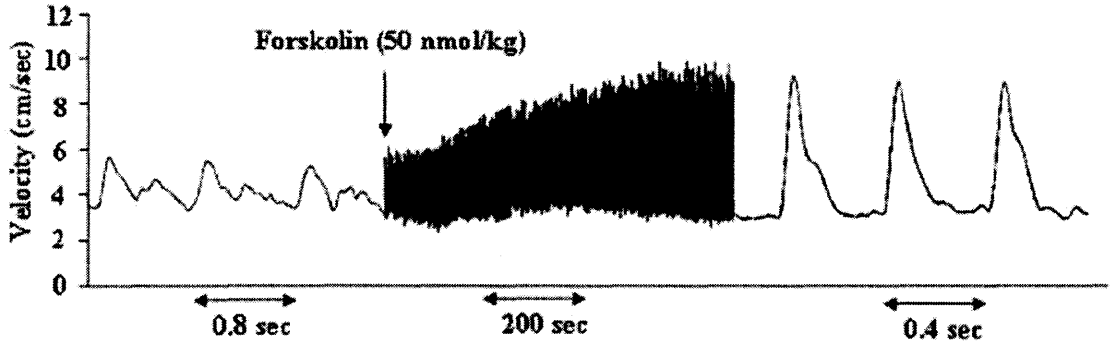

Fig 4.48 Cerebral Blood Flow Velocity pattern in Dog – Introduction of Forskolin

A more specific figure detailing the effect of introduction of Forskolin is shown above. A gradual increase in the velocity values with the absorption of Forskolin is clearly seen above.

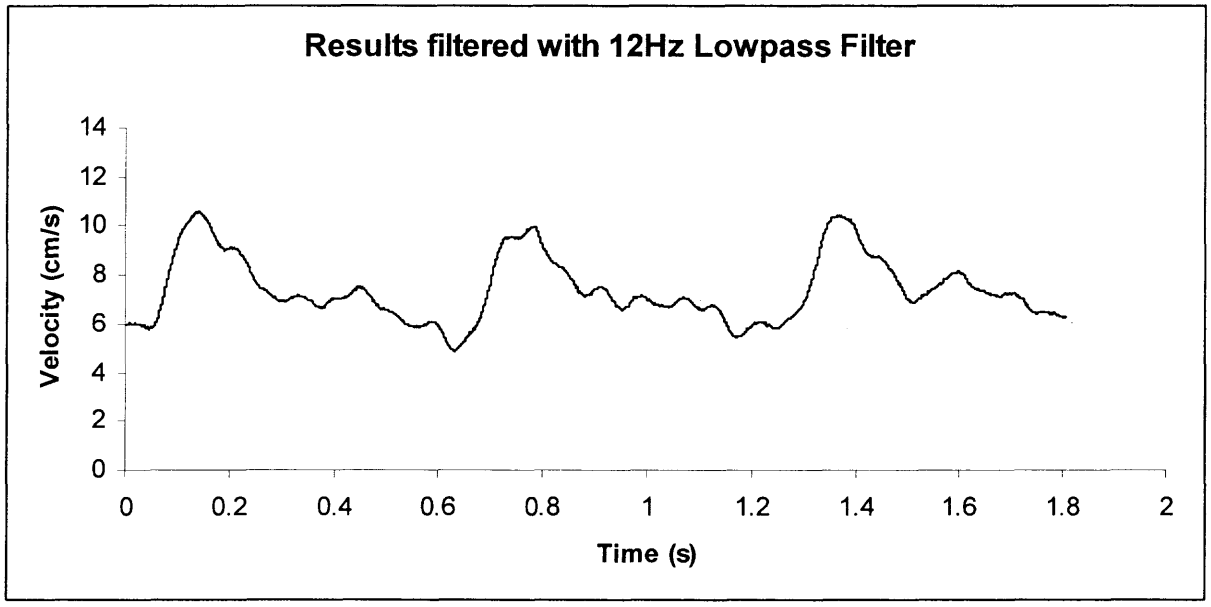

Fig 4.49 Cerebral Blood Flow Velocity pattern in Dog – 12Hz Low Pass Filtering

It was seen that the velocity values varied with increase in pCO2 gradually. This shows that the transducer is sensitive to small changes in pCO2 values. The plot is shown below.

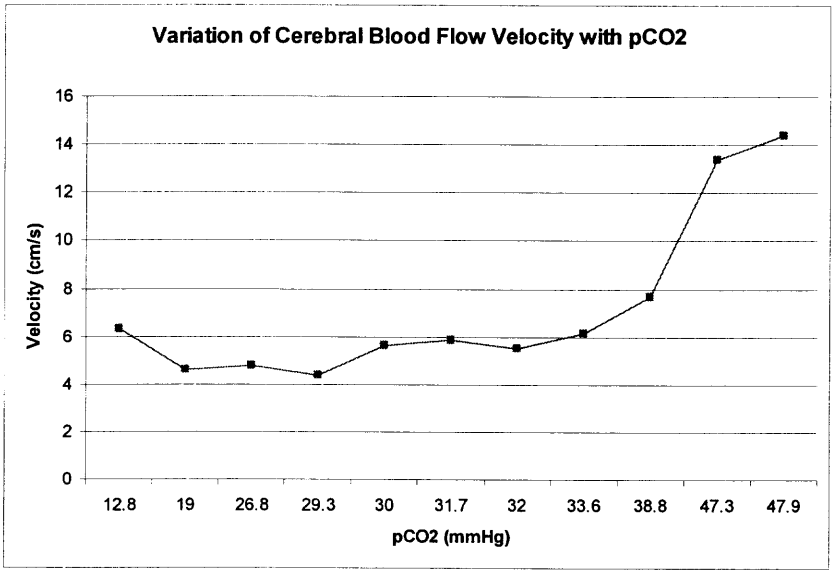

Fig 4.50 Cerebral Blood Flow Velocity increase with change in pCO2 concentration

CHAPTER 5

DISCUSSION AND CONCLUSIONS

Various preliminary tests were performed before the device was tried on any animal. Design changes were made during every step to converge to exact results. The test on the human wrist was considered a standard a testing method for all frequencies and designs of transducers.

The *in vitro* system which was carefully designed and machined became a method of testing the Ultrasound system and the transducer. The in vitro system was used to test every single design of the transducer and only when the transducer produced good enough results it was considered ready for the next test. The system also proved to be a novel method in calibrating the transducer and the ultrasound system. The particles used in the in vitro testing were chosen in a way that the suspension mimicked blood. Care was taken to make sure that there was no leakage during the test. This was done by tight fitting the transducer into the system by using rubber grommets. The in vitro system turned out to be of great help as each trial did not need an animal. For instance, when the effect of different concentrations of agarose gels was tested, the experiment was performed approximately 40 times to get the closest results possible. This would not have been possible without the in vitro system.

When the device was tried on mice, the results produced matched well those published in the literature and the values obtained by earlier researchers. The non-uniformity of the occurrence of peaks is due to human intervention in positioning. Furthermore, as the animal is anesthetized, the blood flow within each artery varies as time increases.

It was then expected in this case that the results would diverge (from the expected values) when the experiment is conducted on the mouse for a long time.

Data analysis of the results obtained, when the device was tried on the mouse, was another method to prove the authenticity and correctness of the results. The power spectrum was considered. The plot gives the power of the frequency of the signals. Observing each of the power spectra, for the femoral, left gastric and mesenteric artery, it is clear that the frequency with the highest power is the frequency at which the peak occurs. This frequency corresponds to the heart rate of the mouse. This leads to a heart rate of the mouse in between 300 to 350 beats per minute, which is lower than the normal heart rate of mice. This is again because the mouse had been anesthetized for a substantial amount of time, before these data were recorded. Looking into the last power spectrum, the Power Spectrum of Mesenteric Artery Blood Flow Velocity Plot using 1% Agarose gel, it can be observed that the value of maximum power is 20. This is a very high value, in comparison to the value of maximum power in the other power spectra. This is evidence that a clearer signal can be obtained if Agarose gel is used in place of Aquagel.

Later, when the device was used on the MCA of a dog, the results obtained did not match those published earlier. The reason for such a large difference in values could be due to mere positioning. As positioning plays a very important role in Doppler experiments, even a slight change in positioning can hinder the signals to a large extent. Theoretically, when the device worked well on a mouse artery of comparable size, it should work well enough on a dog too. One point that needs to be kept in mind is that the

surface of the brain is not flat, but curved to some extent. This could be a reason why the positioning is a problem.

Chronic Implantation

Considering the chronic implantation, the methodology for the surgery has been worked on and is ready to be performed. The surgery will involve the dog being anesthetized and a removal of the skin and muscle from the head of the dog at the appropriate area. All the blood will be cleared and any blood leakage will be stopped. A cranial drill, with a ¼" drill bit, will be used to drill four holes on the skull to an optimum depth without penetrating the dura [31]. The holes will be drilled in a way that they form the four corners of the rectangular piece of skull that is to be sawed off. The Gigli Wire saw will be used to saw a rectangular piece of skull with the required dimensions [30]. Then the surface of the dura will be cleaned of all the blood and any other liquid, and maintained dry. Next, the transducer will be placed on the surface of the dura and positioned accurately to get the best signals of blood flowing inside the middle cerebral artery. It is worth noting that the piece of skull removed will be rather small (a square with sides approximately 4cm) and therefore a good amount of accuracy needs to be employed when the holes are drilled, making sure that the area being exposed contains a part of the middle cerebral artery around the center. This helps immensely the accuracy in positioning the transducer [37].

Once good signals are observed, the transducer will be held firmly at the position and a small, but required, amount of bone cement or dental acrylic will be smeared over it in a way that the polycarbonate casing of the transducer is glued to the surface of the

bone close to it [41] and [43]. The muscle and skin will then be replaced over the surface of the skull and sutured, with only the transducer wire coming out.

All arrangements have been made to try the probe for a chronic implant. The bone cements are tested and ready, and so are the remaining equipments and devices.

Recommendation for Future Work

Future work, if dealing with chronic implantation, should make sure that the positioning does not fluctuate. Although the bone cements will hold the probe well in place, the initial placement matters to a large extent and if that is not performed properly, the experiment cannot go ahead.

Another suggestion will be the use of Agarose gel in place of Aquagel, due to the fact that the use of Agarose gel led to better results in many of the preliminary experiments.

The drawback with Doppler Ultrasound is that the velocity value calculated using this technique cannot be related to the volume flow rate within the same artery at that instant of time, unless the cross sectional area is known. However, the cross-sectional area of arteries changes with the flow of blood inside them [23]. A relation between the two would be a novel concept answering many questions.

APPENDIX A

CEREBROVASCULAR ACCIDENTS

These usually result from pre-existing vascular disease or congenital weakness and may be precipitated by trauma. Most commonly these accidents occur in older persons and animals

Hemorrhage

This usually occurs in atherosclerotic vessels. The resulting blood clot destroys brain tissue, and the neural tissue remaining next to the clot may be softened, leading to later complications. The clot and dead tissue are removed by macrophages, and the damaged area is invaded by connective tissue and glia, often producing a fluid-filled cyst.

Thrombosis

It most commonly involves formation of a clot at a site of vessel lumen constriction due to growth of atherosclerotic plates. Blockage of circulation leads to tissue softening and death, and to congestion of flow and edema in adjacent areas.

Embolism

This is the blockages of a cerebral vessel by a physical object, such as a dislodged clot, air, tumor cells, infectous mass. Often the situation involves multiple embolisms, complicating the clinical picture.

Aneurisms

These are the expansion of a vessel, usually an artery, and these balloons may reach a diameter of several inches. If this occurs within the cranial cavity, the displacement of neural tissue and the compression of other vessels and of cranial nerves

can obviously lead to severe problems. Most arise from the middle cerebral artery or the internal carotid, and if expansion is slow enough, there may be extensive erosion of bone. Clinically there is the added danger that the weakened vessel will rupture, giving the added problems of subarachnoid hemorrhage. Treatment usually involves surgery, if the vessel is accessible. Methods include removal of the sac or reinforcing the vessel wall with muscle or connective tissue, or ensheathing or replacing the weakened vessel with plastic. [19]

APPENDIX B

HEMATOCRIT

The hematocrit is the proportion, by volume, of the blood that consists of red blood cells. The hematocrit (hct) is expressed as a percentage. For example, an hematocrit of 25% means that there are 25 milliliters of red blood cells in 100 milliliters of blood.

The hematocrit is typically measured from a blood sample by an automated machine that makes several other measurements at the same time. Most of these machines in fact do not directly measure the hematocrit, but instead calculate it based on the determination of the amount of hemoglobin and the average volume of the red blood cells. The hematocrit can also be determined by a manual method using a centrifuge. When a tube of blood is centrifuged, the red cells will be packed into the bottom of the tube. The proportion of red cells to the total blood volume can be visually measured.

The normal ranges for hematocrit are dependent on age and, after adolescence, the sex of the individual. The normal ranges are:

Newborns: 55-68%

Adult males: 42-54%

Adult women: 38-46%

Dogs: 40-45%

Very low hematocrit value refers to lack of red blood cells which is anemia.

APPENDIX C

THERMAL CONDUCTIVITY OF BIOLOGICAL TISSUE

Table 8.12. Thermophysical Characteristics of Various Body Tissues, Organs, and Other Materials[80, 567, 817-819, 1665, 2153]

Material, Organ or Tissue	Thermal Conductivity K_e (watts/m-K)	Heat Capacity C_v (MJ/m^3-K)	Approx. Density (kg/m^3)
Skin			
Very warm	7.80	3.77	1000
Normal hand	0.960	3.77	1000
Cool	0.545	3.77	1000
Upper 2 mm	0.376	3.77	1000
Cold hand	0.335	3.77	1000
Subcutaneous fat			
High values	0.450	—	901
Pure fat	0.190	1.96	850
Muscle			
Living muscle	0.642	3.91	1050
Excised, fresh	0.545	3.64	1050
Skeletal muscle, living	0.377	—	1070
Bone			
Mineral	—	—	2982
Cortical	2.28	2.70	1790
Average	1.16	2.39	1500
Cancellous	0.582	2.07	1259
Blood			
Water at 310 K	0.623	4.19	993.4
Plasma (Hct = 0%) at 310K	0.599	4.06	1025
Whole blood (Hct = 40%)	0.549	3.82	1050
Organs			
Heart (excised, near fresh)	0.586	3.91	1060
Liver (excised, near fresh)	0.565	3.78	1050
Kidney (excised, near fresh)	0.544	4.08	1050
Abdomen core	0.544	3.89	1050
Brain (excised, near fresh)	0.529	3.86	1050
Brain (living)	0.680	—	—
Lung (excised, heaving)	0.292	2.24	603
Whole body (average)	—	4.17	1156
Air	0.0092462	0.00119	1.18
Cotton fabric at 310 K	0.0796	0.0267	100
C_{60}/C_{70} bulk compacts/Crystals	0.1-0.4	2.3-2.5	1540-1676
Rubber	0.156	2.41	1290
Ethanol at 310 K	0.163	1.96	789
Teflon	0.399	2.20	2180
Concrete	0.934	1.33	2310
Glass, plate	1.09	1.94	2520
Ice at 249 K (-42°C)	2.21	1.76	913
Sapphire (normal to c axis) at 310 K	2.29	2.89	3970
Stainless steel	13.8	3.68	7910
Aluminum	204	2.45	2710
Silver	406	2.59	10,500
Diamond, natural	2000	1.82	3510

Fig C1 Thermal Conductivity of Biological Tissue [20]

APPENDIX D

MATLAB PROGRAMMING

D.1. To create and display Power Spectrum

```
%Grab Velocity and Time Data from appropriate Excel Spreadsheet
DATA= xlsread('LGA_Aquagel.xls','LGA Aquagel');
TIME=DATA(1:length(DATA),1);
VEL=DATA(1:length(DATA),3);
% Set required sampling frequency
Fs = 1024;
%Determine where NaN occurs
for n=1:length(TIME)
   TF = isnan(TIME(n));
   if TF==1
      break
      end
   end
   b=n-1;
%Create Vectors for Time (T) and Velocity(V)
NaN
for i=1:b
   T(i)=TIME(i);
   V(i)=VEL(i);
```

```
end
% Calculate a power of two that will be equal to the length of VEL and use
% the next highest power to calculate FFT
NFFT= 2^(nextpow2(length(VEL)));
% Take fft, padding with zeros so that length (FFTX) is equal to
% NFFT
FFTX = fft(VEL,NFFT);
% Remove the DC component to remove random extremely high peaks appearing
% at the start of power spectrum
FFTX = fft((VEL-mean(VEL)),NFFT);
% Calculate the numberof unique points
NumUniquePts = ceil((NFFT+1)/2);
% FFT is symmetric, throw away second half
FFTX = FFTX(1:NumUniquePts);
% Take the magnitude of fft of x
MX = abs(FFTX);
% Scale the fft so that it is not a function of the
% length of x
MX = MX/length(VEL);
% Take the square of the magnitude of fft of x.
MX = MX.^2;
% Multiply by 2 because you
% threw out second half of FFTX above
```

```
MX = MX*2;
% DC Component should be unique.
MX(1) = MX(1)/2;
% Nyquist component should also be unique.
if ~rem(NFFT,2)
  % Here NFFT is even; therefore,Nyquist point is included.
  MX(end) = MX(end)/2;
end
% This is an evenly spaced frequency vector with
% NumUniquePts points
f = (0:NumUniquePts-1)*Fs/NFFT;
% Generate the plot, title and labels.
plot(f,MX);
title('Power Spectrum of Mesenteric Artery (Agarose Gel) Velocity-Time PLot');
xlabel('Frequency (Hz)');
ylabel('Power');
```

D.2. To calculate distribution of Peaks

```
%Assign variables for each required range
count05=0;
count510=0;
count2530=0;
count3035=0;
count1416=0;
count2530=0;
%Run a loop to consider each point including the first and last point
for i = 2:4259
   % To identify peaks, consider only those points whose magnitude is
   % greater than that of the point preceding and the point following it.
   % Only peaks will have magnitudes greater than the previous and next
   % points. Calculate this for each separate range required.
   if velocity(i-1)<velocity(i) & velocity(i)>=velocity(i+1)
      if velocity(i)> 5 & velocity(i)<=5
         count05=count05+1;
      end
      if velocity(i)> 5 & velocity(i)<=10
         count510=count510+1;
      end
      if velocity(i)> 25 & velocity(i)<=30
```

```
        count2530=count2530+1;
      end
      if velocity(i)> 30 & velocity(i)<=35
        count3035=count3035+1;
      end
      if velocity(i)>14 & velocity(i)<=16
        count1416=count1416+1;
      end
      if velocity(i)> 25 & velocity(i)<=30
        count2530=count2530+1;
      end
    end
end
```

APPENDIX E

GLOSSARY OF TERMS

Agarose

One of the constituents of agar. Often used in preference to agar because it gels at a lower temperature and does not contain the inhibitors of virus growth frequently present in agar. It is also used widely in gel electrophoresis because it has a more uniform pore size than that of agar

Angle of Insonation

The angle between the Doppler ultrasound beam and the direction of blood flow [8], [33] and [38]

Bone Cements

Adhesives used to fix prosthetic devices to bones and to cement bone to bone in difficult fractures [41]

Cerebrospinal Fluid

The serum-like fluid that circulates through the ventricles of the brain, the cavity of the spinal cord, and the subarachnoid space, functioning in shock absorption [42]

Cerebrovascular

Pertaining to blood vessels in the brain

Chronic

In medicine, a persistent and lasting condition is said to be **chronic** (from Greek *chronos*). For example, a chronic illness is one that persists for a long time, usually more

than three months. By analogy, this adjective has come to describe problems which cannot be solved in a short time, or which will recur regardless of action.

Dental acrylic

Very strong type of Acrylic used in dental applications [43]

Dura

The tough fibrous membrane covering the brain and the spinal cord and lining the inner surface

Femoral Artery

The main artery that supplies blood to the leg.

In vitro

Literally means, "in glass"; in a laboratory dish or test tube; an artificial environment. Anything that is done outside the body is generally known as *in vitro* or *ex vivo*

In vivo

Studies carried out inside living organisms.

Left Gastric Artery

A branch of the celiac artery that supplies the lesser curvature of the stomach and the abdominal part of the esophagus

Matlab

A data-manipulation software package that allows data to be analyzed and visualized using existing functions and user-designed programs

Mesenteric Artery

One of two branches of the aorta that pass between the two layers of the mesentery to the intestines

Peristaltic pump

A pump that moves liquid through tubing by alternate contractions and relaxations on the tubing

PVC

A thermoplastic material composed of polymers of vinyl chloride. PVC is a colorless solid with outstanding resistance to water, alcohols, and concentrated acids and alkalis

Stenosis

A constriction or narrowing of a duct or passage; a stricture

Thermal Conductivity

Measure of the ability of a solid or liquid to transfer heat

REFERENCES

1. "Transcranial Doppler Ultrasonography"; Dr. Joseph F. Smith Medical Library & CHC Medical Library & Patient Information; November 2004.

2. "Doppler Ultrasonography"; Dr. Joseph F. Smith Medical Library & CHC Medical Library & Patient Information; December 2004.

3. Stéphane Carlier, Lisette Okkels Jensen, "An Update on the Use of Intracoronary Doppler and Pressure Measurements"; Cardiovascular Research Foundation, New York; December 2004.

4. "Transducer" from The Encyclopedia; Retrieved from the World Wide Web on the 14th December 2004.

5. http://www.webopedia.com/TERM/T/transducer.html; Retrieved from the World Wide Web on the 12th December 2004.

6. Takuro Ikeda; "Fundamentals of Piezoelectricity"; Publisher: Oxford; New York: Oxford University Press, 1990.

7. Edwin L. Dove, "Medical Ultrasound Imaging"; Retrieved from the World Wide Web on 20th June 2005.

8. http://www.amershamhealth.com/medcyclopaedia/medical/volume%20I/DOPPLER%20ANGLE.ASP; Retrieved from the World Wide Web on the 5th May 2005.

9. External Anatomy; WY003-01 WY003/Joseph November 19, 2003 19:1.

10. "Brain Gross Anatomy"; College of Veterinary Medicine, University of Minnesota (http://vanat.cvm.umn.edu/grossbrain/Ventricles.html; Retrieved from the World Wide Web on the 7th March 2005.

11. "Neurosciences"; School of Veterinary Medicine, University of Pennsylvania (http://cal.vet.upenn.edu/neuro/server/lab4_215_22.html); Retrieved from the World Wide Web on the 7th March 2005.

12. http://noblood.getsmart2.com/rbcs.html; Retrieved from the World Wide Web on the 7th March 2005.

13. W. A. Whitaker III, "Acrylic Polymers: A Clear Focus"; Originally published January,1996.

14. Douglas G. Powell, "Medical Applications of Polycarbonate"; Originally published September 1998.

15. J. S. Fister, V. A. Memoli, J. O. Galante, W. Rostoker, R. M. Urban, "Biocompatibility of Delrin 150: a Creep-Resistant Polymer for Total Joint Prostheses"; Biomed Mater Res. 1985 May-Jun;19(5):519-33.

16. Jaroslaw Krejza, Zenon Mariak, Viken L. Babikian, "Importance of Angle Correction in the Measurement of Blood Flow Velocity with Transcranial Doppler Sonography"; May 2005.

17. http://www.transonic.com/Mouse_Acute_Femoral_Blood_Flow.ppt#263,3,Femoral artery proximal to the epigastria, isolated from the femoral vein, measures ~ 400 μm diameter with a micrometer. Flow measurements can be made in this location easily. ; Retrieved from the World Wide Web on 17th March 2005.

18. David L. Atkins, "Cerebral Blood Flow"; Department of Biological Sciences, George Washington University; March 2005.

19. Stephan J. Schreiber, Stefan Gottschalk, Markus Weih, Arno Villringer, José M. Valdueza, "Assessment of Blood Flow Velocity and Diameter of the Middle Cerebral Artery during the Acetazolamide Provocation Test by Use of Transcranial Doppler Sonography and MR Imaging"; May 2005.

20. Robert A. Freitas Jr., "Nanomedicine, Volume IIA: Biocompatibility"; June 2005.

21. C. S. Ahn, S. G. Lee, S. Hwang, D. B. Moon, T. Y. Ha, Y. J. Lee, K. M. Park, K. H. Kim, Y. D. Kim, K. K. Kim, "Anatomic Variation of the Right Hepatic Artery and its Reconstruction for Living Donor Liver Transplantation Using Right Lobe Graft"; June 2005.

22. A. Garcia Alberola, J. Lacunza Ruiz, J. L. Rojo Alvarez, J. J. Sanchez Munoz, J. Martinez Sanchez, J. Requena Carrion, J. Barnes, M. Valdes, "Early Heart Rate Increase Does Not Predict the Result of the Head-Up Tilt Test Potentiated With Nitroglycerin"; February 2005.

23. Ushio Fikushima, Shu Sasaki, Shozo Okano, Katsuaki Takase, Mitsuyoshi Hagio, "The Comparison between the Cerebral Blood Flow Directly Measures and Cerebral Blood Flow Velocity in the Middle and Basilar Cerebral Arteries Measured by Transcranial Doppler Ultrasonography"; February 2005.

24. A. R. Lupetin, D. A. Davis, I. Beckman, N. Dash, "Transcranial Doppler Sonography II: Evaluation of Intracranial and Extracranial Abnormalities and Procedural Monitoring"; Radiographics 1995; 15:193-209.

25. A. R. Lupetin, D. A. Davis, I. Beckman, N. Dash, "Transcranial Doppler Sonography I: Principles, Technique, and Normal Appearances"; Radiographics 1995; 15:179-191.

26. P. J. Martin, D. H. Evans, A. R. Naylor "Measurement of Blood Flow Velocity in the Basal Cerebral Circulation: Advantages of Transcranial Color-coded Sonography over conventional Transcranial Doppler"; Journal Clin Ultrasound 1995; 23:21-26.

27. L. Garbin, F. Habestswallner, A. Clivati, "Vascular Reactivity in Middle Cerebral Artery and Basilar Artery by Transcranial Doppler in Normal Subjects during Hypoxia"; Ital. J. Neurol. Sci. 1997 18: 135-137.

28. A. H. Koons, D. Wurtzel, J. M. Metcalf, J. Fellus, J. Vannucci, R. Hiatt, T. Hegyi, "Cerebral Blood Flow Measurements in the Newborn Dog"; Biol. Neonate. 1993; 63: 120-128.

29. Shee Yan Fong, Stephen Duplessis, "Minimally Invasive Lateral Mass Plating in the Treatment of Posterior Cervical Trauma: Surgical Technique"; Journal of Spinal Disorders & Techniques. 18(3):224-228, June 2005.

30. A. Brunori, P. Bruni, R. Greco, R. Giuffre, F. Chiappetta, "Celebrating the Centennial (1894-1994): Leonardo Gigli and his Wire Saw"; Division of Neurosurgery, G. M. Lancisi, San Camillo Hospital, Rome, Italy.

31. E. Michael Deppe, Bernd Ringelstein, Stefan Knecht, "The investigation of Functional Brain Lateralization by Transcranial Doppler Sonography"; 6th October 2003.

32. The Society for Neuroanesthesia and Critical Care, Arthur Lam and Michael Mahla; 1998 Annual Meeting.

33. Samir S. Undavia, Valentia Berger, Gabor Kaley, Edward J. Messina, "Myogenic Responses of Isolated Adipose Tissue Arterioles"; Department of Physiology, New York Medical College, Valhalla, September 2004.

34. William E. Woodward, Gerald F. Appell, "Current Velocity Measurements using Acoustic Doppler Backscatter: A Review".

35. J. A. Clark, W. D. Scherer, "Remote acoustic Doppler Measurements of Ocean Currents"; Acousto-Optic Lab, School of Engineering and Architecture, The Catholic University of America, Washington, DC, Rep. 7-82, July 1982.

36. "Observations of Water Flow with High Resolution Doppler Sonar"; Geophys. Res. Lett., vol. no.2, Feb 1981.

37. Stephen F. Vatner, W. Thomas Manders, Roderick Bronson, Lawerence L. Priano, "Carotid Chemoreceptor Reflex Induced Sympathetic Vasoconstriction of the Cerebral Circulation"; Department of Medicine, Harvard Medical School and peter Bent Brigham Hospital, Boston, Massachusetts, and the New England Regional primate Research Center, Southboro, Massachusetts, November 2004.

38. J. Krejza, Z. Mariak, V. L. Babikian, "Importance of Angle Correction in the Measurement of Blood Flow Velocity with Transcranial Doppler Sonography"; AJNR Am. J. Neuroradiol., October 1, 2001; 22(9): 1743 – 1747.

39. J. Klingelhöfer, D. Sander, M. Holzgrafe, C. Bischoff, B. Conrad, "Cerebral Vasospasm Evaluated by Transcranial Doppler Ultrasonography at Different Intracranial Pressures"; J Neurosurg 1991;75:752-758.

40. J. Krejza, Z. Mariak, J. Lewko, "Standardization of Flow Velocities with Respect to Age and Sex Improves the Accuracy of Transcranial Color Doppler Sonography of Middle Cerebral Artery Spasm"; Am. J. Roentgenol., July 1, 2003; 181(1): 245 - 252.

41. T. J. Puolakka, K. J. Pajamaki, P. O. Pulkkinen, J. K. Nevalainen, "Poor survival of Cementless Biomet total Hip: a report on 1,047 hips from the Finnish Arthroplasty Register"; Department of Surgery, University Hospital of Tampere, Finland.

42. E.V. Capparelli, D. Holland, C. Okamoto, B. Gragg, J. Durelle, J. Marquie-Beck, G. Van Den Brande, R. Ellis, S. Letendre, "Lopinavir Concentrations in Cerebrospinal Fluid exceed the 50% inhibitory concentration for HIV"; Pediatric Pharmacology Research Unit, University of California San Diego, La Jolla, California, USA.

43. M. A. Parada, M. Puig de Parada, L. Hernandez, E. Murzi, F. Garcia, "A Practical Method for Simultaneous Multiple Intracerebral Implantations for Microdialysis in Rats"; Los Andes University, Department of Physiology, School of Medicine, Merida, Venezuela. marcop@ing.ula.ve.

44. V. E. Nelson, "Cracked Acrylic Ventricular Assist Devices after using a Doppler Stethoscope and Ultrasound Transmission Gel to predict Impending Pump Failure: A Case Report"; St Louis University Health Sciences Center Perfusion Department, MO 63110-0250, USA.

45. Race Foster, Marty Smith, Holly Nash, "Complete Blood Count (CBC)"; Retrieved from the World Wide Web on 23rd April 2005.

46. Interstellar Research, "Fourier Transform: Theory"; Retrieved from the World Wide Web on 15th June 2005.

47. Erhard Wielandt, "The Fourier Transformation"; Retrieved from the World Wide Web on 15th June 2005.

48. Wikipedia, "Fast Fourier transform"; Retrieved from the World Wide Web on the 15th June 2005.

49. Michael Barr, Brian Wagner, "Introduction to Digital Filters"; Retrieved from the World Wide Web on the 15th June 2005.

50. R W Hamming, "Digital Filters"; Retrieved from the World Wide Web on the 16th June 2005.

51. Kerry Lacanette, "A Basic Introduction to Filters - Active, Passive, and Switched-Capacitor", National Semiconductor Application Note 779, April 1991.

52. Ferroperm Optics, "Bandpass Filters"; Retrieved from the World Wide Web on the 16th June 2005.

53. J. Karen Carlson, A. Stephanie Eisenstat, Terra Ziporyn, "'Ultrasound' In The Harvard Guide to Women's Health" Cambridge, MA: Harvard University Press, 1996.

54. Barry L. Zaret, et al., "'Ultrasound Studies' In The Patient's Guide to Medical Tests", Boston: Houghton Mifflin, 1997.

55. Edward Robert Berkow, "'Ultrasonography (US)' In The Merck Manual of Diagnosis and Therapy" 16th ed., Rahway, NJ: Merck Research Laboratories, 1992.

56. WholehealthMD.com, "Forskolin"; Retrieved from the World Wide Web on the 16th June 2005.

57. Robert Deegan, Huai Bing He, Yuri Krivoruk, Alastair Wood, Margaret Wood, "Regulation of Norepinephrine Release by beta sub 2-Adrenergic Receptors during Halothane Anesthesia" Anesthesiology" 82(6):1417-1425, June 1995.

58. Drug Guide by Healthwise, "Isoproterenol Inhalation"; Retrieved from the World Wide Web on 21st July 2005.

59. Science Blog. Copyright, University of Michigan Health System http://www.scienceblog.com/community/older/2000/E/200004629.html;Retrieved from the World Wide Web on the 15th June 2005.

60. R. Aaslid, "The Doppler Principle applied to Measurement of Blood Flow Velocity in Cerebral Arteries" in R. Aaslid(ed): "Transcranial Doppler sonography", Springer, Vienna-New York, 1986.

61. K. Martin, D. Spinks, "Measurement of the Speed of Sound in Ethanol/Water Mixtures"; Ultrasound in Medicine and Biology, Volume 27, Number 2, February 2001, pp. 289-291(3).

62. J. Azevedo, M. Moreno, J. Bermejo, N. Pérez-Castellano, P. Puerta, M. Desco, C. Antoranz, J. A. Serrano, E. García, J. L. Delcán, "Regional Diastolic function in Ischaemic Heart Disease using Pulsed Wave Doppler Tissue Imaging"; Laboratory of Ecocardiography, Service of non-Invasive Cardiology, Department of Cardiology, General Hospital University Gregorio Marañón, Madrid, Spain.

63. L. E. Drain, "The laser doppler technique", Publisher: Chichester[Eng.], New York : J. Wiley.

64. J. W. Doucette, P. D. Corl, H. M. Payne, A. E. Flynn, M. Goto, M. Nassi, J. Segal, "Validation of a Doppler Guide Wire for Intravascular Measurement of Coronary Artery Flow Velocity"; Cardiovascular Research Institute, University of California, San Francisco.

65. Takuro Ikeda, "Fundamentals of piezoelectricity"; Publisher: Oxford; New York : Oxford University Press, 1990.

66. Takuro Ikeda,. "Fundamentals of piezoelectric materials science"; Oxford University Press, London, 1990.

67. Hanna Damasio, "Human brain anatomy in computerized images"; New York, N.Y. : Oxford University Press.

68. Nancy A. Brunzel, "Fundamentals of Urine and Body Fluid Analysis"; Division of Medical Technology, Department of Laboratory Medicine and Pathology, University of Minnesota, Minneapolis, MN.

69. H. J. Deuling, W. Helfrich, "A Theoretical Explanation for the Myelin Shapes of Red Blood Cells"; Blood Cells, 1977, 3:713-720.

70. Kenneth B. Seamon, John W. Daly, "Forskolin its Biological and Chemical Properties"; Adv Cyclic Nucleotide Protein Phosphorylation Res. 1986;20:1-150.

71. S. S. Haykin, "An Introduction to Analog and Digital Communications"; 1989 - New York: Wiley.

72. R. W. Erickson, D. Maksimovic, "Fundamentals of Power Electronics"; 2001 - print.google.com. Retrieved from the World Wide Web on 24th June 2005.

73. P. S. Heckbert, "Fundamentals of texture mapping and image warping"; 1989 - cs.cmu.edu. Retrieved from the World Wide Web on 24th June 2005.